EQUILIBRIUM AND DYNAMICS OF SURFACTANT ADSORPTION MONOLAYERS AND THIN LIQUID FILMS

by

Krassimir D. Danov, Peter A. Kralchevsky and Ivan B. Ivanov
Faculty of Chemistry, University of Sofia, Sofia, BULGARIA

TABLE OF CONTENTS

Part 2

(Part 1 can be found at http://www.lcpe.uni-sofia.bg/publications/1999/pdf/1999-10-1-KD-PK-II.pdf)

VI. SURFACE FORCES IN THIN LIQUID FILMS

In the present section, we review the molecular theory of surface forces with a special attention to the effect of surfactant adsorption and surfactant micelles on the interactions in the thin liquid films and between the particles in dispersions.

In the *absence of adsorbed surfactants* the interactions in the foam or emulsion films are dominated by the attractive van der Waals and hydrophobic forces, which lead to a fast drainage and rupture of the films. It should be noted that even the pure water-air and water-oil interfaces are charged [22, 279], however the resulting electrostatic repulsion is too weak to stabilize the films.

The adsorption of ionic surfactants gives rise to a relatively high surface potential and strong *electrostatic repulsion*, which may counterbalance the *van der Waals attraction* and stabilize films and dispersions. This classical concept of dispersion stability was formulated by Derjaguin, Landau, Verwey and Overbeek (DLVO), see Section A below.

More recent experimental data [4] show that considerable deviations from the conventional DLVO theory appear for short surface-to-surface distance (*hydration repulsion*) and in the presence of bivalent and multivalent counterions (*ionic correlation force*). Both effects can be interpreted as contributions to the double layer interaction not accounted for in the DLVO theory, see Section B below.

Special *oscillatory structural forces* appear in thin films containing small colloidal particles like surfactant micelles, polymer coils, protein macromolecules, latex or silica particles [268, 280-283]. For larger particle volume fractions these forces are found to stabilize thin films and dispersions, whereas at low particle concentrations the oscillatory

force degenerates into the *depletion attraction*, which has the opposite effect, see Section C below.

When nonionic surfactants, like those having polyoxiethylene moieties, are adsorbed at the film or particle surfaces, the formed polymer brushes give rise to a *steric interaction* between such two surfaces [4, 284]. Its quantitative description is reviewed in Section D below.

The surfactant molecules in adsorption monolayers or lamellar bilayers are involved in a thermally exited motion, which brings about the appearance of *fluctuation capillary waves*. The latter also cause a steric interaction (though a short range one) when two thermally corrugated interfaces approach each other, see Section E below.

Finally, in Section F we discuss the effect of surface forces on the interaction between surfactant micelles.

A. DLVO theory

A.1. Van der Waals surface forces

The van der Waals forces represent an averaged dipole-dipole interaction, which is a superposition of three contributions: (i) *orientation interaction*: interaction between two permanent dipoles [285]; (ii) *induction interaction*: interaction between one permanent dipole and one induced dipole [286]; (iii) *dispersion interaction*: interaction between two induced dipoles [287]. The energy of van der Waals interaction between molecules i and j obeys the law [288]

$$u_{ij}\left(r\right) = -\frac{\alpha_{ij}}{r^6}$$

(185)

where u_{ij} is the potential energy of interaction, r is the distance between the two molecules and α_{ij} is a constant characterizing the interaction. The microscopic theory yields [4, 288]

$$\alpha_{ij} = \frac{p_i^2 p_j^2}{3kT} + \left(p_i^2 \alpha_{0j} + p_j^2 \alpha_{0i}\right) + \frac{3\pi\alpha_{0i}\alpha_{0j}\hbar v_i v_j}{v_i + v_j}$$

(186)

where p_i and α_{0i} are molecular dipole moment and electronic polarizability, $\hbar$ is the Planck constant and v_i can be interpreted as the orbiting frequency of the electron in the Bohr atom.

The *orientation* interaction can yield from 0% (nonpolar molecules) up to 70% (molecules of large permanent dipole moment, like H_2O) of the value of α_{ij}; the contribution of the *induction* interaction in α_{ij} is usually low, about 5-10%; the contribution of the *dispersion* interaction might be between 24% (water molecules) and 100% (nonpolar hydrocarbons); for numerical data - see e.g. Ref. [4]. Note that these estimates hold for the interaction between two molecules in a gas phase; the percentage of the respective contributions to the Hamaker constant of condensed phases can be quite different, see Eq. (190) below.

The van der Waals interaction between two macroscopic bodies can be found by integration of Eq. (185) over all couples of interacting molecules followed by subtraction of the interaction energy at infinite separation between the bodies. This approach, called the *microscopic* theory, is essentially based on the assumption that the van der Waals interaction in a condensed medium is pair-wise additive. The result of integration depends on the geometry of the system. For a plane-parallel film from component 3 located between two semiinfinite phases composed of components 1 and 2, the van der Waals interaction energy per unit area and the respective disjoining pressure, stemming from Eq. (185), are [289]:

$$ f_{vw} = -\frac{A_H}{12\,\pi h^2} \,, \quad \Pi_{vw} = -\frac{\partial f_{vw}}{\partial h} = -\frac{A_H}{6\,\pi h^3} \tag{187} $$

where, as usual, h is the thickness of the film and A_H is the compound Hamaker constant [290]:

$$ A_H = A_{33} + A_{12} - A_{13} - A_{23}\,; \qquad A_{ij} = \pi^2\,\rho_i\,\rho_j\,\alpha_{ij}\,, \qquad i,j = 1,2,3 \tag{188} $$

A_{ij} is the Hamaker constant of components i and j; ρ_i and ρ_j are the molecular number densities of phases i and j built up from components i and j, respectively. If A_{ii} and A_{jj} are known, one can calculate A_{ij} by using the Hamaker approximation

$$ A_{ij} = \left(A_{ii}\, A_{jj} \right)^{\frac{1}{2}} \tag{189} $$

In fact, Eq. (189) is applicable only to the dispersion contribution in the van der Waals interaction [4]. The Hamaker constant A_{ii} can be estimated by means of the microscopic theory, Eqs. (186) and (188). When components 1 and 2 are identical, A_H is positive. Therefore, the van der Waals interaction between identical bodies, in any medium, is always

attractive. Besides, two dense bodies (even if nonidentical) will attract each other when placed in medium 3 of low density (gas, vacuum).

When the phase in the middle (component 3) has intermediate Hamaker constant between those of bodies 1 and 2, A_H can be negative and the van der Waals disjoining pressure can be repulsive (positive). Such is the case of an aqueous film between mercury and gas.

An alternative approach to the calculation of the Hamaker constant, A_H, in condensed phases is provided by the Lifshitz *macroscopic* theory [292, 293], which is not limited by the assumption for pair-wise additivity of the van der Waals interaction, see Refs. [2, 4, 294]. For the symmetric case of two identical phases 1 interacting across a medium 3 the macroscopic theory provides the expression [4]

$$A_H = \frac{3}{4} kT \left(\frac{\varepsilon_1 - \varepsilon_3}{\varepsilon_1 + \varepsilon_3} \right)^2 + \frac{3\hbar\omega_e \left(n_1^2 - n_3^2 \right)^2}{16\sqrt{2} \left(n_1^2 + n_3^2 \right)^{3/2}} \tag{190}$$

where ε_1 and ε_3 are the dielectric constants of phases 1 and 3; n_1 and n_3 are the respective refractive indices; ω_e is a characteristic electronic absorption frequency which is about 1.85×10^{15} s^{-1} for water and the most organic liquids [4]. The first term in the right-hand side of Eq. (6.6) expresses the contribution of the orientation and induction interactions, which can never exceed $\frac{3}{4} kT \approx 3 \times 10^{-21}$ J. The last term in Eq. (190) accounts for the dispersion interaction.

When the film surfaces represent two surfactant adsorption monolayers, they can be modeled as multilayered structures (say, one layer for the headgroup region, another layer for the hydrocarbon tails, etc.). There is a general formula for the interaction between two such multilayered structures [294]:

$$f_{vw} = -\sum_{i=1}^{N_L} \sum_{j=1}^{N_R} \frac{A(i,j)}{12\pi h_{ij}^2}, \qquad A(i,j) \equiv A_{i,j} - A_{i,j-1} - A_{i-1,j} + A_{i-1,j-1} \tag{191}$$

where N_L and N_R denote the number of layers on the *left* and on the *right* from the central layer, the latter denoted by index "0" - see Fig. 23 for the notation. Equation (191) reduces to Eq. (187) for $N_L = N_R = 1$ and $h_{11} = h$.

Both Eqs. (187) and (191) correspond to *infinite* plane-parallel film surfaces. On the other hand, in the case of a film of *finite* area, formed between two deformed emulsion

droplets (see Fig. 15), the droplet-droplet interaction energy can be expressed in the form [295]

$$U(h,r) = -\frac{A_H}{12}\left[\frac{3}{4} + \frac{a}{h} + 2\ln\left(\frac{h}{a}\right) + \frac{r^2}{h^2} - \frac{2r^2}{ah}\right] \qquad (h,r \ll a) \qquad (192)$$

where h and r are the thickness and the radius of the film formed between the two deformed drops and a is the radius of the spherical part of the drop surface. Eq. (192) is a truncated series expansion; the exact formula, which is more complicated, can be found in Ref. [295]. Expressions for U for other geometrical configurations are also available [294].
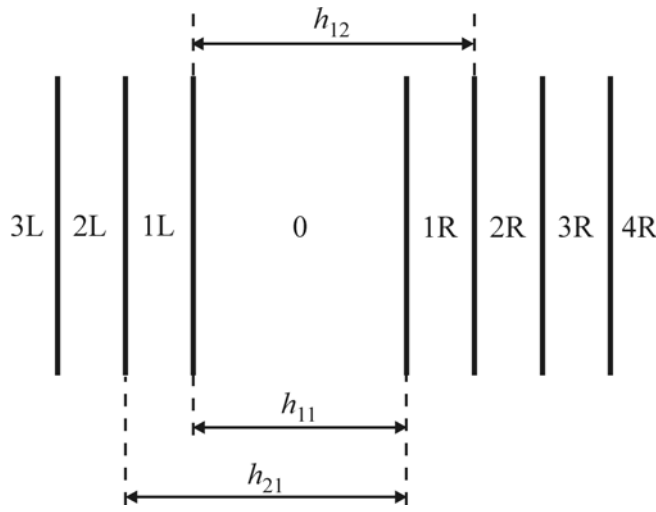
Fig. 23. Two multilayered bodies interacting across a medium "0". The layers are counted from the central film "0" outwards to the left (L) and right (R).

The asymptotic behavior of the *dispersion* interaction at large intermolecular separations does not obey Eq. (185); instead $u_{ij} \propto 1/r^7$ due to the electromagnetic retardation effect established by Casimir and Polder [296]. Various expressions have been proposed to account for this effect in the Hamaker constant [294].

The *orientation* and *induction* interactions are *electrostatic* effects; so, they are not subjected to electromagnetic retardation. Instead, they are influenced by the Debye screening due to the presence of electrolyte ions in the liquid phases. Thus for the interaction across an electrolyte solution the screened Hamaker constant is given by the expression [297]

$$A_H = 2\kappa h A_0 e^{-2\kappa h} + A_d \qquad (193)$$

where A_0 denotes the contribution of orientation and induction interaction into the Hamaker constant and A_d is the contribution of the dispersion interaction; κ is the Debye screening parameter:

$$\kappa^2 = \frac{2 e^2 I}{\varepsilon \varepsilon_0 k T}, \qquad I = \frac{1}{2} \sum_i Z_i^2 n_i \qquad (194)$$

where e is the elementary electric charge, ε and ε_0 are the relative and vacuum dielectric constants, respectively, and I is the ionic strength of the electrolyte solution; Z_i and n_i denote the valence and the number density of the ions.

It should be noted, that the experiment sometimes gives values of the Hamaker constant, which are markedly larger than the values predicted by the theory. In part this effect could be attributed to the strong attractive *hydrophobic force*, which is found to appear in aqueous films in contact with hydrophobic surfaces. The experiments showed, that the nature of the hydrophobic force is different from the van der Waals and double layer interactions [298-302]. It turns out that the hydrophobic interaction decays exponentially with the increase of the film thickness, h. The hydrophobic free energy per unit area of the film can be described by means of the equation [4]

$$f_{\text{hydrophobic}} = -2\gamma e^{-h/\lambda_0} \qquad (195)$$

where typically $\gamma = 10\text{-}50$ mJ/m^2, and $\lambda_0 = 1\text{-}2$ nm in the range $0 < h < 10$ nm. Larger decay length, $\lambda_0 = 12\text{-}16$ nm, was reported by Christenson *et al.* [302]for the range 20 nm $< h < 90$ nm. This amazingly long-ranged attraction entirely dominates over the van der Waals forces. In particular, it can lead to rupture of foam films containing small oil droplets or larger hydrophobic surfaces.

There is no generally accepted explanation of hydrophobic forces. Nevertheless, many authors agree that H-bounding in water and other associated liquids is the main underlying factor [4, 303]. Another hypothesis for the physical origin of the hydrophobic force considers the possible role of the spontaneous bubble nucleation between two hydrophobic surfaces as they approach each other [304-306].

A.2. Electrostatic surface forces

The electrostatic (double layer) interactions across an aqueous film are due to the overlap of the double electric layers formed at two charged interfaces, e.g. interfaces covered by ionic surfactants. Moreover, electrostatic repulsion is observed even between interfaces covered by adsorption monolayers of nonionic surfactants [22, 307-310].

Let us first consider the electrostatic (double layer) interaction between two identical charged plane parallel surfaces across a solution of symmetrical $Z{:}Z$ electrolyte. If the separation between the two planes is very large, the number concentration of both counterions and coions would be equal to its bulk value, n_0, in the middle of the film. However, at finite separation, h, between the surfaces the two electric double layers overlap and the counterion and coion concentrations in the middle of the film, n_{10} and n_{20}, are no longer equal. As pointed out by Langmuir [311], the electrostatic disjoining pressure, Π_{el}, can be identified with the excess osmotic pressure in the middle of the film:

$$\Pi_{el} = kT\left(n_{10} + n_{20} - 2n_0\right) \tag{196}$$

To find the dependence of Π_{el} on the film thickness, h, one solves the Poisson-Boltzmann equation for the distribution of the electrostatic potential inside the film. The solution provides the following connection between Π_{el} and h for symmetric electrolytes [2]:

$$\Pi_{el} = 4n_0 kT \cot^2\theta, \qquad \kappa h = 2\mathrm{F}(\varphi, \theta)\sin\theta \tag{197}$$

where $\mathrm{F}(\varphi, \theta)$ is an elliptic integral of the first kind and φ is related with θ as follows:

$$\cos\varphi = \cot\theta / \sinh\left(Z\Phi_s/2\right) \quad \left(\text{fixed surface potential } \Phi_s\right) \tag{198}$$

$$\tan\varphi = \tan\theta\sinh\left(Z\Phi_\infty/2\right) \quad \left(\text{fixed surface charge } \sigma\right) \tag{199}$$

$$\cosh Z\Phi_\infty = 1 + \frac{1}{2}\left(\frac{Ze\sigma_s}{\varepsilon\varepsilon_0 kT\kappa}\right)^2; \quad \Phi_s \equiv \frac{e\psi_s}{kT} \tag{200}$$

Here Φ_s is the dimensionless surface potential and Φ_∞ is the value of Φ_s for $h \to \infty$; Z is the valency of the counterion ($Z = \pm1, \pm2, ...$) Eq. (197) expresses the dependence $\Pi_{el}(h)$ in a parametric form: $\Pi_{el}(\theta)$, $h(\theta)$.

In principle, there is a possibility neither the surface potential nor the surface charge to be constant when h varies. In such a case a condition for *charge regulation* is applied, which in fact represents the condition for dynamic equilibrium of the counterion exchange between the Stern and diffuse parts of the electric double layer. The Stern layer itself can be considered as an adsorption layer of counterions. Then the Langmuir adsorption isotherm can be applied to yield [1, 290]

$$\frac{\sigma_{max} - \sigma_s}{\sigma_{max}} = \left[1 + \left(\frac{\sigma_{max}}{Zed_i n_0}\left(\exp\left(\Phi_a + Z\Phi_s\right)\right)\right]^{-1} \tag{201}$$

where d_i is the diameter of the hydrated counterion, σ_{max} is the maximum possible surface charge density due to all surface ionizable groups, σ_s is the effective surface charge density, which is smaller (by magnitude) than σ_{max} because some ionizable groups are blocked by adsorbed counterions; Φ_a is the energy of adsorption of a counterion in kT units (Φ_a is a negative quantity). The product $Z\Phi_s$ is always negative. At high surface potential, when $Z\Phi_s \to -\infty$, from Eq. (201) one obtains $\sigma_s \to 0$, that is all surface ionizable groups are blocked by adsorbed counterions.

When the film thickness is large enough ($\kappa h \geq 1$) the difference between the regimes of constant potential, constant charge and charge regulation becomes negligible [290], i.e. the usage of each of them leads to the same results for $\Pi_{el}(h)$.

When the dimensionless electrostatic potential in the middle of the film

$$\Phi_m = \frac{e}{kT}\psi_m = \frac{1}{2Z}\ln(n_{20}/n_{10}) \tag{202}$$

is small enough (the film thickness, h, is large enough), one can suppose that $\Phi_m \approx 2\Phi_1(h/2)$, where Φ_1 is the dimensionless electric potential at a distance $h/2$ from the surface (of the film) when the other surface is removed at infinity. Since

$$Z\Phi_1(h/2) = 4\,e^{-\frac{\kappa h}{2}}\tanh\left(\frac{Z\Phi_s}{4}\right) \tag{203}$$

from Eqs. (196), (202) and (203) one obtains a useful asymptotic formula [3]

$$\Pi_{el} \approx n_0 kTZ^2\Phi_m^2 \approx 64n_0kT\left(\tanh\frac{Z\Phi_s}{4}\right)^2 e^{-\kappa h} \tag{204}$$

It is interesting to note, that when Φ_s is large enough, the hyperbolic tangent in Eq. (204) will be identically 1, and Π_{el} (as well as f_{el}) becomes independent of the surface potential (or charge).

Eq. (204) can be generalized [312] for the case of 2:1 electrolyte (bivalent counterion) and 1:2 electrolyte (bivalent coion):

$$\Pi_{el} = 432n_{(2)}kT\left(\tanh\frac{v_{i:j}}{4}\right)^2 e^{-\kappa h} \tag{205}$$

where $n_{(2)}$ is the concentration of the bivalent ions, the subscript "$i{:}j$" takes value "2:1" or "1:2", and

$$v_{2:1} = \ln\left[3/\left(1+2\,e^{-\Phi_s}\right)\right], \quad v_{1:2} = \ln\left[\left(2\,e^{\Phi_s}+1\right)/3\right] \tag{206}$$

Eq. (204) can be generalized also for the case of two *non-identically* charged interfaces of surface potentials ψ_{s1} and ψ_{s2} for *Z:Z* electrolytes [2,3]

$$\Pi_{el}(h) = 64 n_0 kT \gamma_1 \gamma_2 \frac{e^{-\kappa h}}{} , \quad \gamma_k \equiv \tanh\left(\frac{|Z|\, e\, \psi_{sk}}{4kT}\right) \quad k = 1, 2 \tag{207}$$

Eq. (207) is valid for both low and high surface potentials, if only $\exp(-\kappa h) \ll 1$.

A.3. DLVO - criterion for the stability of dispersions

A quantitative theory of interactions in thin liquid films and dispersions was proposed by Derjaguin and Landau [313] and Verwey and Overbeek [3]. In this theory, called DLVO after the authors' names, the total interaction is supposed to be a superposition of van der Waals and double layer interactions. In other words, the total disjoining pressure, Π, and the particle-particle interaction energy, U, are presented in the form:

$$\Pi = \Pi_{vw} + \Pi_{el}; \quad U = U_{vw} + U_{el} \tag{208}$$

U could be calculated by means of the Derjaguin formula, Eq. (183). A typical curve Π vs h exhibits a maximum representing a barrier against coagulation, and two minima, called primary and secondary minimum, see Fig. 17a. If the particles cannot overcome the barrier, coagulation (flocculation) does not take place and the dispersion is stable due to the electrostatic repulsion, which gives rise to the barrier. With larger colloidal particles ($R > 0.1$ μm) the secondary minimum (that for $h > h_1$ in Fig 17a) could be deep enough to cause coagulation and even formation of ordered structures of particles [314].

By addition of electrolyte or by decreasing the surface potential of the particles one can suppress the electrostatic repulsion, thus lowering the height of the barrier. According to the DLVO-theory the critical condition determining the onset of rapid coagulation is

$$U(h_{\max}) = 0, \quad \left.\frac{dU}{dh}\right|_{h_{\max}} = 0 \tag{209}$$

where $h = h_{\max}$ denotes the position of the barrier.

Based on Eqs. (161), (182), (187) and (204) one can derive from Eqs. (208) - (209) the following criterion for the threshold of rapid coagulation of identical particles [3, 313]:

$$\frac{\kappa^6}{n_0^2} = \left[\frac{768\pi}{A_H} kT e^{-1} \tanh^2\left(\frac{Z e \psi_s}{4kT}\right)\right]^2 \tag{210}$$

where $e = 2.718...$ is the Napper number. For a *Z:Z* electrolyte the substitution of κ^2 from Eq. (194) into Eq. (210) yields

$$n_0\left(\text{critical}\right) \propto \frac{1}{Z^6} \tanh^4\left(\frac{Z\,\text{e}\,\psi_s}{4kT}\right) \tag{211}$$

When ψ_s is high enough the hyperbolic tangent equals 1 and Eq.(211) yields n_0(critical) $\propto Z^6$ which in fact is the empirical rule established earlier by Schulze [315] and Hardy [316].

B. Hydration repulsion and ionic-correlation force

After 1980 a number of surface forces have been found out which are not taken into account by the conventional DLVO theory. They are considered separately in Sections B-E below.

B.1. Repulsive hydration forces

Effects of different physical origin are termed "hydration forces" in the literature, see Ref. [317] for review. For that reason from the very beginning we specify that here we call *hydration force* the short-range monotonic repulsive force which appears as a deviation from the DLVO theory for short distances between two molecularly smooth electrically charged surfaces. Such a force may appear in foam or emulsion films stabilized by ionic surfactants, as well as between the surfactant micelles in a solution. Experimentally the existence of this force was established by Israelachvili *et al*. [318, 319] and Pashley [320, 321] who examined the validity of DLVO-theory at small film thickness in experiments with films from aqueous electrolyte solutions confined between two mica surfaces. At electrolyte concentrations below 10^{-4} mol/l (KNO$_3$ or KCl) they observed the typical DLVO maximum, cf. Fig. 17a. However, at electrolyte concentrations higher than 10^{-3} mol/l they did not observe the expected DLVO maximum; instead a strong short range repulsion was detected; cf. Fig. 24. Empirically, this force, called the hydration repulsion, appears to follow an exponential law [4]

$$f_{\text{hydr}}\left(h\right) = f_0\,e^{-h/\lambda_0} \tag{212}$$

where, as usual, h is the film thickness; the decay length $\lambda_0 \approx 0.6$ - 1.1 nm for 1:1 electrolytes; the pre-exponential factor, f_0, depends on the hydration of the surfaces but is usually about 3-30 mJ/m^2.

The physical importance of the hydration force is that it stabilizes thin films and dispersions preventing coagulation in the primary minimum (that between points 2 and 3 in Fig. 17a). It is believed that the hydration force is connected with the binding of strongly hydrated ions at the interface. This is probably the explanation of the experimental results of

Healy *et al*. [322], who found that even high electrolyte concentrations cannot cause coagulation of amphoteric latex particles due to binding of strongly hydrated Li$^+$ ions at the particle surfaces. If the Li$^+$ ions are replaced by weakly hydrated Cs$^+$ ions, the hydration repulsion becomes negligible, compared with the van der Waals attraction, and the particles coagulate as predicted by the DLVO-theory.

For the time being there is no generally accepted theory of the repulsive hydration force. It has been attributed to various effects: solvent polarization and H-bonding [323], image charges [324], non-local electrostatic effects [325], existence of a layer of lower dielectric constant, ε, in a vicinity of the interface [326, 327]. It seems, however, that the main contribution to the hydration repulsion between two charged interfaces originates from the *finite size* of the hydrated counterions [328], an effect which is not taken into account in the DLVO theory (the latter deals with *point* ions).

The *volume excluded by the ions* becomes important in relatively thin films, in so far as the counterion concentration is markedly higher only in a close vicinity of the film surfaces. Paunov *et al*. [328] took into account this effect by means of the Bikerman equation [329, 330]

$$n_i(x) = \frac{1 - v\sum_k n_k(x)}{1 - v\sum_k n_{k0}}\, n_{i0}\exp U_i; \qquad U_i = -\frac{Z_i e\psi}{kT} \tag{213}$$

Here x is the distance to the charged surface, n_i and U_i are the number density and the potential energy (in kT units) of the i-th ion in the double electric layer; n_{i0} is the value of n_i in the bulk solution; the summation is carried out over all ionic species; v has the meaning of an average excluded volume per counterion; the theoretical estimates [328] show that v is approximately equal to 8 times the volume of the hydrated counterion.

The problem for the distribution of the electric potential across the film accounting for the effect of the ionic excluded volume can be formulated as follows [328]. The electric potential in the film, $\psi(x)$, satisfies the Poisson equation

$$\varepsilon_0 \frac{d}{dx}\left(\varepsilon\frac{d\psi}{dx}\right) = -\rho(x) \tag{214}$$

where the surface charge density, $\rho(x)$, is determined from Eq. (213):

$$\rho(x) = \frac{\sum_i Z_i e\, n_i^*\exp U_i}{1 + v\sum_i n_i^*\exp U_i}; \qquad n_i^* \equiv \frac{n_{i0}}{1 + v\sum_k n_{k0}} \tag{215}$$

79

For v = 0 Eq. (215) reduces to the expression used in the conventional DLVO theory. Eq. (214) can be solved numerically. Then the total electrostatic disjoining pressure can be calculated by means of the expression [328]

$$\Pi_{el}^{tot} \equiv -\int_{0}^{\psi_m} \rho_m \, d\psi = \frac{kT}{v} \ln\left[\frac{1 + v\sum_k n_k^* \exp(-Z_k e\psi_m / kT)}{1 + v\sum_k n_k^*}\right] \qquad (216)$$

where the subscript "m" denotes values of the respective variables at the midplane of the film. Finally, the non-DLVO *hydration* force can be determined as an excess over the conventional DLVO electrostatic disjoining pressure:

$$\Pi_{hr} \equiv \Pi_{el}^{tot} - \Pi_{el}^{DLVO} \qquad (217)$$

where Π_{el}^{DLVO} is defined by Eq. (196), which can be deduced from Eq. (216) for v → 0. Note that the effect of v ≠ 0 leads to a larger value of ψ_m, which contributes to a positive (repulsive) Π_{hr}. Similar, but quantitatively much smaller, is the effect of the lowering of the dielectric constant, ε, in the vicinity of the interface, which has been also taken into account in Ref. [328].

The theory based on Eqs. (214) - (217) is found [328] to give an excellent numerical agreement with experimental data of Pashley [320, 321], Claesson *et al*. [331] and Horn *et al*. [332]. In Fig. 24 theoretical predictions for $F/R \equiv 2\pi f$ vs h are presented; here F is the force measured by the surface force apparatus between two crossed cylinders of radius R; as usual, f is the total surface free energy per unit area, see Eq. (161). The dependence of hydration repulsion on the concentration of electrolyte (KCl) is investigated. All theoretical curves are calculated for v = 1.2×10^{-27} m³ (8 times the volume of the hydrated K⁺ ion), $A_H = 2.2 \times 10^{-20}$ J and $\psi_s = -128.4$ mV; the boundary condition of constant surface potential is used. The theoretical curves in Fig. 24 resemble very much the experimental findings, see e.g. Fig. 13.9 in Ref. [4]. In particular, for $C_{el} = 5 \times 10^{-5}$ and 10^{-4} M a typical DLVO maximum is observed, without any indication about the existence of short range repulsion. However, for $C_{el} = 10^{-3}$, 10^{-2} and 10^{-1} M maximum is not seen but instead, the short range hydration repulsion appears. Note that the increased electrolyte concentration increases the hydration repulsion, but suppresses the long-range double layer repulsion.
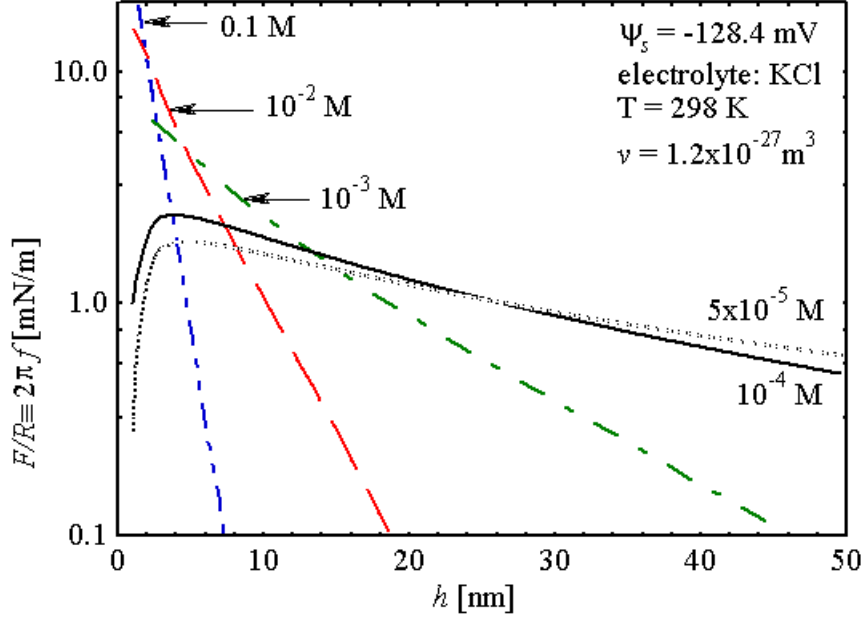
Fig. 24. Theoretical plot of $F/R \equiv 2\pi f$ vs. h for various concentrations of KCl denoted on the curves. All curves are drawn for the same values of the surface potential, $\psi_s = -128$ mV, excluded volume per K^+ ion $v = 1.2 \times 10^{-27}$ m^3 and $T = 298$ K.

B.2. Ionic Correlation Force

Because of the strong electrostatic interaction between the ions in solution their positions are correlated in such a way that a counterion atmosphere appears around each ion thus screening its Coulomb potential. As shown by Debye and Hückel [333, 334], the energy of formation of the counterion atmospheres gives a contribution to the free energy of the system called "correlation energy" [24]. The correlation energy provides also a contribution to the osmotic pressure of the electrolyte solution, which can be presented in the form [333, 334]

$$\Pi_{OSM} = kT \sum_{i=1}^{k} n_i - \frac{kT\kappa^3}{24\pi} \tag{218}$$

The first term in the right-hand side of the Eq. (218) corresponds to an ideal solution, whereas the seconds term takes into account the effect of electrostatic interaction between the ions (the latter is accounted for thermodynamically by the activity coefficient [335]). The expression for Π_{el} in the DLVO-theory, Eq. (196), obviously corresponds to an ideal solution (i.e. to the first term in Eq. 218), the contribution of the ionic correlations being neglected. Hence, in a more general theory instead of Eq. (208) one is to write

$$\Pi = \Pi_{vw} + \Pi_{el} + \Pi_{cor} \tag{219}$$

where Π_{cor} is the contribution of the ionic correlations into disjoining pressure; Π_{cor} can be interpreted as a surface excess of the last term in Eq. (218). In other words, the ionic

correlation force originates from the fact that the counterion atmosphere of a given ion in a thin film is different from that in the bulk of the solution. There are two reasons for this difference: (i) the ionic concentration in the film differs from that in the bulk and (ii) the counterion atmospheres are affected by the presence of the film surfaces. Both numerical [336, 337] and analytical [338, 339] methods have been developed for calculating Π_{cor}.

In the case when the electrolyte is symmetrical ($Z:Z$) and $\exp(-\kappa h) \ll 1$ one can use the asymptotic formula [338]

$$\Pi_{cor} = \Pi_{el} \frac{Z^2 e^2 \kappa}{16 \pi \varepsilon \varepsilon_0 kT} \left(\ln 2 + 2I_C \right) + O\left(e^{-\kappa h} \right) \tag{220}$$

where Π_{el} is the conventional DLVO electrostatic disjoining pressure,

$$I_C = \frac{1}{2}(1+J)\ln 2 + \frac{2 - 2z^3 + z}{2z(2z^2 - 1)^2} - \frac{1}{2}(1-J)\ln(z + z^2)$$

$$- \frac{\sqrt{z^2 - 1}}{z}\left[1 + J + 4(2z^2 - 1)^{-3} \right] \arctan\sqrt{\frac{z-1}{z+1}}$$

$$J \equiv \frac{2z^2 - 3}{(2z^2 - 1)^3}, \qquad z \equiv \left[1 + \left(\frac{e\sigma_s}{2\varepsilon\varepsilon_0 kT\kappa} \right)^2 \right]^{1/2}$$

The results for the case of symmetric electrolytes are the following. Π_{cor} is negative and corresponds to attraction, which can be comparable by magnitude with Π_{vw}. In the case of 1:1 electrolyte Π_{cor} is usually a small correction to Π_{el}. In the case of 2:2 electrolyte, however, the situation can be quite different: the attractive forces, $\Pi_{cor} + \Pi_{vw}$, prevail over Π_{el} and the total disjoining pressure, Π, becomes negative. These results show that in general Π_{cor} is not a small correction over Π_{el}: in the presence of bivalent and multivalent counterions Π_{cor} becomes the dominant surface force.

The above results are obtained for two overlapping electric double layers inside the film. Such films can appear between two colliding droplets in an *oil-in-water* emulsion. In the opposite case of *water-in-oil* emulsion the double layers are outside the film. Nevertheless, in the latter case Π_{cor} is not zero because the ions belonging to the two outer double layers interact across the thin dielectric (oil) film. The theory for such a film [340] predicts that Π_{cor} is negative (attractive) and strongly dependent on the dielectric permittivity of the oil film; for such films Π_{cor} can be comparable by magnitude with Π_{vw}; $\Pi_{el} = 0$ in this case.

In the case of secondary thin liquid films, stabilized by ionic surfactant ($h = h_2$ in Fig. 17a), the measured contact angles are considerably larger than the theoretical value predicted

if only van der Waals attraction is taken into account [262]. The experimentally detected additional attraction in these very thin films ($h \approx 5$ nm) can be attributed to short range ionic correlation effects [263] as well as to the discreteness of the surface charge [2,261,341].

C. Oscillatory Structural and Depletion Forces

C.1. Experiments with micellar surfactant solutions

In the beginning of this century Johnott [342] and Perrin [343] observed that soap films decrease their thickness by several step-wise transitions. The phenomenon was called "stratification". Bruil and Lyklema [344] and Friberg *et al.* [345] studied systematically the effect of ionic surfactant and electrolyte on the occurrence of the step-wise transitions. Keuskamp and Lyklema [346] anticipated that some oscillatory interaction between the film surfaces must be responsible for the observed phenomenon. Kruglyakov [347] and Kruglyakov and Rovin [348] reported the existence of stratification with emulsion films.

Some authors [348, 349] suggested that a possible explanation of the phenomenon can be the formation of surfactant lamella liquid-crystal structure inside the film. Such lamellar micelles are observed to form in surfactant solutions, however, at concentrations much higher than those used in the experiments with stratifying films. The latter fact makes the explanation with lamella liquid crystal problematic. Nikolov *et al.* [280, 350, 351]observed stratification not only with micellar surfactant solutions but also with suspensions of latex particles of micellar size. The step-wise changes in the film thickness were approximately equal to the diameter of the spherical particles, contained in the foam film [280-282, 352]. The experimental observations show that stratification is observed always, when spherical colloidal particles are present in the film at sufficiently high concentration. The observed multiple step-wise decrease of the film thickness (see e.g. Fig. 25) can be attributed to the layer-by-layer thinning of a colloid-crystal-like structure inside the film [280].

The mechanism of stratification was studied theoretically in Ref. [353], where the appearance and expansion of black spots in the stratifying films was described as a process of condensation of vacancies in a colloid crystal of ordered micelles within the film.

Recently, oscillatory structural forces due to micelles and microemulsion droplets were directly measured by means of a surface force balance [283]. The stable branches of the oscillatory disjoining pressure isotherm have been measured [268] with micellar solutions by means of the experimental cell of Mysels [354]. Moreover, Denkov *et al.* [355] took pictures

of spherical surfactant micelles in a foam film at different stages of stratification by using cryoelectron microscopy. The micrographs show that the micelles do not form crystal-like structure in *lateral* direction; however, some ordering in *normal* direction should be expected in so far as the film thickness varies in a step-wise manner. On the other hand, the application of the interference method, developed in Ref. [356], to free vertical stratifying films, containing 100 nm latex particles, confirms that the particles form a colloid crystal structure of hexagonal packing within these films. Similar result was obtained by cryoelectron microscopy [355]: the micrographs of vitrified stratifying films containing latex particles (144 nm in diameter) showed well ordered two-dimensional particle array. These results suggest that smaller particles like micelles (exhibiting more intensive Brownian motion and interacting by relatively "soft" screened Coulomb potential) form less ordered structure within the stratifying film. On the contrary, larger particles, interacting like hard spheres, are expected to form colloid-crystal like structure within the films.
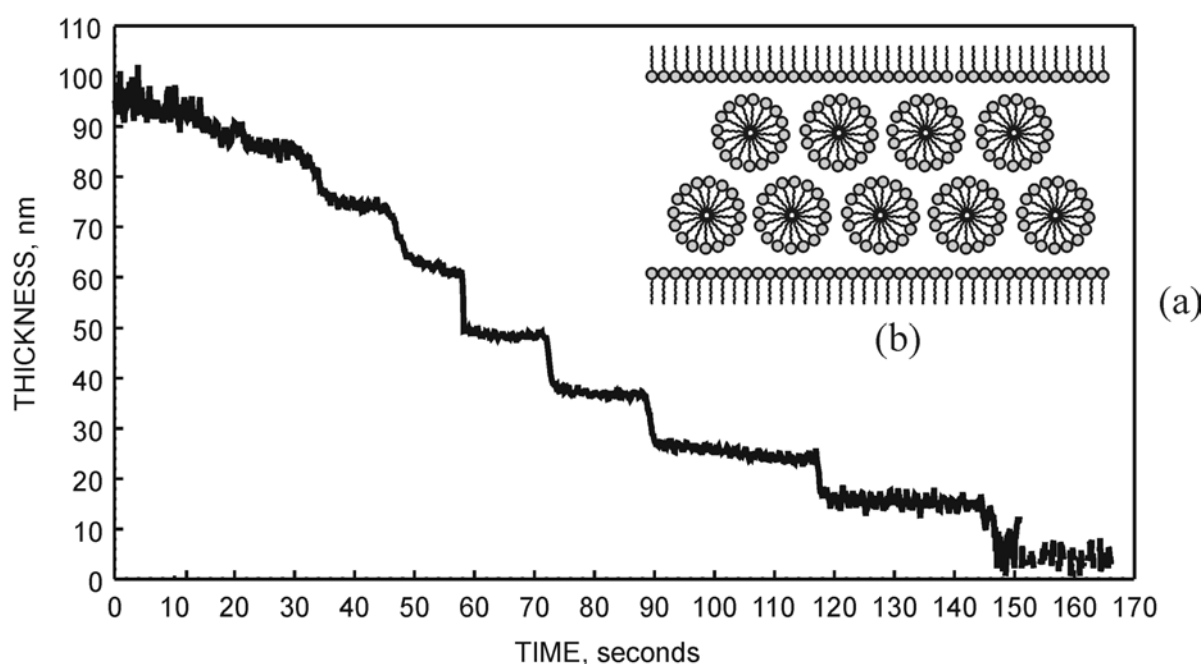
**Fig. 25.** (a) Experimental curve (from Ref. 374) showing the decrease of the thickness, *h*, of an emulsion film with time. The film is formed from 33.5 mM aqueous solution of sodium nonylphenol polyoxyethylene-25 sulfate with 0.1 M NaCl added. The "steps" of the curve represent metastable states corresponding to different number of micelle layers inside the film. (b) Sketch of a film containing two micelle layers.

C.2 Physical origin of the oscillatory structural forces

In general, oscillatory structural forces appear in two cases: (i) in thin films of pure solvent between two smooth *solid* surfaces; (ii) in thin liquid films containing colloidal particles (including macromolecules and surfactant micelles). In the first case, the oscillatory forces are called the "solvation forces" [4, 357]; they could be important for the short-range interactions between solid particles in dispersions. In the second case, the structural forces affect the stability of foam and emulsion films as well as the flocculation processes in various colloids. At higher particle concentrations the structural forces stabilize the liquid films and colloids [280, 281]. At lower particle concentrations the structural forces degenerate into the so called *depletion attraction*, which is found to destabilize various dispersions [358, 359].

In all cases, the oscillatory structural forces appear when monodisperse spherical (in some cases ellipsoidal or cylindrical) particles are confined between the two surfaces of a thin film. Even one "hard wall" can induce ordering among the neighboring molecules. The oscillatory structural force is a result of overlap of the structured zones at two approaching surfaces [360-363].

It is worthwhile noting that the wall can induce structuring in the neighboring fluid only if the magnitude of the surface roughness is negligible compared with the particle diameter, *d*. Indeed, when surface irregularities are present, the oscillations are smeared out and oscillatory structural force does not appear. If the film surfaces are fluid, the role of the surface roughness is played by the interfacial fluctuation capillary waves, whose amplitude (usually between 1 and 5 Å) is comparable with the diameter of the solvent molecules. In order for structural forces to be observed in foam or emulsion films, the diameter of the colloidal particles must be much larger than the amplitude of the surface corrugations.

The period of the oscillations is close to the particle diameter [4, 350, 352]. In this respect the structural forces are appropriately called the "volume exclusion forces" by Henderson [364], who derived an explicit (though rather complex) formula for calculating these forces. Numerical simulations [365, 366] and density-functional modeling [367] of the step-wise thinning of foam films are also available.

Recently, a semiempirical formula for the oscillatory structural component of disjoining pressure was proposed [368]

$$
\begin{aligned}
\Pi_{osc}(h) &= P_0 \cos\left(\frac{2\pi h}{d_1}\right) \exp\left(\frac{d^3}{d_1^2 d_2} - \frac{h}{d_2}\right) \quad \text{for } h > d \\
&= -P_0 \qquad\qquad\qquad\qquad\qquad\qquad\quad \text{for } 0 < h < d
\end{aligned}
\tag{221}
$$

where d is the diameter of the hard spheres, d_1 and d_2 are the period and the decay length of the oscillations which are related to the particle volume fraction, φ, as follows [368]

$$\frac{d_1}{d} = \sqrt{\frac{2}{3}} + 0.237\,\Delta\varphi + 0.633(\Delta\varphi)^2 \; ; \qquad \frac{d_2}{d} = \frac{0.4866}{\Delta\varphi} - 0.420 \qquad (222)$$

Here $\Delta\varphi = \varphi_{max} - \varphi$ with $\varphi_{max} = \pi/(3\sqrt{2})$ being the value of φ at close packing. P_0 is the particle osmotic pressure determined by means of Carnahan-Starling formula [369]

$$P_0 = nkT\,\frac{1 + \varphi + \varphi^2 - \varphi^3}{(1-\varphi)^3}, \qquad n = \frac{6\varphi}{\pi d^3}, \qquad (223)$$

where n is the particle number density. For $h < d$, when the particles are expelled from the slit into the neighboring bulk suspension, Eq. (221) describes the so called *depletion attraction*. On the other hand, for $h > d$ the structural disjoining pressure oscillates around P_0 (defined by Eq. 223) in agreement with the finding of Kjellander and Sarman [370]. The finite discontinuity of Π_{osc} at $h = d$ is not surprising as, at this point, the interaction is switched over from oscillatory to depletion regime. As demonstrated in Ref. [368], the quantitative predictions of Eq. (221) compare well with the Henderson theory [364] as well as with numerical results of Mitchell *et al.* [371], Karlström [372], Kjellander and Sarman [370].

It is interesting to note that in oscillatory regime the concentration dependence of Π_{osc} is dominated by the decay length d_2 in the exponent, cf. Eq. (222). Roughly speaking, for a given distance h the oscillatory disjoining pressure Π_{osc} increases five times when φ is increased with 10%, see Ref. [368].

The contribution of the oscillatory structural forces to the interaction free energy per unit area of the film can be obtained by integrating Π_{osc}:

$$
\begin{aligned}
f_{osc}(h) &= \int_h^\infty \Pi_{os}(h')dh' = F(h) && \text{for } h \geq d \\
&= F(d) - P_0(d-h) && \text{for } 0 \leq h \leq d
\end{aligned}
\qquad (224)
$$

$$F(h) \equiv \frac{P_0 d_1 \exp\left[(d^3/d_1^2 d_2) - (h/d_2)\right]}{4\pi^2 + (d_1/d_2)^2}\left[\frac{d_1}{d_2}\cos\left(\frac{2\pi h}{d_1}\right) - 2\pi\sin\left(\frac{2\pi h}{d_2}\right)\right]$$

C.3. Comparison between theory and experiment

It should be noted that Eqs. (221) and (224) refer to hard spheres of diameter d. In practice, however, the interparticle potential can be "soft" because of the action of some long-

range forces. If such is the case, one can obtain an estimate of the structural force by introducing an effective hard core diameter [352]

$$d(T) = \left[\frac{3}{4\pi} \beta_2(T) \right]^{1/3}, \qquad (225)$$

where β_2 is the second virial coefficient in the virial expansion of the particle osmotic pressure: $P_{osm}/(nkT) = 1 + \beta_2 n/2 + ...$ In the case of charged particles, like ionic surfactant micelles, the following approximate expression can be also used [350]

$$d = d_{\mathrm{H}} + 2\kappa^{-1} \qquad (226)$$

where d_{H} is the hydrodynamic diameter of the particle, determined, say, by dynamic light scattering. It was found [350, 368] that Eq. (226) compares well with the experimental data for stratifying films.

Two pronounced effects with stratifying films deserve to be mentioned. (i) The increase of electrolyte concentration leads to smoother and faster thinning of the foam films from *ionic* surfactant solutions. When the electrolyte concentration becomes high enough, the step-wise transitions disappear. This can be explained by suppression of the oscillatory structural forces due to decrease of the effective micelle volume fraction because of shrinkage of the counterion atmospheres [350]; (ii) In the case of *nonionic* surfactant micelles the *increase* of temperature leads to a similar effect: disappearance of the step-wise character of the film thinning [352]. This can be attributed to the change of the intermicellar interaction from repulsive to attractive with the increase of temperature [373]. The electrolyte and temperature dependence of the colloid structural forces provides a tool for control of the stability of dispersions.

As an illustration let us consider experimental data [374] for micellar solutions of the ionic surfactant *sodium nonylphenol polyoxyethylene-25 sulfate* (SNP-25S) at concentration 3.35×10^{-2} M. The step-wise thinning of a film formed from such a micellar solution is shown in Fig. 25. Comparative experiments with 0.1 M added NaCl and without any added NaCl have been carried out. From the experimental number concentration of the micelles, n, their effective diameter and volume fraction, φ, have been calculated by means of Eqs. (223) and (226).

Table 3. Data for stratifying films stabilized by SNP-25S at concentration 3.35×10^{-2} M.

C_{el} M NaCl	φ	d nm	d_1 nm	d_2 nm	f_{el} (10^{-3} erg /cm^2)	f_{vw} (10^{-3} erg /cm^2)	f_{osc} (10^{-3} erg /cm^2)	θ theory deg	θ experim. deg
0.1	0.18	7.7	8.8	3.5	0.03	-0.40	-1.99	1.02	1.0±0.04
0	0.38	9.8	9.7	9.1	15.47	-0.37	-23.51	1.92	1.89±0.08

The calculated values of φ and d are listed in Table 3 One sees that the addition of 0.1 M electrolyte (NaCl) decreases the volume fraction of the micelles from 0.38 to 0.18 due to the shrinkage of the micelle counterion atmospheres. The period and decay length of the oscillations, d_1 and d_2, are calculated from Eq. (222); one sees that d_2 is markedly lower than d_1 and d for the lower volume fraction $\varphi = 0.18$. The electrostatic and van der Waals surface free energies, f_{el} and f_{vw}, are calculated by means of Eqs. (187) and (204) with $A_H = 5 \times 10^{-21}$ J and area per surface charge 76 Å^2, whereas, the oscillatory free energy, f_{osc}, is determined from Eq. (224). For that purpose, the experimental (interferometric) thickness of films containing *one layer* of surfactant micelles have been used; corrections for the thickness of the two surfactant adsorption monolayers are taken into account when calculating f_{el} and f_{osc}. The experimental values of the contact angle, θ, of the respective films are also shown in Table 3. The theoretical values of θ are calculated by means of Eq. (161), where

$$f = f_{el} + f_{vw} + f_{osc} \tag{227}$$

is substituted ($\sigma = 7.5$ mN/m). One sees that the theoretical and the experimental values of θ coincide in the framework of the experimental accuracy [374]. The theoretical plot of f_{osc} vs. h calculated by means of Eq. (224) with the parameters values taken from Table 3 is shown in Fig. 26. Note that the experimental thickness of the film containing one layer of surfactant micelles corresponds to the first minimum of f_{osc} (that at $h \approx 12$ nm in Fig. 26). In general, the *metastable* states of the film (the steps in Fig. 25) correspond (approximately) to the *minima* of f vs h curve.

The numerical results in Table 3 and Fig. 26 call for some discussion. First, one sees that the contribution of the oscillatory structural force, f_{osc}, to the total surface free energy, f, is the greatest one, cf. Eq. (227). Moreover, the magnitude of f_{osc} (the depth of the first minimum in Fig. 26) increases with the decrease of the electrolyte concentration because of

the increase of the micelle effective volume fraction φ. As a result, the contact angle, θ, increases with the decrease of electrolyte concentration. This tendency is exactly the opposite to that in the absence of micelles, when oscillatory structural forces are missing.
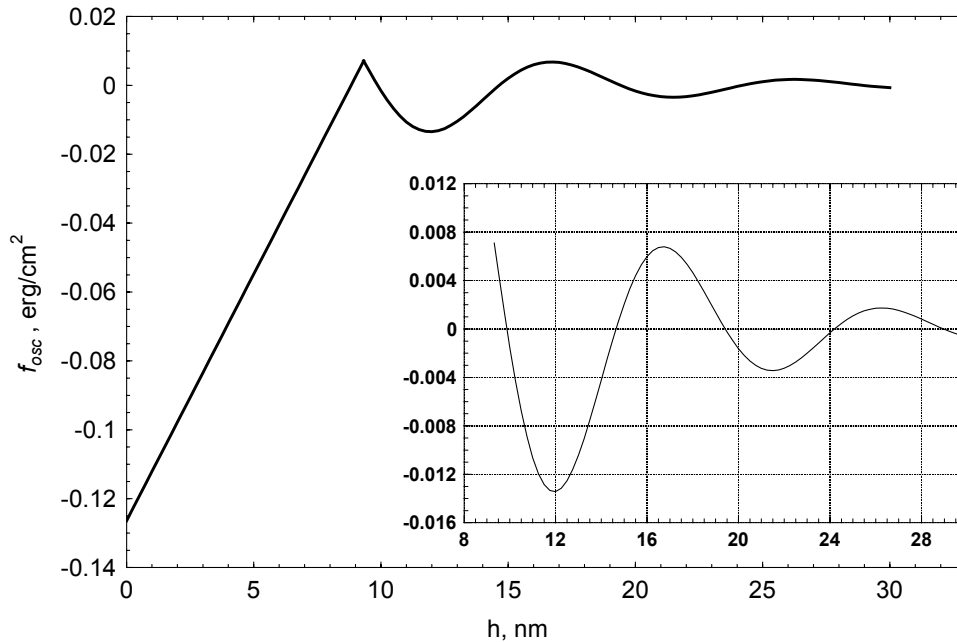

Fig. 26. Plot of the oscillatory free energy, f_{osc}, vs. the film thickness, h, calculated from Eq. (224) with the parameters values from Table 3 for SNP-25S micelles: $\varphi = 0.32$, $d = 9.3$ nm, $d_1 = 9.5$ nm and $d_2 = 7.0$ nm. The inset shows the region 8 nm $< h <$ 28 nm in an enlarged scale.

C.4. Depletion interaction

With the decrease of particle (micelle) volume fraction φ the amplitude of the oscillations (Fig. 26) decreases and the oscillatory structural force degenerates into the depletion interaction. The latter interaction manifested itself in the experiments by Bondy [375], who observed coagulation of rubber latex in presence of polymer molecules in the disperse medium. Asakura and Oosawa [358] published a theory, which attributed the observed interparticle attraction to the overlap of the depletion layers at the surfaces of two approaching colloidal particles - see Fig. 27. The centers of the smaller particles, of diameter, d, cannot approach the surface of a bigger particle (of diameter D) at a distance shorter than $d/2$, which is the thickness of the depletion layer. When the two depletion layers overlap (Fig. 27) some volume between the large particles becomes inaccessible for the smaller particles. This gives rise to an osmotic pressure, which tends to suck out the solvent between the bigger particles thus forcing them against each other. The total depletion force experienced by one of the bigger particles is [358]

$$F_{dep} = -kTnS(h_0) \qquad (228)$$

where the effective depletion area is

$$S(h_0) = \frac{\pi}{4}(2D + d + h_0)(d - h_0) \qquad \text{for } 0 \le h_0 \le d$$

$$S(h_0) = 0 \qquad \text{for } d \le h_0 \qquad (229)$$
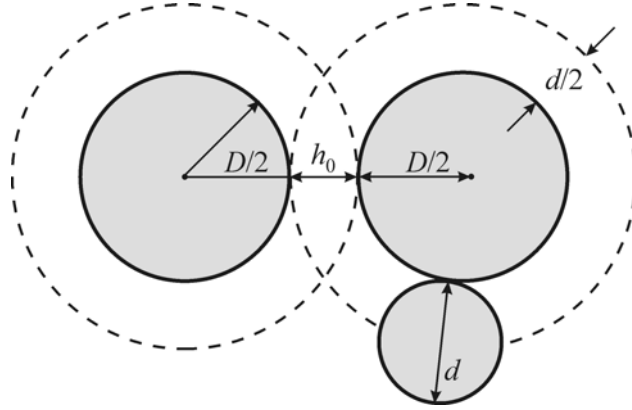
Fig. 27. Overlap of the depletion zones around two particles of diameter D separated at a surface-to-surface distance h_0; the smaller particles have diameter d.

Here h_0 is the shortest distance between the surfaces of the larger particles and n is the number density of the smaller particles. By integrating Eq. (228) one can derive an expression for the depletion interaction energy between the two larger particles, $U_{dep}(h_0)$. For $D \gg d$ this expression reads

$$U_{dep}(h_0)/kT \approx -\frac{3}{2}\varphi\frac{D}{d^3}(d - h_0)^2 \qquad 0 \le h_0 \le d \qquad (230)$$

where $\varphi = \pi n d^3/6$ is the volume fraction of the small particles. The maximum value of U_{dep} at $h_0 = 0$ is $U_{dep}(0)/kT \approx -3\varphi D/(2d)$. For example, if $D/d = 50$ and $\varphi = 0.1$, then $U_{dep}(0) = -7.5kT$. This depletion attraction turns out to be large enough to cause flocculation in dispersions. De Hek and Vrij [359]studied systematically the flocculation of sterically stabilized silica suspensions in cyclohexane, induced by polystyrene molecules. Patel and Russel [376] investigated the phase separation and rheology of aqueous polystyrene latex suspensions in the presence of polymer (Dextran T-500). The stability of dispersions is often determined by the competition between electrostatic repulsion and depletion attraction [377]. An interplay of steric repulsion and depletion attraction was studied theoretically by van Lent *et al.* [378] for the case of polymer solution between two surfaces coated with anchored polymer layers. Joanny *et al.* [379] and Russel *et al.* [284] re-examined the theory of depletion interaction by

taking into account the internal degrees of freedom of the polymer molecules; their analysis confirmed the earlier results of Asakura and Oosawa [358].

In the case of plane-parallel films the depletion component of disjoining pressure is

$$\Pi_{dep}(h) = -P_0 \quad h < d$$
$$\Pi_{dep}(h) = 0 \qquad h > d$$

(231)

which is a special case of Eq. (221) for small d_2. Evans and Needham [380] succeeded to measure the depletion energy of two interacting bilayer surfaces in a concentrated Dextran solution; their results confirm the validity of Eq. (231).

The depletion interaction is present always when a film is formed from micellar surfactant solution; the micelles play the role of the smaller particles. At higher micellar concentrations the volume exclusion interaction becomes more complicated: it follows the oscillatory curve depicted in Fig. 26. In this case only the region of the small thickness (the linear portion for $0 < h < d$ in Fig. 26) corresponds to the conventional depletion force.

D. Steric Polymer Adsorption Force

Steric interaction can be observed in foam or emulsion films stabilized with nonionic surfactants, or with various polymers, including proteins. The nonionic surfactants molecules are anchored (grafted) to the liquid interface by their hydrophobic moieties (Fig. 28a).
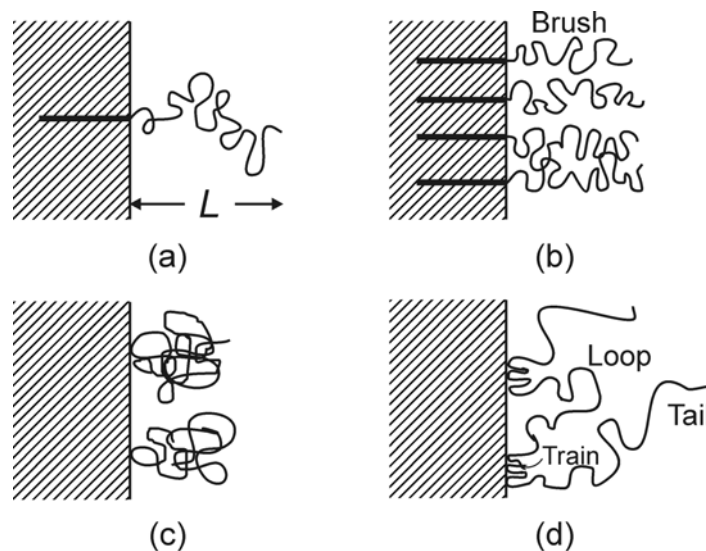

Fig. 28. Polymeric chains adsorbed at an interface: (a) terminally anchored polymer chain of mean end-to-end distance L; (b) a "brush" of anchored chains; (c) adsorbed (but not anchored) polymer coils; (d) complex conformation of an adsorbed polymeric molecule: "loops", "tails" and "trains" are formed.

When two such surfaces approach each other the following effects take place [4, 381-383]: (1) The entropy decreases due to the confining of the dangling chains which results in a repulsive osmotic force known as "*steric*" or "*overlap*" *repulsion*. (2) In a poor solvent the segments of the chain molecules attract each other; hence the overlap of the two approaching layers of polymer molecules will be accompanied with some intersegment *attraction*; the latter can prevail for small overlap, however at the distance of larger overlap it becomes negligible compared with the osmotic repulsion. (3) Each polymeric chain in an adsorption monolayer (brush), see Fig. 28b, is subjected to an elastic stress (extension) because of the repulsive interactions with the chains of neighboring molecules in the brush. This elastic stress can be partially released when two such monolayers are pressed against each other in a thin film; this brings about an effective attractive contribution to the steric surface force.

D.1. Adsorption of polymeric molecules

Adsorbed polymeric molecules may form not only brushes (Fig. 28b), but coils of macromolecules, like proteins, which can also adsorb at a liquid surface - Fig. 28c. Sometimes the configurations of the adsorbed polymers are very different from the statistical coil: loops, trains and tails can be distinguished (Fig. 28d).

The osmotic pressure of either dilute or concentrated polymer solutions can be expressed in the form [384]

$$\frac{P_{osm}}{n\,k\,T} = \frac{1}{N} + \frac{1}{2}n\,v + \frac{1}{3}n^2\,w + \dots \qquad (232)$$

Here N is the number of segments in the polymer chain, n is the number segment density, v and w account for the pair and triplet interactions between segments. In fact v and w are counterparts of the second and third virial coefficients in the theory of non-ideal gases [12]. v and w can be calculated if information about the polymer chain and the solvent is available [284]

$$w^{1/2} = \bar{v}\,m\,/\,N_A\,, \qquad v = w^{1/2}\left(1 - 2\chi\right), \qquad (233)$$

where $\bar{v}$ (m^3/kg) is the specific volume per segment, m (kg/mol) is the molecular weight per segment, N_A is the Avogadro number and χ is the Flory parameter. The latter depends on both the temperature and the energy of solvent-segment interaction. Then v can be zero (cf. Eq. 233) for some special temperature, called the *theta temperature*. The solvent at theta temperature is known as *theta solvent* or *ideal solvent*. At the theta temperature the intermolecular (intersegment) attraction and repulsion in polymer solutions are exactly counterbalanced. In a *good solvent*, however, the repulsion due mainly to the excluded volume effect dominates the attraction and $v > 0$. In contrast, in a *poor solvent* the intersegment attraction prevails, so $v < 0$.

The steric interaction between two approaching surfaces appears when the film thickness becomes of the order of, or smaller than $2L$ where L is the mean-square end-to-end

distance of the hydrophilic portion of the chain. If the chain were entirely extended, then L would be equal to Nl with l being the length of a segment. However, due to the Brownian motion $L < Nl$. For an anchored chain, like that depicted in Fig. 28a, in a theta solvent L can be estimated as [284]

$$L \approx L_0 \equiv l\sqrt{N} \tag{234}$$

In a *good solvent* $L > L_0$, whereas in a *poor solvent* $L < L_0$. In addition, L depends on the surface concentration, Γ, of the adsorbed chains, i.e. L is different for an isolated molecule and for a brush - cf. Figs. 28a and 28b. The mean field approach [284, 385] applied to polymer solutions provides the following equation for calculating L

$$\tilde{L}^3 - \left(1 + \frac{1}{9}\tilde{\Gamma}^2\right)\tilde{L}^{-1} = \frac{1}{6}\tilde{v} \tag{235}$$

where $\tilde{L}, \tilde{\Gamma}$ and $\tilde{v}$ are the dimensionless values of L, Γ and v defined as follows:

$$\tilde{L} = L/\left(l\sqrt{N}\right), \quad \tilde{\Gamma} = \Gamma N\sqrt{w}/l, \quad \tilde{v} = v\Gamma N^{3/2}/l \tag{236}$$

For an isolated adsorbed molecule $\left(\tilde{\Gamma} = 0\right)$ in an ideal solvent $\left(\tilde{v} = 0\right)$ Eq. (235) predicts $\tilde{L} = 1$, i.e. $L = L_0$.

D.2. Interaction of two polymeric adsorption monolayers

Dolan and Edwards [386] calculated the steric interaction free energy per unit area, f_{st}, for two polymeric adsorption monolayers (Fig. 28b) in a *theta solvent* as a function of the film thickness, h,:

$$f_{st}(h) = \Gamma kT\left[\frac{\pi^2}{3}\frac{L_0^2}{h^2} - \ln\left(\frac{8\pi}{3}\frac{L_0^2}{h^2}\right)\right] \qquad \text{for } h < L_0\sqrt{3} \tag{237}$$

$$f_{st}(h) = 4\Gamma kT\exp\left(-\frac{3h^2}{2L_0^2}\right) \qquad \text{for } h > L_0\sqrt{3} \tag{238}$$

where L_0 is the end-to-end distance as defined by Eq. (234). The boundary between the power-law regime ($f_{st} \propto 1/h^2$) and the exponential decay regime is at $h = L_0\sqrt{3} \approx 1.7L_0$, the latter being slightly less than $2L_0$ which is the intuitively expected beginning of the steric overlap. The first term in the right-hand side of Eq. (237) comes from the osmotic repulsion between the brushes, which opposes the approach of the two surfaces; the second term is negative and accounts effectively for the decrease of the elastic energy of the initially extended chains with the decrease of the film thickness, h.

In the case of a *good solvent* the disjoining pressure $\Pi_{st} = -df_{st}/dh$ can be calculated by means of Alexander-de Gennes theory [387, 388] as

$$\Pi_{st}(h) = kT\Gamma^{3/2}\left[\left(\frac{2L_g}{h}\right)^{9/4} - \left(\frac{h}{2L_g}\right)^{3/4}\right] \quad \text{for } h < 2L_g; \ L_g = N\left(\Gamma l^5\right)^{1/3} \tag{239}$$

where L_g is the thickness of a brush in a good solvent [389]. The positive and the negative terms in the right-hand side of Eq. (239) correspond to osmotic repulsion and elastic

attraction. The validity of Alexander-de Gennes theory was experimentally confirmed by Taunton *et al.* [390] who measured the forces between two brush layers grafted on the surfaces of two crossed mica cylinders.

Claesson *et al.* [373] studied the effect of temperature on the interaction between monolayers of the nonionic surfactant $C_{12}E_5$. These authors observed that the f_{St} vs. h curves exhibit a minimum related to attraction, whose depth increases with the increase of temperature (Fig. 29). Most probably this is an effect of the intersegment attraction of hydrophobic origin, which cannot be described by the Alexander-de Gennes theory. Theories applicable to this case are reviewed by Russel *et al.* [284].

In the case of adsorbed molecules, like these in Figs. 28c and 28d, which are not anchored to the surface, the measured surface forces can depend on the rate of approaching of the two surfaces [391, 392]. The latter effect can be attributed to the comparatively low rate of exchange of polymer between the adsorption layer and the bulk solution. This leads to a hysteresis of the surface force: different interaction on approach and separation of the two surfaces [4]. In the case of more complicated configuration of the adsorbed polymers (Fig. 28d) one can observe two regimes of steric repulsion: (1) weaker repulsion at larger separations due to the overlap of the *tails* and (2) stronger repulsion at smaller separations indicating overlap of the *loops* [393].
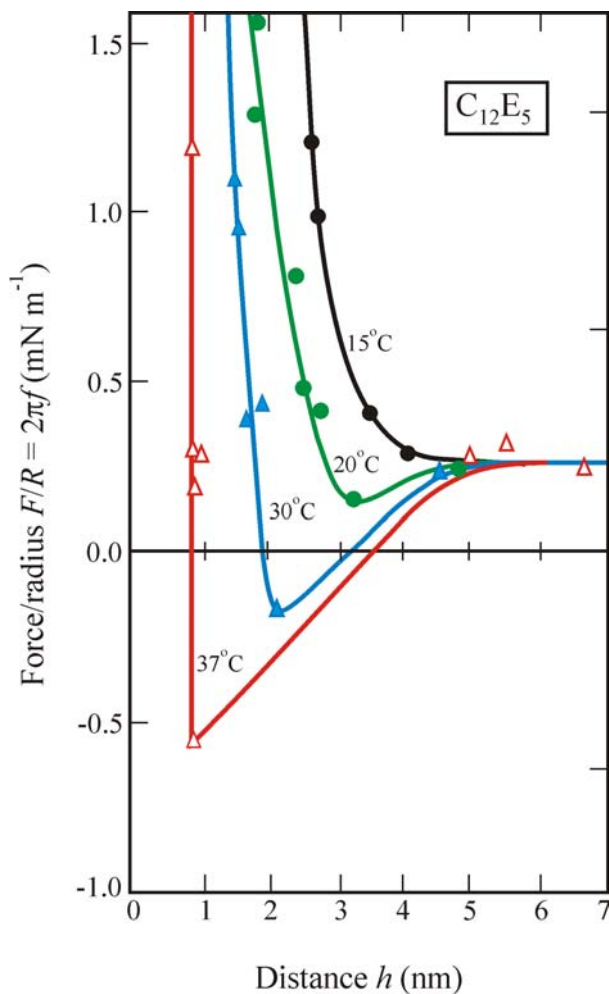

Fig. 29. Plot of experimental data for measured forces, $F/R \equiv 2\pi f$ vs. h, between two surfaces covered by adsorption monolayers of the nonionic surfactant $C_{12}E_5$ for various temperatures. The appearance of minima on the curves indicate that the water becomes a poor solvent for the polyoxyethylene chains with the increase of temperature (from Claesson et al., [373]).

E. Fluctuation Wave Forces

The adsorption monolayers at fluid interfaces and the bilayers of amphiphilic molecules in solution (lipid membranes, surfactant lamellas) are involved in a thermal fluctuation wave motion. The configurational confinement of such thermally exited modes within the narrow space between two approaching interfaces gives rise to short-range repulsive surface forces, which are briefly presented below.

E.1. Protrusion force

Due to the thermal motion the protrusion of an amphiphilic molecule from an adsorption monolayer (or micelle) may fluctuate about the equilibrium position of the molecule, Fig. 30a. In other words, the adsorbed molecules are involved in a *discrete* wave motion, which differs from the *continuous* modes of deformation considered in sections E.2 and E.3 below. Aniansson *et al.* [394, 395] analyzed the energy of protrusion in relation to the micelle kinetics. These authors assumed energy of molecular protrusion of the form $u(z) = \alpha z$, where z is the distance out of the surface ($z > 0$); they determined $\alpha \approx 3 \times 10^{-11}$ J/m for single-chained surfactants.
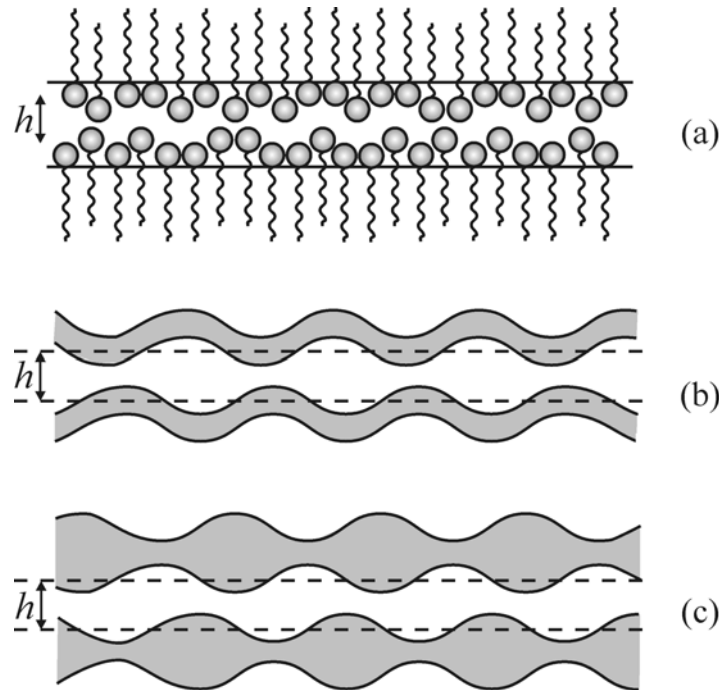
**Fig. 30.** Surface forces due to configurational confinement of thermally exited modes into a narrow region between two approaching interfaces: (a) fluctuating protrusion of adsorbed amphiphilic molecules gives rise to the *protrusion* surface force; (b) bending mode of membrane fluctuations gives rise to the *undulation* force; (c) squeezing (peristaltic) mode of membrane fluctuations gives rise to the *peristaltic* force.

By using a mean-field approach Israelachvili and Wennerström [317] derived the following expression for the protrusion disjoining pressure which appears when two protrusion zones overlap (Fig. 30a):

$$\Pi_{protr}(h) = \frac{\Gamma\alpha(h/\lambda)\exp(-h/\lambda)}{1-(1+h/\lambda)\exp(-h/\lambda)}, \quad \lambda \equiv \frac{kT}{\alpha}. \tag{240}$$

λ has the meaning of protrusion decay length; $\lambda = 0.14$ nm at 25°C; Γ denotes the number of protrusion sites per unit area. Note that Π_{protr} decays exponentially for $h \gg \lambda$, but $\Pi_{protr} \propto h^{-1}$ for $h < \lambda$, i.e. Π_{protr} is divergent at $h \to 0$.

E.2. Undulation force

The undulation force arises from the configurational confinement related to the *bending mode* of deformation of two fluid bilayers, like surfactant lamellas or lipid membranes. This mode consists in undulation of the bilayer thickness and constant area of the bilayer midsurface, Fig. 30b. Helfrich *et al.* [396, 397] established that two such bilayers, at a mean surface-to-surface distance h apart, experience a repulsive disjoining pressure given by the expression

$$\Pi_{und}(h) = \frac{3\pi^2(kT)^2}{64 k_t h^3} \tag{241}$$

where k_t is the bending elastic modulus of the bilayer as a whole. The experiment [398] and the theory [233] show that k_t is of the order of 10^{-19} J for lipid bilayers. The undulation force has been measured and the dependence $\Pi_{und} \propto h^{-3}$ confirmed experimentally [399-401].

E.3. Peristaltic force

Similar to the undulation force, a *peristaltic force* [317] can appear between two surfactant lamellas or lipid bilayers. It originates from the configurational confinement related to the peristaltic (squeezing) mode of deformation of a fluid bilayer, Fig. 30c. This mode of deformation consists in fluctuation of the bilayer thickness without bending of the bilayer midsurface. The peristaltic deformation is accompanied with extension of the bilayer surfaces. Israelachvili and Wennerstöm [317] demonstrated that the peristaltic disjoining pressure is related with the stretching modulus, k_S, of the bilayer:

$$\Pi_{per}(h) \approx \frac{2(kT)^2}{\pi^2 k_s h^5} \tag{242}$$

The experiment [206] gives value of k_s varying between 135 and 500 mN/m depending on temperature and composition of the lipid membrane.

F. Surface Forces and Micelle Growth

As an illustration in the present section we consider the effect of the surface forces on the interactions between surfactant micelles and the growth of rod-like micelles in solution.

A useful experimental method, providing quantitative information for the micelle-micelle interactions (in not too concentrated solutions), is the static light scattering (SLS). As known, this method is based on the measurement of the concentration dependence of the scattered light and the solution refractive index [402, 403]. From the intensity of the scattered light the Rayleigh ratio, R_θ, is determined and the data are plotted in accordance with the Debye equation [402-404]

$$\frac{K_S c_{SM} M_1}{R_\theta} = 1 + 2 A_2 c_{SM} + ...; \quad K_S \equiv \frac{4\pi^2 n_0^2}{\lambda^4 N_A}\left(\frac{dn_r}{dc_{SM}}\right)^2 \tag{243}$$

where K_S is the so called optical constant of the solution, n_0 and n_r are the refractive indices of the pure solvent and the solution, λ is the light wavelength *in vacuo*, N_A is the Avogadro number, M_1 (g/mol) is the micelle mass, c_{SM} is the concentration of surfactant micelles in the solution; A_2 is the second virial coefficient. A_2 is *positive* when the micelles *repel* each other, whereas A_2 is *negative* when the *attractive* interaction between the micelles is predominant.

In Fig. 31 we present SLS data for micelles of ionic surfactant (sodium dodecyl dioxyethylene sulfate: SDP-2S) in the presence of added NaCl (the upper line) and mixture of NaCl and AlCl$_3$ (the lower line); in both cases the ionic strength of the solutions is the same, $I = 24$ mM. The surfactant concentration is small enough to have only small spherical micelles in the solution. The ratio

$$\xi = c_{SM}/(3 c_{Al}) \tag{244}$$

(c_{Al} is the concentration of Al^{3+}), is kept constant, $\xi = 1.15$, for the solution with AlCl$_3$. As seen in Figure 31, the presence of Al^{3+} ions inverts the sign of A_2 from positive to negative. In other words, the micelle-micelle interaction is repulsive in the presence of Na$^+$ counterions only, whereas it becomes attractive if Al^{3+} counterions are present. This can be attributed to the fact that the *ionic-correlation attraction* dominates over the *double layer repulsion* in the presence of divalent and trivalent counterions [336, 339]. SLS data with Mg^{2+} and Ca^{2+} (not shown in Figure 31) also give negative A_2, as it could be expected if the ionic correlations are the source of the attraction between the micelles. Note however, that at higher surfactant

concentrations the transition from spherical to elongated micelles could give an apparent negative value of A_2, which should not be attributed to micelle-micelle attractive interactions, such as van der Waals or the ionic correlation forces [404].
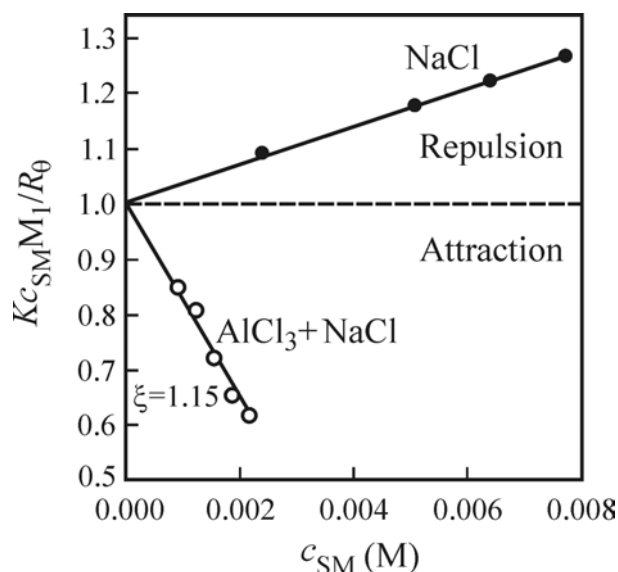
Fig. 31. Static light scattering data for SDP-2S micelles plotted in accordance with Eq (243). The full dots correspond to solutions with NaCl, whereas the empty dots are measured with mixtures of AlCl$_3$ and NaCl; the total ionic strength, $I = 24$ mM, is fixed.

As known, the spherical surfactant micelles undergo a transition to larger rod-like aggregates with the increase of surfactant concentration [4]. It was found out experimentally that the formation of rod-like micelles is enhanced by the addition of electrolyte and/or decreasing the temperature [405-413], as well as by increasing the length of the surfactant hydrocarbon chain [414-416]. It was recently established [417] that the presence of multivalent counterions (Ca^{2+}, Al^{3+}) in solutions of anionic surfactant (sodium dodecyl dioxyethylene sulfate) strongly enhances the formation of rod-like micelles. A qualitative explanation of this fact is that a multivalent counterion, say Al^{3+}, can bind together three surfactant headgroups at the micelle surface thus causing a decrease of the area per headgroup [417]. In accordance with the theory by Israelachvili et al. [4, 418] this will induce a transition from spherical to cylindrical micelles.

From a practical viewpoint it is important to note that the giant cylindrical micelles formed in the presence of Ca^{2+} and Al^{3+} exhibit a markedly larger solubilization efficiency than the common spherical micelles [417], see Figure 32. In other words, the same amount of surfactant solubilizes more oil when it is organized as large cylindrical (rather than small spherical) micelles. This finding could be employed in detergency. The light scattering experiments [417] reveal that in the process of solubilization the giant rod-like micelles

disassemble to smaller spherical swollen micelles (their hydrodynamic radius, R_h is also shown in Fig. 32). Therefore, it turns out that in this case the process of solubilization is a rather complex one.
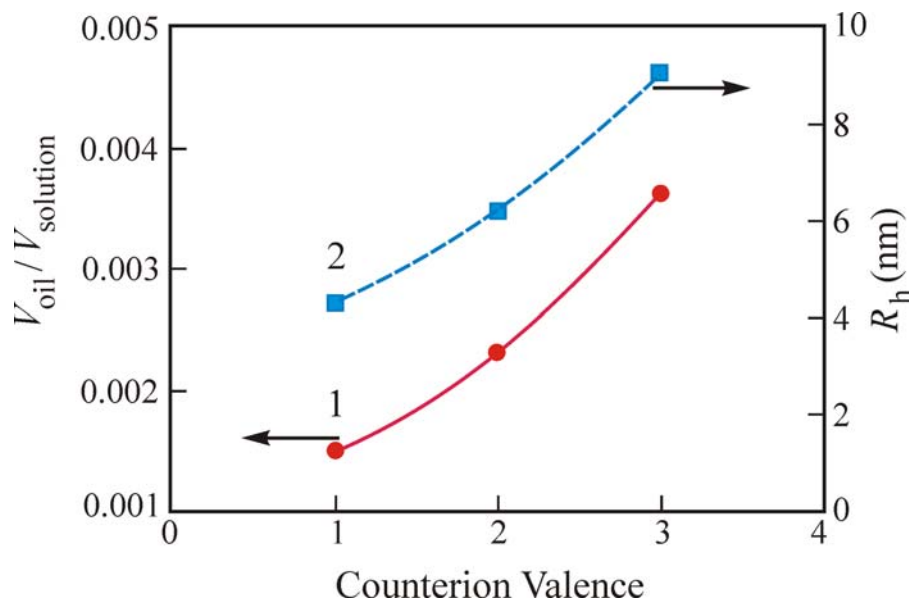
Fig. 32. Solubilisation of oil (di-isopropyl benzene) in 8 mM solution of SDP-2S in the presence of added electrolyte (NaCl, CaCl$_2$ or AlCl$_3$) of fixed ionic strength, $I = 24$ mM. The volume of solubilized oil per unit volume of solution, $V_{oil}/V_{solution}$, is plotted against the valence of the counterions (Na$^+$, Ca^{2+} or Al^{3+}). The measured apparent hydrodynamic radius of the swollen micelles, R_h, is also plotted vs the counterion valence.

VII. HYDRODYNAMIC FORCES IN THIN LIQUID FILMS

It is now generally recognized that the presence of surfactants plays an important role for the drainage velocity of thin liquid films and the hydrodynamic forces in these films. The surfactants change not only the disjoining pressure (see Section VI above), but also the tangential mobility of the interface of the droplet or bubble. This affects the flocculation and coalescence rate constants, which determine the rates of reversible and irreversible coagulation of the dispersions [419], and emulsions [420-422]. The role of the film properties for the foam stability is discussed in [267]. Depending on the behavior of the interdroplet film, two kinds of foam and emulsion stability can be distinguished: (i) thermodynamic stability governed by repulsive disjoining pressure, and (ii) kinetic stability affected by hydrodynamic and diffusion fluxes inside the film. These two types of stability are actually

interrelated and both are involved in the theoretical interpretation of the Bancroft rule [419,420,423-425,488].

When two colloidal particles come close to each other, they experience two types of forces. The first one, the *surface forces of intermolecular origin* (the disjoining pressure), which are due to the van der Waals, electrostatic, steric, etc. interactions, have been discussed in Section VI above. The second type represent the *hydrodynamic* forces which originate from the interplay of the hydrodynamic flows around two moving colloidal particles or two film surfaces. It becomes important when the separation between the particle surfaces is of the order of the particle radius and increases rapidly with the decrease of the gap width.

The simultaneous action of disjoining pressure and hydrodynamic forces determines the stages of the formation and evolution of a liquid film of fluid surfaces [5,426]:

(i) Two slightly deformed fluid particles approach each other (see Fig. 33a and Section VII.A).

(ii) Dimple is formed at a certain small separation between the fluid particles (see Fig. 33b and Section VII.B). The dimple initially grows, but latter becomes unstable and quickly outflows.

(iii) Then a plane-parallel film of radius R and typical thickness from 15 to 200 nm forms (see Fig. 33c and Section VII.C). When the long range repulsive forces are strong, an equilibrium (but thermodynamically metastable) primary film forms, cf. point 1 in Fig. 17a. (This film is also called the common black film (CBF)).

(iv) The film surface corrugations, caused by thermal fluctuations or other disturbances, amplified by attractive disjoining pressure may increase their amplitude so much that the film either ruptures or a spot of thinner Newton black film (NBF) forms (see point 2 in Fig. 17b, Fig. 33d and Section VIII).

(v) If the short-range repulsive disjoining pressure is large enough the black spots (secondary films of very low thickness, $h_2 \approx 5 - 10$ nm) are stable. They either coalescence or grow in diameter, forming an equilibrium secondary (NBF) thin film (see Fig. 33e).

(vi) After the whole film area is occupied by the Newton black film, the equilibrium between the film and the meniscus is violated and the NBF expands until reaching its final equilibrium radius, R_{NBF}, corresponding to an equilibrium contact angle θ (see Fig. 33f). Sometimes no plane-parallel film forms, but instead the dimple persists until rupture or formation of NBF occurs. For more details - see part IV.C of ref. 267.
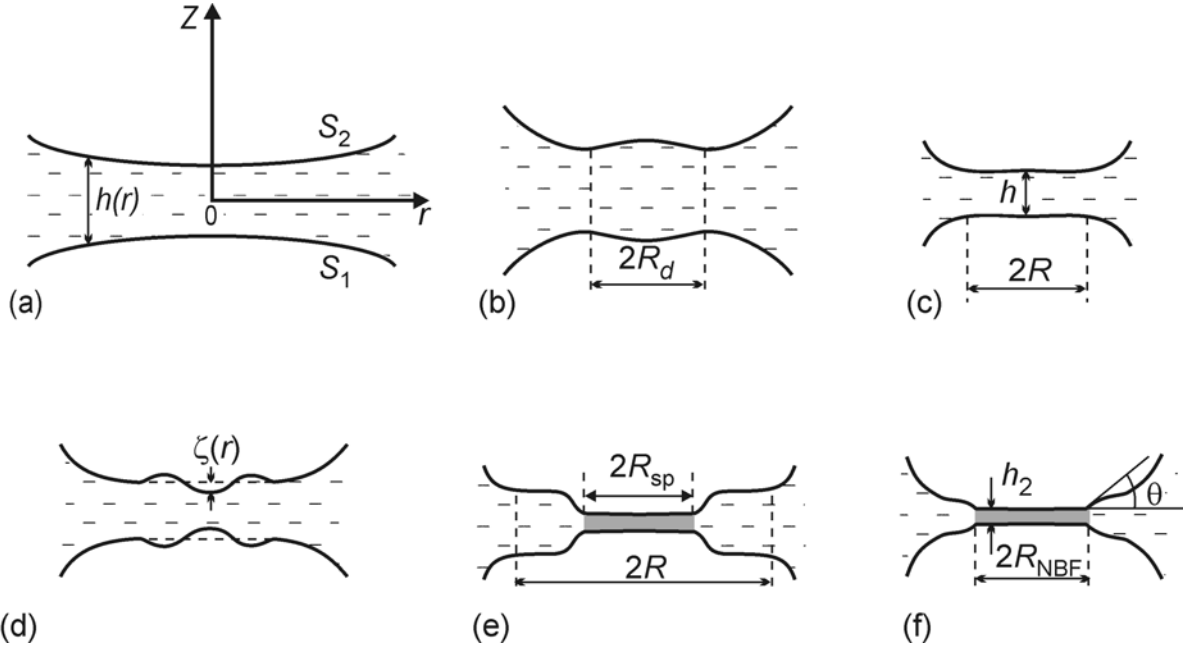
Fig. 33. Consecutive stages of evolution of a thin liquid film between two bubbles or drops: (a) mutual approach of slightly deformed surfaces; (b) the curvature at the film center inverts its sign and a "dimple" arises; (c) the dimple disappears and an almost plane-parallel film forms; (d) due to thermal fluctuations or other disturbances the film either ruptures or transforms into a thinner Newton black film (e) which expands until reaching the final equilibrium state (f).

A. Films of Uneven Thickness between Colliding Fluid Particles

For the sake of simplicity we will assume that the colloidal particles approach each other along their axes of symmetry (see Fig. 33a). The driving force can be the buoyancy, the Brownian force, etc. The hydrodynamic interaction is stronger in the front zones and leads to a weak deformation of the fluid particles (drops, bubbles) in this front region. The deformation is proportional to the hydrodynamic capillary number Ca = $\eta V R_c/(\sigma h)$, where V is the velocity of thinning, R_c is the particle radius, and h is the minimal distance between the particle surfaces.

When the surfactant is soluble only in the continuous (film) phase, the velocity of particle approach can be calculated from the following formula stemming from the lubrication approximation [5]:

$$V = V_{\mathrm{Ta}}\left(1 + \frac{3\eta D}{h_e E_G} + \frac{2\eta D_s}{h E_G}\right) \quad , \qquad V_{\mathrm{Ta}} = \frac{2Fh}{3\pi\eta R_c^2} \tag{245}$$

where $h_e \equiv (\partial \Gamma / \partial c)_e$ is the characteristic adsorption distance for a given equilibrium surfactant concentration (see Table 1), D_s is the surface diffusion coefficient of the surfactant (see Section III, Eq. 3.3), and V_{Ta} is the well known Taylor velocity [427] of approach of two non-deformable solid spheres under the action of an external force F. From Eq. (245) we can deduce that the velocity of particle approach, V, increases with the increase of the bulk and surface surfactant diffusivities, D and D_s, as well as with the decrease of the Gibbs elasticity, E_G, and the slope of the adsorption isotherm, $h_e \equiv (\partial \Gamma / \partial c)_e$. A more general treatment, valid for droplets of different radii and different interfacial properties, can be found in Ref. [428]. In emulsion systems, containing surfactant soluble in *both* continuous phase and the droplets, the velocity, V, depends on the surfactant distribution between the phases [429].

In the case of emulsion films with surfactant soluble *only* in the drop phase, the presence of surfactant does not influence the approach of the two film surfaces (the particles behave as droplets of *pure* liquid), see Section C.3 below. The approach of two *nondeformed*, spherical, drops or bubbles in *pure* liquid phases (in the absence of any surfactant) has been investigated by many authors [5,430-439]. All results show that the approaching velocity at small distances ($h/R_c \ll 1$) is much larger than that for solid spheres; it is proportional to the Taylor velocity, V_{Ta}, multiplied by factors larger than unity:

$$V / V_{\text{Ta}} = 0.75 R_c / \left[h \ln(R_c / h) \right] \qquad \text{for bubbles without surfactant [420],}$$

and

$$V / V_{\text{Ta}} = 0.811 \eta \sqrt{R_c} / \left(\eta_{dr} \sqrt{h} \right) \qquad \text{for droplets without surfactant [438];}$$

the viscosities of the droplets and of the medium are η_{dr} and η, respectively. It turns out that even small amount of surfactant soluble in the *continuous medium* decreases the approaching velocity by several orders of magnitude because the surfactant immobilizes the drop (bubble) surfaces and then $V \approx V_{\text{Ta}}$.

The shape of the gap between two pure liquid drops for different characteristic times is calculated numerically in Refs. [440,441]. Experimental investigations of these effects for symmetric and asymmetric drainage of foam films were carried out by Joye *et al*. [442,443]. In some special cases the deformation of the fluid particle can be very fast: for example, the bursting of a small air bubble at an air/water interface is accompanied by a complex motion resulting in the production of a high-speed liquid jet [444]. Unfortunately, in Refs. [440,441,444] the effect of surfactant is not investigated.

B. Inversion Thickness and Dimple Formation

At a given gap width the curvature in the middle of the film surfaces, at $r = 0$, changes its sign and the surfaces acquire a concave lens-shape form, called „dimple" [445] (see Fig. 33b). This stage is observed also for asymmetric films [443]. This stage is possible if the force acting on the fluid particles is high enough, so that the energy barrier, created by the increase of surface energy during the deformation, can be overcome [446]. For example, in the case of Brownian flocculation of small droplets at low electrolyte concentration such a dimple might not appear [446]. The parallel experiments [447] on the formation and thinning of emulsion films of macroscopic and microscopic areas, prepared in the Scheludko cell [448] and in a miniaturized cell, show that the patterns and the time scales of the film evolution in these two cases are significantly different. There is no dimple formation in the case of thin liquid films of small diameters [447]. Other effect of the quasistatic surface forces is the prevention of the dimple formation in the case of large van der Waals attraction [440] when a reverse bell-shape deformation appears and the film ruptures quickly.

There is a number of theoretical studies describing the development of a dimple at the initial stage of film thinning [442,443,449-452]. The distance at which the dimple forms is called the *inversion thickness* h_i. From Eq. (57) in the paper by Ivanov *et al*. [428] the following expression for h_i could be derived for the case when the surfactant is soluble only in the continuous phase:

$$h_i = \frac{F}{4\pi\sigma}\left[1+\left(1-\frac{4}{3}\frac{2\pi\sigma}{F}\frac{h_s}{1+b_s}\right)^{1/2}\right], \tag{246}$$

where the dimensionless parameter b_s and the characteristic surface diffusion thickness h_s are defined as

$$b_s \equiv \frac{3\eta D}{h_e E_G}, \quad h_s \equiv \frac{6\eta D_s}{E_G}; \qquad h_e \equiv \left(\partial\Gamma / \partial c\right)_e \tag{247}$$

From Eq. (246) it follows that the presence of surfactants in the continuous phase decreases the inversion thickness if we keep the interfacial tension, σ, and the exerted force, F, constant. For most surfactant solutions one has $b_s \ll 1$, and then only the surface diffusivity and Gibbs elasticity influence the inversion thickness. For large inversion thicknesses from Eq. (246) one can derive the following asymptotic equation

$$h_i \approx F / \left(2\pi\sigma\right),$$

which is valid also when the surfactant is soluble in the droplet phase.

With parameter values typical for foams, $\sigma = 30$ dyn/cm, and $R_c = 50$ μm, and with the buoyancy as driving force, from Eq. (246) one obtains $h_i = 14$ nm, which is an unrealistically small value. This means that the buoyancy force might be insufficient to explain the formation of films during the hydrodynamic interaction of two bubbles. Another outer force that can be important for the emulsion and foam stability is the hydrodynamic force in a shear or non-turbulent flows [461]. An attempt to treat the case of turbulence was performed by Kumar *et al*. [462,463]. For micron-size liquid droplets the Brownian force is still several orders of magnitude greater than the buoyancy force due to gravity. Following the scheme of Smoluchowski [464,465], Danov *et al*. [446] investigated the diffusion of deformable miniemulsion drops toward a given „central" drop by taking into account also the van der Waals attraction and the electrostatic repulsion. The total force acting on the particles is obtained as a sum of the Brownian (diffusion) force and the potential force, which is due to non-hydrodynamic interactions between the particles. The detailed solution leads to the calculation of the inversion thickness. These authors pointed out that: (i) the van der Waals attraction promotes the film formation, (ii) at bigger droplet radii the film formation is enhanced, (iii) the interfacial mobility does not influence significantly the inversion thickness, (iv) with the increase of the dimensions the role of the Brownian force decreases, but it is predominant over the buoyancy force at small particle dimensions. Therefore, the surfactants influence the inversion thickness only due to the change of the interfacial tension and the electrostatic interaction between the particles. Indeed, when the electrostatic repulsion is taken into account (Fig. 34), the inversion thickness decreases with the decrease of electrolyte concentration C_{el}. The points in Fig. 34 correspond to concentration at which the kinetic energy of the drops is not large enough to overcome the energy barrier accompanying the drop deformation, and the particles behave like non-deformable charged spheres.
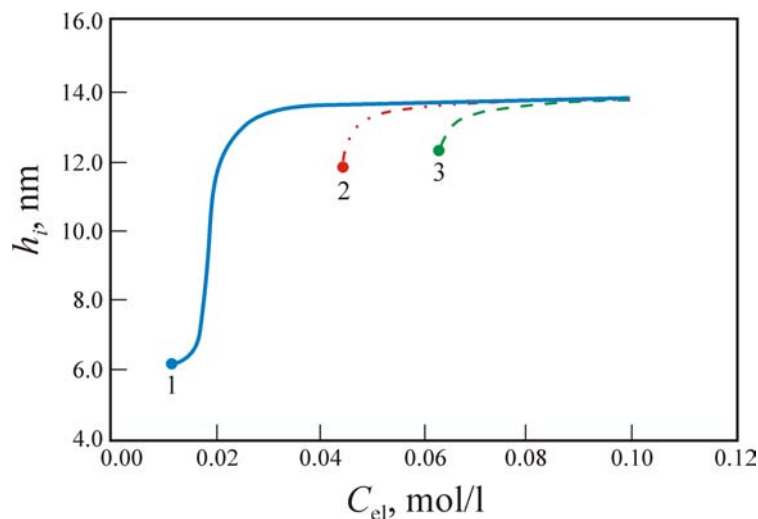
**Fig. 34.** Influence of the electrolyte concentration, C_{el}, on the inversion thickness, h_i. The physical parameters of the system are $A_H = 10^{-13}$ erg, $R_c = 5$ μm and $\sigma = 1$ dyn/cm. Curves 1, 2 and 3 correspond to $\psi_S = 50$ mV, $\psi_S = 25$ mV and $\psi_S = 10$ mV, respectively. The full points at the ends of the curves corresponds to concentrations, at which the drop deformation becomes important [446].

C. Effect of the Surfactant on the Rate of Film Thinning

After the dimple disappears the resulting almost plane-parallel film thins at constant radius R. The theoretical description of thin film drainage is based on the lubrication theory [59,466], in which the following assumptions are made: (i) the thickness of the film, h, is smaller than the film radius, R, and the film radius is smaller than the particle radius, R_c:

$$h^2 << R^2 << R_c^2,$$

and (ii) the Reynolds number, $\text{Re} = vh/v$ (where $V = -dh/dt$ is the velocity of film thinning, and v is the kinematic viscosity of the continuous phase), is small enough to neglect the convective term in the classical Navier-Stokes equation of the liquid motion in the film phase. The general solution of this problem in the film phase reads [5,267,419,420]

$$p = p_s(r,t), \quad u = \frac{1}{8\eta}\frac{\partial p_s}{\partial r}\left(z^2 - h^2\right) + u_s \tag{248}$$

where r and z are the cylindrical coordinates, the midplane of the film corresponds to $z = 0$, p and u are the pressure and the radial component of the velocity inside the film, and p_s and u_s are the corresponding pressure and the radial component of the velocity at the film surfaces. Equation (248) shows that the liquid motion in the film is a superposition of the flow with constant velocity profile, u_s (which corresponds to the interfacial mobility rate), and of the parabolic velocity profile (which represent the Poiseuille flow between tangentially immobile interfaces). In the droplet phase the pressure does not change in radial direction [5] and the velocity decreases (see Fig. 35).
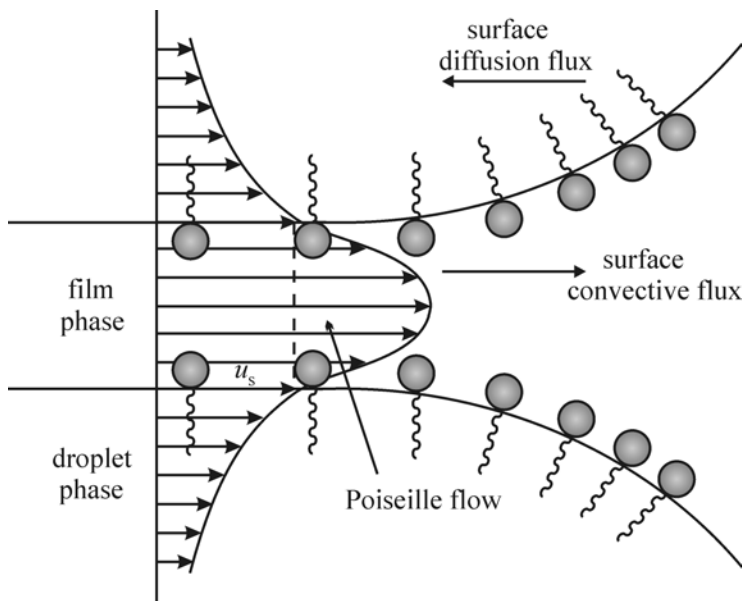

Fig. 35. Fluid motion in the film and droplet phases. The flow in the film phase is superposition of the Poiseuille flow and a flow of constant velocity u_s. Due to the nonuniform interfacial surfactant distribution surface diffusion and convective fluxes appear.

From the integral mass balance of the liquid in the film and the from the solution of Eq. (248), the equation for determining the local film thickness can be deduced [5,267]

$$\frac{\partial h}{\partial t} + \frac{1}{r}\frac{\partial}{\partial r}\left(rhu_s\right) = \frac{1}{r}\frac{\partial}{\partial r}\left(\frac{rh^3}{12\eta}\frac{\partial p_s}{\partial r}\right) \tag{249}$$

The generalization of the lubrication problem for a film between droplets of different radii was first solved by Ivanov $et\ al.$ [428]. In all systems of practical interest the Peclet number (Pe = Vh/D) is small enough to neglect the convective flux in the bulk diffusion equation, Eq. (18), for the continuous phase, which leads to slow dependence of the surfactant concentration inside the film on the z-coordinate. Thus the concentration throughout the film is close to that in the subsurface, $c \approx c_s(r,t)$; the latter depends on the interfacial adsorption mass balance expressed by Eqs. (20)-(22). Then if the surfactant is soluble only in the continuous phase the surface convective flux of surfactant is compensated only by the surface and the bulk diffusion fluxes:

$$\Gamma u_s = D_s \frac{\partial \Gamma}{\partial r} + \frac{hD}{2}\frac{\partial c_s}{\partial r} \tag{250}$$

Equations (249) and (250), along with the balance of the stresses on the interface, Eq. (80), and the adsorption isotherm or the kinetic rate expression (see Sections III.B and III.C), describe the influence of the surfactant on the film drainage. From Eq. (249) a generalization of the known formula of Charles and Mason [467] can be derived:

$$F = 6\pi\eta V \int_0^R \frac{r^3}{h^3}\left(1 - \frac{2h}{r}\frac{u_s}{V}\right)dr \tag{251}$$

It shows that as a rule the presence of surfactant decreases the interfacial mobility and decreases the velocity of thinning under the action on an outer force, F. The following particular cases are given in the literature: (i) tangentially immobile interfaces, (ii) partially immobilized interfaces, and (iii) completely mobile interfaces. These three cases are considered in Sections C.1 - C.3 below.

C.1. *Film surfaces immobilized by dense adsorption monolayers*

For surfactant concentrations close or above CMC the Gibbs elasticity and the interfacial viscosity are large enough to immobilize the interface, $u_s \approx 0$ (see refs. 5,58,267,420). Similar effect is observed when the droplet dynamic viscosity is much larger than the dynamic viscosity of the continuous phase (for example in the bitumen emulsions

η_{dr} is about 150 000 poises at room temperature). For the case of film with immobile surfaces from Eq. (251) on e can deduce the well known Reynolds formula [466], in which the disjoining pressure, Π, can be also included:

$$V_{\text{Re}} = \frac{2Fh^3}{3\pi\eta R^4} = \frac{2(P_c - \Pi)h^3}{3\eta R^2}$$ (252)

where $P_c = 2\sigma/R_c$ is the capillary pressure, and F is identified with $(P_c - \Pi)\pi R^2$. Therefore in such a case the surfactant influence on the film drainage is mainly due to the disjoining pressure: repulsive or attractive surface forces (see Section VI) can decrease or increase the velocity of thinning.

C.2. *Films of partially mobile surfaces: surfactant soluble in the film phase*

When the surfactants are soluble only in the film phase and their concentrations are below CMC, the solution of Eqs. (249)-(251), (80) reads [470,471]

$$\frac{V}{V_{\text{Re}}} = 1 + \frac{1}{\varepsilon_f} , \quad \frac{1}{\varepsilon_f} \equiv b_s + \frac{h_s}{h}$$ (253)

where ε_f is the so called *foam parameter*, and b_s and h_s are defined by Eq. (247). For film thickness of the order of h_s only the bulk diffusion affects the interfacial mass balance of surfactant. For surfactant concentrations, for which the Langmuir adsorption isotherm is obeyed, Ivanov and Dimitrov [5] reported the following values of these parameters: $h_s \approx 100$ nm and $b_s \ll 1$.

The negligible role of the bulk diffusion in thin films is due to the overlap of the diffusion layers at the two film interfaces. This leads to a more uniform surfactant distribution across the film and hence to a smaller concentration gradient and bulk diffusion flux. Under such conditions the *surface* diffusion becomes important. In the range of large concentrations the Gibbs elasticity, E_G, is high and $h_s \to 0$. For low molecular surfactants $b_s \to 0$ and $V \to V_{\text{Re}}$, but for organic solvents, especially at a liquid/liquid interface, saturated adsorption monolayers are usually not obtained [28], That is the reason why in such cases the surface diffusion will be dominant factor determining the film drainage all surfactant concentrations.

Expressions for the rate of thinning, similar to Eq.(253), which are valid for various ranges of values of the interfacial parameters, can be found in the literature [5,267,428,476,478]. The validity of the Eq. (253) was checked experimentally with several systems: $CH_3(CH_2)_3COOH$ in water [5,420,472], aniline films containing dodecanol

[5,420,473], and for more than fifty systems by Jeelany and Hartland [474]. A typical plot of V/V_{Re} vs. h^{-1} is shown in Fig. 36 for free nitrobenzene films stabilized by dodecanol. In agreement with Eq. (253), the dependence is linear and from the intersection point of the curves the surface diffusion coefficient was calculated to be $D_s = 7 \times 10^{-9}$ m^2/s. The latter value of D_s is comparable by magnitude with the values obtained by Teissie *et al.* [475], Vollhardt [476], and Feng [477] by means of various methods.
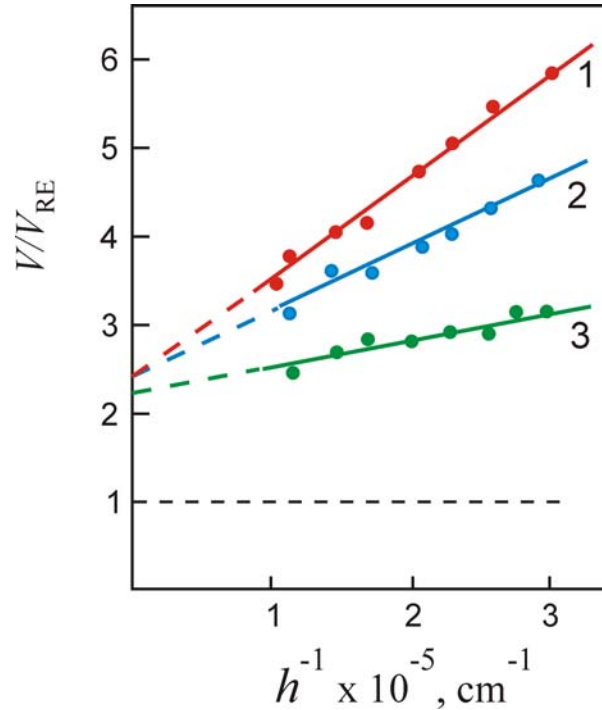
Fig. 36. A typical plot of V/V_{Re} vs. h^{-1} for nitrobenzene films stabilized with various concentrations of dodecanol: (1) 11×10^{-2} M; (2) 4.4×10^{-2} M; (3) 17.8×10^{-2} M; after Ref. [471].

When the surfactant adsorption is *barrier controlled* (see Section III.C) the equilibrium adsorption isotherm is replaced by the equation of adsorption balance, Eq. (43). If such is the case, instead of Eq. (253) one should apply the following formula for the film drainage velocity [5]:

$$\frac{V}{V_{Re}} = \left(1 + \frac{h_s}{h}\right)\frac{q^2}{8}\frac{I_0(q)}{I_2(q)}, \quad q \equiv R\left[\frac{6\eta\beta}{E_G(h+h_s)}\right]^{1/2}, \tag{254}$$

where the dimensionless film radius q is defined by Eq. (254), $I_n(q)$ are the modified Bessel functions of the first kind, n-th order, and the kinetic rate parameter $\beta \equiv \partial(r_{ad} - r_{des})/\partial\Gamma$ is assumed to be constant (independent of h). In the limiting case $q \to 0$, $V/V_{Re} \to 1 + h_s/h$ and the adsorption flux from the bulk phase of the liquid is negligible. In other words, the

surfactant behaves like insoluble one and its interfacial distribution is determined by the surface diffusion and convection. The exchange of surfactant between bulk and interface becomes important for not too small values of q, i.e. when the film radius R increases, the Gibbs elasticity E_G decreases and the film thickness h decreases, cf. Eq. (254).

The investigation of the influence of the interfacial viscosity on the rate of film thinning and the shape of the film surfaces is a computationally difficult task, which could be solved only numerically. The results for a symmetrical plane-parallel foam and emulsion films, obeying the classical Boussinesq-Scriven constitutive law (see Section III.F) are presented in [5,58,267,479,480]. Ivanov and Dimitrov [5,481] showed that to solve this problem it is necessary to use the boundary conditions on the film ring (at $r = R$); for that reason the calculations given in Refs. [479,480] may not be realistic. The only correct way to solve the boundary problem is to include the influence of the Plateau border in the boundary conditions; however this makes the explicit solution much more difficult. As a first approximation, in Ref. [267] an appropriate asymptotic procedure foam films is applied to foam films and the following formula for the velocity of thinning was obtained

$$\left(1+\frac{1}{\varepsilon_f}\right)\frac{V_{\text{Re}}}{V} = 1+\frac{\Delta_\eta\left(R_\eta\right)}{\varepsilon_f}, \quad R_\eta \equiv R\left[\frac{6\eta\left(1+\varepsilon_f\right)}{h\eta_s}\right]^{1/2} \tag{255}$$

where η_s is the sum of the interfacial dilatational and shear viscosities (cf. Section III.F above), and the function Δ_η, which is parametrically presented in Fig. 37, depends only upon the dimensionless radius R_η. Therefore, the increase of the film thickness h, film radius R, and the parameter ε_f (ε_f is proportional to E_G) lead to decrease of the influence of the surface viscosity on the film thinning rate.
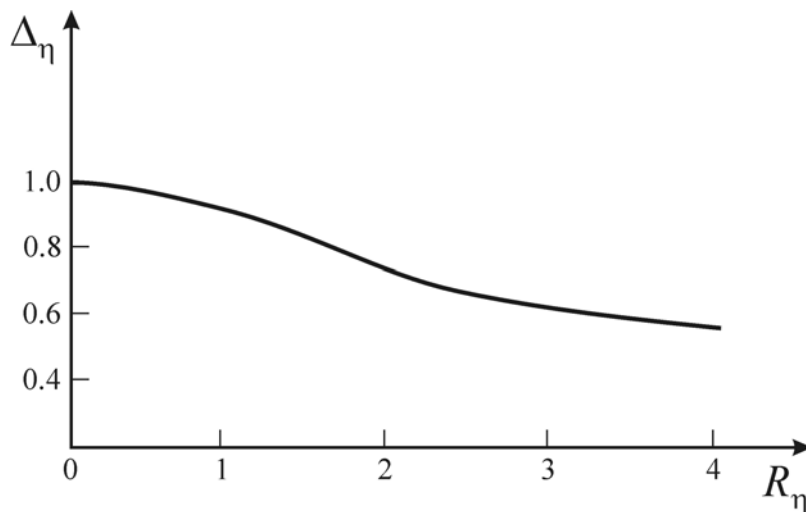
Fig. 37. Function Δ_η vs. dimensionless film radius R_η, defined by Eq. (255) (cf. Ref. 267).

Model of more complicated surface rheology was proposed by Tambe and Sharma [482], who studied the hydrodynamics of drainage of thin liquid films surrounded by *viscoelastic* interfaces, which obey a generalized Maxwell model for the interfacial stress tensor.

C.3. *Films of completely mobile surfaces: surfactant soluble in the drop phase*

When the surfactants are soluble in the drop phase, the film drainage is practically the same as in the case of a film between pure solvent phases; this has been proven both theoretically and experimentally [484-487]. The flow in the droplet phase is very complicated and the full Navier-Stokes equation have been used by Ivanov and Traykov [486] to obtain the following exact expression for the film drainage velocity:

$$V = \left[\frac{32(P_c - \Pi)^2}{\rho_{dr}\eta_{dr}R^4} \right]^{1/3} h^{5/3}; \qquad \frac{V}{V_{\text{Re}}} = \frac{1}{\varepsilon_e} \quad , \quad \varepsilon_e \equiv \left(\frac{\rho_{dr}\eta_{dr}Fh^4}{108\pi\eta^3 R^4} \right)^{1/3} , \qquad (256)$$

where ρ_{dr} and η_{dr} are respectively the droplet density and dynamic viscosity, and ε_e is the so called *emulsion parameter*. Substituting typical parameter values in Eq. (256) one can demonstrate that at a given constant force the velocity of thinning of an emulsion film (the velocity of approach of two *deformed* emulsion drops, Fig. 15) is smaller than the velocity of approach of two *non-deformed* droplets (see ref. 419), but much larger than V_{Re}. It is interesting to note that the velocity of thinning does not depend on the viscosity of the continuous phase, η, and its dependence on the drop viscosity, η_{dr}, is rather weak, see Eq. (256). There are experimental observations confirming this prediction (see Ref. 28, p. 381, and Refs. 419,420,423-425).

In Ref. [429] it was established that for micron-size *non-deformed* droplets the surfactant in the drop phase can slightly influence the velocity of film thinning, (in contrast with the case of deformed drops, Fig. 15, described by Eq. 256).

Based on Eqs. (253) and (256) one may give an explanation of the Bancroft rule for the stability of emulsions, and of the process of chemical demulsification, see Refs. [419,420,423-425,488]

D. Role of Surfactant Transfer across the Film Surfaces

Nonionic surfactants are often soluble in both water and oil phases. In the practice of emulsion preparation the surfactant (the emulsifier) is initially dissolved in one of the liquid phases and then the emulsion is prepared by homogenization. In such a case, the initial distribution of the surfactant between the two phases of the emulsion is non-equilibrium. Therefore, surfactant diffusion fluxes appear across the surfaces of the emulsion droplets. The process of surfactant redistribution usually lasts from several hours, up to several days, until the final equilibrium distribution is established. The diffusion fluxes across the interfaces, directed either from the continuous phase toward the droplets or in the opposite direction, are found to stabilize both the thin films and the emulsions [310,489-491]. In particular, even films which are thermodynamically unstable may exist for several days because of the surfactant diffusion transfer; however, they rupture immediately after the diffusive equilibrium has been established. Experimentally this effect manifests itself in a phenomena called *osmotic swelling* [489] and *cyclic dimpling* [490,491].

D.1. Stabilization due to osmotic swelling
Velev *et al*. [310] reported that emulsion films, formed from preequilibrated phases containing the nonionic surfactant Tween and 0.1 M NaCl, spontaneously thin down to Newton Black Films (thickness ≈ 10nm), and then rupture. However, when the nonionic surfactant (Tween 20 or Tween 60) is initially dissolved in the xylene drops and the film is formed from the non-preequilibrated phases, neither black film formation, nor rupture is observed [489]. Instead, the films have a thickness above 100 nm, and one observes formation of channels of larger thickness connecting the film periphery with the film center (Fig. 38b). One may observe that the liquid is circulating along the channels for a time period from several hours to several days. The phenomenon continues until the redistribution of the surfactant between the phases is accomplished. These observations can be interpreted in the following way:

Since the surfactant concentration in the oil phase (the disperse phase) is higher than the equilibrium one, the surfactant molecules cross the oil-water boundary and enter the aqueous phase; there it forms micelles (denoted by black dots in Fig. 38a) in so far as the background surfactant concentration is above CMC. Thus surfactant micelles accumulate within the film, because the bulk diffusion through the film is not fast enough to promptly transport the excess micelles into the Plateau border. Thus the film is subjected to *osmotic*

swelling because of the increased concentration of *micelles* in its interior. The excess osmotic pressure

$$P_{osm} = kT\, C_{mic} \geq P_c \qquad\qquad (257)$$

counterbalances the outer capillary pressure and prevents further thinning of the film. Moreover, the excess osmotic pressure in the film gives rise to a convective outflow of liquid: this is the physical origin of the observed channels (Fig. 38b).
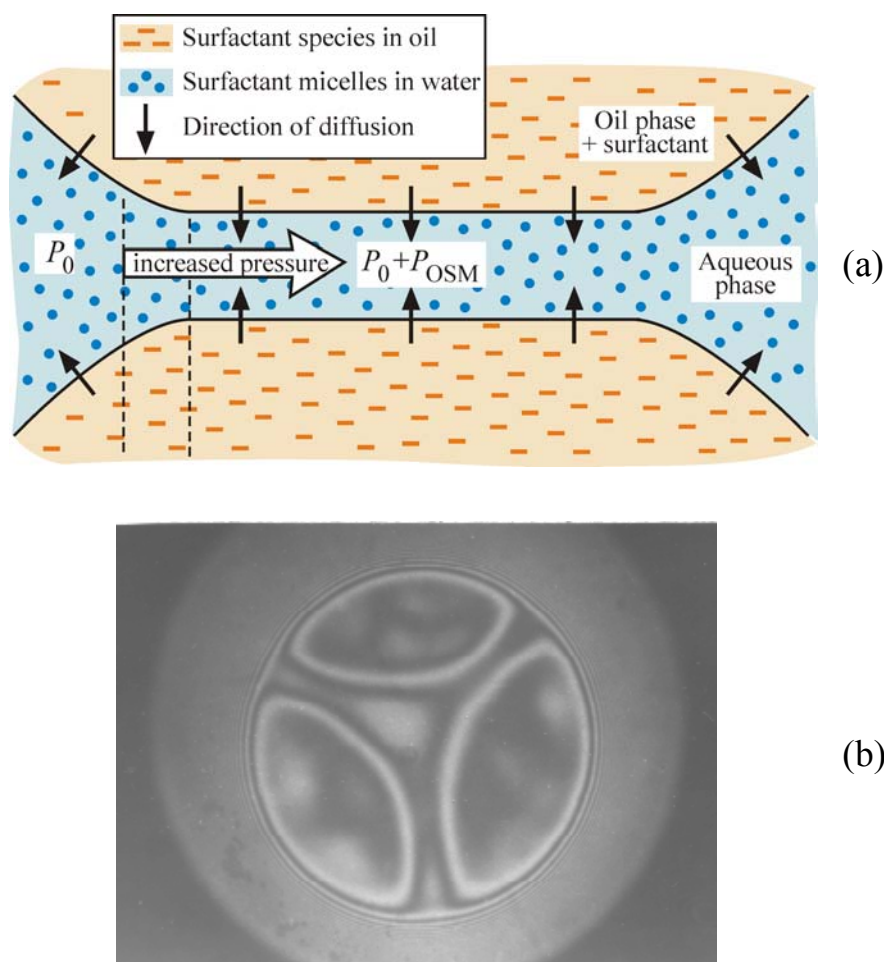
Fig. 38. Osmotic swelling of an aqueous film formed between two oil droplets: (a) The surfactant dissolved in the oil is transferred by diffusion toward the film; there it forms micelles whose osmotic effect increases the local pressure. (b) Photograph of a typical pattern from a circular film with channels.

The experiment [489] shows that the occurrence of the above phenomenon is the same for initial surfactant concentration in the water varying from 1 up to 500 times the CMC, if only a small fraction of surfactant is initially dissolved also in the oil. This fact implies that the value of the surfactant chemical potential inside the oil phase is much greater than that in the aqueous phase, the latter being closer to its value at the CMC in the investigated range of

concentrations. This large difference between the surfactant chemical potentials in the two non-preequilibrated liquid phases is the driving force of the observed process, whose main feature is the transport of surfactant from the droplets toward the continuous phase. The complementary case, which corresponds to surfactant transport of the opposite direction, is considered in the next subsection.

D.2. Stabilization due to cyclic dimpling

This phenomenon is driven by surfactant transfer from the continuous phase toward the droplets. It manifests itself as a cyclic dimpling of emulsion films. The phenomenon was first observed [490] with aqueous films between two xylene droplets in the presence of the nonionic emulsifier Tween 20 or Tween 80 (initially dissolved in water, but also soluble in oil). The same phenomenon has been observed also with other emulsion systems [491].

After the formation of such an emulsion film, it thins down to a certain thickness (usually above 100 nm), at which a dimple spontaneously forms in the film center and starts growing (Fig. 39a). When the dimple becomes bigger and approaches the film periphery, a channel connecting the dimple with the aqueous phase outside the film forms (Fig. 39b). Then the liquid inside in the dimple flows out leaving an almost plane-parallel film behind. Just afterwards a new dimple starts to grow and the process repeats again. The period of this cyclic dimpling remains approximately constant for many cycles and depending on the concrete system could be from a couple to a dozen of minutes. It was established that this process is driven by the depletion of the surfactant concentration on the film surfaces due to the dissolution of surfactant in the adjacent drop phases. The depletion triggers a surface convective flux of surfactant along the two film surfaces directed from the periphery toward the center. This flux, driven by the interfacial tension gradient (Marangoni effect), causes a tangential movement of the film surfaces; the latter drags along a convective influx of solution in the film, which feeds the dimple (Fig. 39a). Thus the cyclic dimpling appears to be a process leading to stabilization of the emulsion films and emulsions due to the influx of additional liquid in the region between the droplets. This influx prevents the droplets from a closer approach and coalescence.
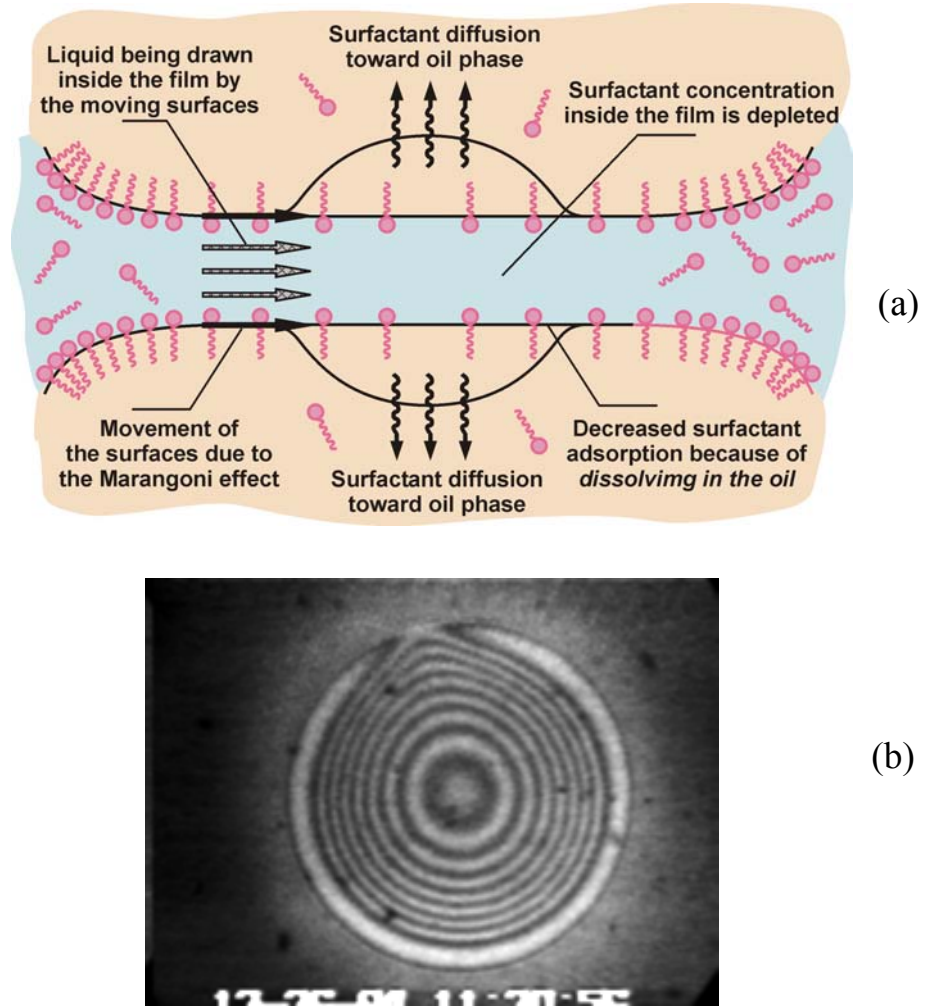
Fig. 39. Cyclic formation of dimples caused by the surfactant diffusion from the film surfaces toward the two adjacent oil phases: (a) schematic presentation of the process; (b) photograph of a large dimple just before flowing out; the interference fringes in reflected light allow to determine the dimple shape.

Combining the general hydrodynamic equations for films of partially mobile surfaces, the interfacial mass balance, and the boundary conditions for the surface stresses, one can derive [491] the following governing equation for the time evolution of the dimple profile, $h(r,t)$:

$$\frac{\partial h}{\partial t} + \frac{1}{3\eta r}\frac{\partial}{\partial r}\left\{ rh^3 \frac{\partial}{\partial r}\left[\frac{\sigma}{r}\frac{\partial}{\partial r}\left(r\frac{\partial h}{\partial r} \right) + \Pi(h) \right] \right\} = \frac{1}{2r}\frac{\partial}{\partial r}\left(\frac{jhr^2}{\Gamma} \right) \tag{258}$$

where j is the diffusion flux from the film surfaces toward the drop phase, and as usual, r is the radial coordinate, σ is the surface tension, Γ is the adsorption, and Π is the disjoining pressure.

114

The comparison between the numerical calculations based on Eq. (258) and the experimental data for the cyclic dimpling is shown in Fig. 40. The experimental points are obtained from the interference fringes, see Fig. 39b. The shape at the initial moment, t=0, serves as an initial condition for determining $h(r,t)$ by solving Eq. (258); the flux j is determined from this curve as an adjustable parameter. With this value of j the curves for $t = 3$, 9, 17 and 29 s are drawn without the usage of any adjustable parameter; one sees that the theory agrees very well with the experiment, Fig. 40.

In Ref. [491] the profile of the radial velocity inside the film was computed as a function of the vertical coordinate. Near the central region the velocity changes its sign along the z-line. This is an important finding which proves the existence of a vortex. Indeed, the flow near the surface is directed towards the film center, whereas close to the midplane $z = 0$ the fluid moves to the opposite direction. Around the film periphery the vortex disappears due to the liquid influx from the outside. This behavior is time-dependent. The vortex shows up after c.a. 40 seconds of the dimple time evolution. It occupies larger parts of the film as the dimple grows, and may have a share in causing instabilities which ultimately lead to dimple expulsion. Fig. 41 presents a very simplified sketch of the vortex; the drawing is not in scale (we recall that even in the case of a dimple $h/R \approx 10^{-2}$).
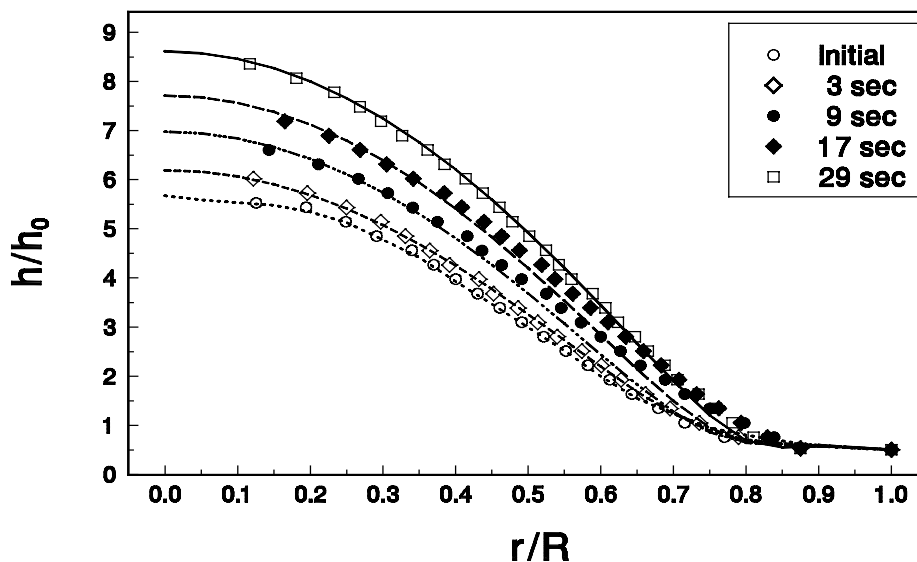
Fig. 40. Comparison between the theory of cyclic dimpling (the lines) and the experimental data (the points) for the dimple shape, $h(r)$, determined from the interference fringes (cf. Fig. 39b); emulsifier: nonylphenol polyoxyethylene-40; the oil phase is styrene; the scaling parameters are $h_0 = 350$ nm and $R = 320$ μm.
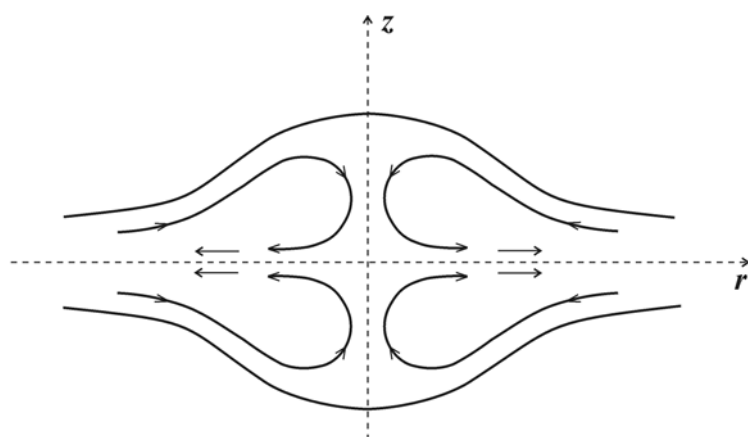
Fig. 41. A sketch of the flow pattern inside a growing cyclic dimple.

VIII. INFLUENCE OF SURFACTANT ON CAPILLARY WAVES

As a result of thermodynamic fluctuations or outer disturbances the surfaces of a thinning liquid film are corrugated (see Fig. 33d). When the derivative of the disjoining pressure, $\partial\Pi/\partial h$, is positive, the amplitude of the film surface corrugations spontaneously grows with the decrease of the film thickness [5,6,420,492]. The appearance of unstable fluctuations is possible even in the relatively thick primary equilibrium films as a result of fluctuations in the electric potential [6,493]. The evaporation or condensation of solvent at the film surface(s) have also destabilizing effect [7]. The mass transfer of solutes, which do not exhibit surface activity, across the film surfaces can influence significantly the film stability [494].

At large separation (thick film) the film surfaces are independent from each other and the film stability depends on the stability of the separate phase boundaries. In this case the short waves, which obey the relation $Dk^2/\omega \geq 1$, with k being the wave number in the plane of the film and ω being the frequency, have a large decrement due to the energy dissipation and the surfactant does not influence the stability. The viscosity of the bulk phases affects the wave propagation and must be taken into account (see Section VIII.F).

In the case of *thin* liquid film the different lateral and normal length-scales and the small wavelength of the fluctuations lead to significant energy dissipation due to the bulk viscous effect. That is why the waves with length longer than the film thickness ($kh \ll 1$) are predominant (see Section VIII.B).

A. Waves in Surfactant Adsorption Monolayers

A surfactant monolayer (or thin layer of oil) spread at a fluid interface damps the surface waves. This phenomenon is due to the fact that as the surfactant monolayer is compressed and expanded during the wave motion, the oscillations of the local surfactant concentration result in oscillations of the local interfacial tension. As a result a combination of Marangoni and interfacial viscosity effects damp the surface waves. Following the classical approach of small-amplitude waves Hansen and Ahmad [495] and Hedge and Slattery [496] derived the dispersion relation between the wave number k and wave frequency ω (see also Ref. [58]):

$$\left(-i\rho\omega^2 - 2\eta k^2\omega + i\sigma k^3 + i\rho gk\right)\left[i\eta\left(n^2 + k^2\right)\omega - nk^2\left(E_* - i\omega\eta_s\right)\right] + \\ + \left(2\omega\eta ikn + \sigma k^3 + \rho gk\right)\left[2\eta k^2\omega + ik^3\left(E_* - i\omega\eta_s\right)\right] = 0 \tag{259}$$

where ρ is the liquid density, g is the gravity acceleration, $\eta_s = \eta_{sh} + \eta_d$ is the sum of the interfacial shear and dilatational viscosities (see Section III.F), $n = (k^2 - i\omega/v)^{1/2}$ is the vertical complex wave number, the complex dilatational modulus E_* is defined in the following way

$$E_* \equiv E_G \frac{1 + \sqrt{q} - i\sqrt{q}}{1 + 2\sqrt{q} + 2q}, q \equiv \frac{D}{2\omega h_e^2}, \tag{260}$$

and the interfacial fluctuations are proportional to $\exp[I(kx - \omega t)]$. The study of such waves at the surface of a droplet (see Eq. (87)) allow measurement of the Gibbs elasticity and the interfacial viscosity. That is why dispersion relations, such as Eqs. (259)-(260), are employed in the analyses of capillary and longitudinal waves. The wave techniques can be classified as capillary, longitudinal and light scattering wave methods.

The *capillary wave method* corresponds to small frequency fluctuations. For pure transverse wave motion Eq. (259) leads to:

$$\rho\omega^2 = 2i\eta k^2\omega + \sigma k^3 + \rho gk \qquad \text{(for damped waves)}$$

$$\rho\omega^2 = \sigma k^3 + \rho gk \qquad \text{(for non-damped waves)} \tag{261}$$

The latter relation is known as Kelvin's equation. Methods for creating propagating capillary ripples typically involve either a mechanical or electrocapillary disturbance of the fluid interface [189-191]. The laser is more appropriate because it does not necessitate physical contact with the fluid surface [497]. The wave characteristics, which are necessary for the evaluation of the interfacial properties through the dispersion relation, are often determined by reflection of a laser beam from the fluid surface to a position-sensitive photodiode.

The longitudinal wave method was first described by Lucassen [498]. Since Lucassen's original work, propagation characteristics of longitudinal waves have been widely used for measuring dilatational elasticity and interfacial viscosity of adsorbed surfactant monolayers. The pure longitudinal waves motion obeys the dispersion relation

$$i\eta\left(n^2 + k^2\right)\omega = nk^2\left(E_* - i\omega\eta_s\right) \qquad (262)$$

which is a special case of Eq. (259). The longitudinal wave techniques involve the oscillation of a barrier within the plane of a fluid interface and the detection of longitudinal wave characteristics by either Wilhelmy plate or an electrocapillary method. If the frequency of oscillation is large, so that the surface wave expands and contracts at a rate sufficiently larger than the rates of surfactant adsorption and desorption, the surfactant monolayer is rendered insoluble and the complex dilatational elasticity E_* may be regarded as Marangoni elasticity, defined as $E_M = \partial\sigma/\partial\ln A$. The experimental results for Marangoni elasticity for poly-L-lysine/SDS aqueous mixtures are given in Ref. [111]. If the frequency of the wave oscillation is small, the wave disturbance will cause only a small deviation from the equilibrium state of the interface and the complex dilatational elasticity E_* is close to the Gibbs elasticity. The experimental results for the Gibbs elasticity of aqueous solution of decanoic acid are reported in Ref. [499], and for the interfacial viscosity in Refs. [191,194,500,501].

Using the light scattering method, thermally-induced capillary waves of very small amplitude may be observed to propagate at equilibrium fluid interfaces. The accuracy of the measurement obtainable with this method combined with the linear surface wave theory of thermal capillary waves of high frequency, render the light scattering techniques attractive for measuring dynamic surface properties [193,502-504].

All the waves discussed above are stable. To illustrate the opposite case of normal mode instability, let us consider two fluid phases, A and B, of densities ρ_A and ρ_B; say $\rho_A > \rho_B$. By placing the heavier fluid A above the lighter fluid B, the superposed configuration will generally be unstable to any mechanical deviation of the interface from its equilibrium planar shape. The corresponding dispersion relation, which governs the non-damped wave, is [505]

$$\left(\rho_A + \rho_B\right)\omega^2 = \sigma k^3 - \left(\rho_A - \rho_B\right)gk \qquad (263)$$

Two opposing effects may be distinguished in this relation: (i) the buoyancy force causes the wave amplitude to grow, rendering the system unstable, whereas the effect of interfacial tension tends to diminish the amplitude growth and suppress the instability; (ii) the short

wavelength capillary waves enhance the stabilizing effect of interfacial tension (the term σk^3 increases), while long wavelength gravity waves lead to an opposite effect. It turns out that the increase of the surfactant concentration decreases the interfacial tension and decreases the stability of the interface. The critical wavelength for a surfactant solution surface is from 0.2 to 0.3 cm.

The *interfacial turbulence* is another effect which leads to destabilization of interfaces and thin films. It appears in the presence of intensive spontaneous transfer of a solute across the interface. The various dynamic phenomena of interfacial turbulence range from a subtle twitching of the interface, to the kicking of drops in one of the phases or formation of long, narrow streams of one phase penetrating into the other one, breaking finally into small emulsion droplets (spontaneous emulsification) [506-508]. Similar effect in a thin film stabilized by nonionic surfactant was reported in Ref. [489]. In the classical theoretical study of Sterling and Scriven [144] the origin of interfacial turbulence was attributed to local interfacial fluctuations in the surface concentration of the solute. The latter induce interfacial tension gradients, which lead to a local interfacial agitation and to the ultimate appearance of interfacial motion. Hennenberg et al. [509] have summarized the factors which affect the interfacial turbulence as follows.

Let us consider the transfer of a solute from phase "a" to phase "b". The conditions for *instability* of the interfaces between these two phases are multiform, i.e. various sufficient conditions are present: (i) at least one of the following relations holds:

$$\frac{D_a}{D_b} > \frac{v_a}{v_b} > 1, \quad \text{or} \quad \frac{D_a}{D_b} > 1 > \frac{v_a}{v_b}, \quad \text{or} \quad \frac{v_b}{v_a} > \frac{D_b}{D_a} > 1 \,;$$

where v is bulk kinematic viscosity, D is the bulk diffusivity of the solute which is being transferred, and the subscripts "a" and "b" denote the respective phases. (ii) Other sufficient condition for instability is the viscosities v_a and v_b, and the diffusivities, D_a and D_b to be small. (iii) Another sufficient condition is the Gibbs elasticity, E_G, to be high in order to withstand large interfacial tension gradients and the interfacial viscosity, η_s, to be small.

On the other hand, the sufficient conditions for *stability* of an interface can be formulated as follows:

$$k^2(\eta_a + \eta_b)(D_a + D_b) / \sigma \gg 1, \quad \text{or} \quad k^3 \eta_s D_s / \sigma \gg 1.$$

The last two relations show that the interfacial turbulence is suppressed (i) by large bulk viscosities and diffusivities, or (ii) by large interfacial viscosity and diffusivity.

Interfacial instability due to fluctuations of the electric potential is investigated by Felderhof [493]. Theoretical description of the stability of an evaporating liquid surface is given by Prosperetti and Plesset [510]. They established that at large evaporation flow rates the instability is very strong with growth time of a millisecond or less. This theory has found an interesting practical application for providing a stable regime of light-water cooled nuclear power plants.

B. Waves in Surfactant Stabilized Liquid Films

The stability of thin liquid films and membranes (of thickness of the order of 10–100 nm) against thermal capillary waves and other disturbances is an important issue in many areas of science and technology. Some examples of systems and processes are: foams and emulsions [267,419-425,511]; displacement of the petroleum in rock pores by gas and foams [512,513]; coating and deposition processes in various technologies like semiconductor chip deposition [514] and fiber optic coating [515-520]; the rupture of the tear film in the human eye [521,522]; bio-membrane and lipid vesicle deformations [523-526]; fusion, flicker and engulfing of cells [527-533]; etc. There are many factors which can give rise to hydrodynamic instability in thin liquid films: capillary forces, gravitational effects (Rayleigh-Taylor instabilities), temperature gradients (Bénard convection), tangential stresses caused by interfacial tension gradients (Marangoni instability), hydrodynamic effects arising from the presence of parallel flows in the film (Kelvin-Helmholtz and shear flow instabilities), and the action of surface forces (see Section VI), which can be treated in the framework of the so called *body force* approach [6,534-536].

The inability to obtain general analytical solution of the problem makes the linear instability analysis the most widely applied mathematical approach [487,537,538]. Below we review the application of this approach to free and wetting thin liquid films (see Sections VIII.B.1 and VIII.B.2).

B.1. *Influence of surfactant on the stability of free liquid films*

A detailed linear analysis of the fluctuations in a quasi-equilibrium plane-parallel thin liquid film intervening between two different phases is given by Maldarelli *et. al.* [6,534-536]. The authors have derived complex dispersion relations (relations between frequency ω and wave number k, see Eqs. (88), (89) in Ref. [6]) which include the influence of the van der Waals and electrostatic interactions, and the Marangoni effect. These dispersion relations can

be analyzed only numerically and the influence of the different factors cannot be explicitly extracted. Nevertheless two general conclusions can be drawn:

(i) Most important for the thin liquid film stability are the long waves, whose wavelength is much greater than the film thickness, $kh \ll 1$.

(ii) There are two types of eigenmodes of a symmetrical film system, so called *squeezing* and *bending* modes (see Fig. 42). The bending mode is not effective to cause film rupture; therefore the investigation of the squeezing mode instabilities is sufficient to determine the conditions for film stability.

(a)   (b)
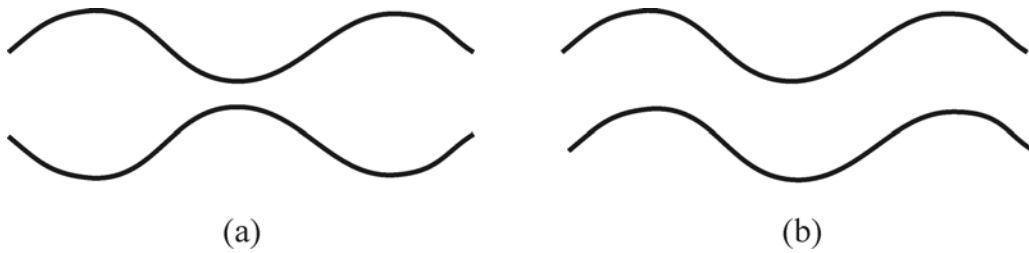
Fig. 42. Symmetric "squeezing" (a) and anti-symmetric "bending" (b) modes of the film surface fluctuations.

In the case of a squeezing mode fluctuations in a symmetrical foam film the dispersion relation can be expressed in the following simplified form [539]

$$\Omega^2 = \frac{\sigma k^2 h^5}{96\eta D R^4}\left[\frac{2R^2}{\sigma}\left(\frac{\partial \Pi}{\partial h}\right) - k^2\right](1+F_s), \Omega \equiv \left(\frac{\omega h^2}{4D}\right)^{1/2} \tag{264}$$

where Ω is the dimensionless increment; the fluctuation of the film thickness is

$$h(r,t) \propto \exp(\omega t)\, \mathrm{J}_0\left(kr/R\right);$$

for positive (negative) ω the disturbances will grow (decay); k is the dimensionless Fourier-Bessel wave number, and

$$F_s \equiv \frac{2R^2}{k^2h^2}\frac{d_s B_s}{1+\dfrac{\eta_s}{3\eta h}d_s B_s}\ ,\ d_s \equiv \frac{12\eta D}{hE_G}\ ,\ B_s \equiv \Omega^2 + \frac{h}{2h_e}\Omega\tanh\Omega + \frac{D_s k^2 h^2}{4DR^2}$$

is a dimensionless factor taking into account the influence of the interfacial viscosity and diffusivity.

Eq. (264) provides an expression for the dependence $\omega(h,k)$. When the film is thick enough ω is *negative* for all h and k; therefore all corrugations decay with time and the film is stable. As the film thickness decreases in the process of film drainage, a certain thickness,

$h = h_t$, will be reached, for which ω becomes zero for some wave special value, k_t, of the wave number:

$$\omega(h_t, k_t) = 0 \, ; \qquad\qquad \omega(h_t, k) < 0 \qquad \text{for} \quad k \neq k_t$$

Combining the last equation with Eq. (264) and the condition that the film has a finite area, πR^2, one derives a simple criterion for the destabilization of the film by small perturbations:

$$\frac{2R^2}{\sigma}\left(\frac{\partial\Pi}{\partial h}\right) \geq j_1^2 \approx 5.783 \tag{265}$$

where j_1 s the first zero of the Bessel function J_0. The thickness, h_t at which the first unstable mode (that with $k = k_t$) appears, is called the *transitional thickness*. In fact, when a thinning film reaches thickness $h = h_t$, it undergoes a transition from *stability* (damped corrugations) to *instability* (growing corrugations). Eq. (265) shows that the inequality $\partial\Pi/\partial h > 0$ is a necessary, but not sufficient, condition for this transition to happen. De Vries [540,541] was the first to point out that local fluctuations of the film thickness lead to two opposite effects: positive contribution to the free energy due to the increase of the film area and negative contribution resulting from the increased negative surface energy of attraction in the thinner part of the film (Fig. 42).

The presence of surfactant increases the film stability. To demonstrate that we will use the special case of Eq. (264) for $\Omega \ll 1$:

$$\omega = \frac{\sigma k^2 h^3}{24\eta R^4}\left[\frac{2R^2}{\sigma}\left(\frac{\partial\Pi}{\partial h}\right) - k^2\right]\left[1 + \frac{6\eta}{h}\left/\left(\frac{E_G}{D_s} + \frac{\eta_s}{R^2}k^2\right)\right.\right], \tag{266}$$

Let us assume that the sign of ω, which is determined by the term in the first brackets, is positive, and consequently, the perturbation grows. Eq. (266) shows that all factors, leading to decrease of ω decelerate the destabilization of the film; such factors are the increase of Gibbs elasticity E_G and surface viscosity, η_s, both of them stemming from the presence of adsorbed surfactant. On the contrary, larger surface diffusivity, D_s, accelerates the growth of the corrugations.

Vrij [542] and Vrij and Overbeek [543] considered the growth of a single wave, of a given wavelength. On the other hand, the real corrugation is rather a superposition of waves of various wavelengths, than a single wave. This idea was incorporated in the theory by Ivanov *et al*. [492], who investigated the stability of a planar foam film of tangentially immobile surfaces. These authors derived a set of two equations for determining the critical

thickness of film rupture, h_{cr}, and the thickness, h_m, at which the harmonic, which breaks the film (the critical harmonic), starts growing:

$$h_{cr}^2 \ln\left[\frac{P_c - \Pi(h_{cr})}{P_c - \Pi(h_m)}\right] = \frac{2k_B T}{\Pi'(h_m)R^2}\left[\frac{P_c - \Pi(h_{cr})}{P_c - \Pi(h_m)}\right]^{\Pi'(h_m)R^2/(4\sigma)}$$

$$2\Pi'(h_m)\int_{h_{cr}}^{h_m}\frac{dh}{P_c - \Pi} = \ln\left[\frac{P_c - \Pi(h_{cr})}{P_c - \Pi(h_m)}\right] \quad (267)$$

In general $h_t \geq h_m \geq h_{cr}$; by definition $\omega(h_m, k_{cr}) = 0 = 0$, whereas h_{cr} is defined as the film thickness for which the amplitude of the critical wave is so large, that the corrugated film surfaces touch each other [492]. Numerical solution of the above set of equation confirms that the theory correctly predicts the experimentally observed [544] increase of h_{cr} with the increase of the film radius, R. Note, however, that h_{cr} depends not only on the film radius, but also on the bulk surfactant concentration c_0 : $h_{cr}(R,c_0)$; the effect of c_0 is not accounted for in Eq. (267).

Systematic experimental studies of the influence of the bulk surfactant concentration, c_0, and the film radius, R, upon the stability of foam [420,492,545] and emulsion [420,487,546] films are available. The general conclusions are that the critical thickness, h_{cr}, increases when R increases and c_0 decreases. In Fig. 43 the dependence of the critical thickness of rupture of aniline films on the concentration of dodecanol is shown [420].
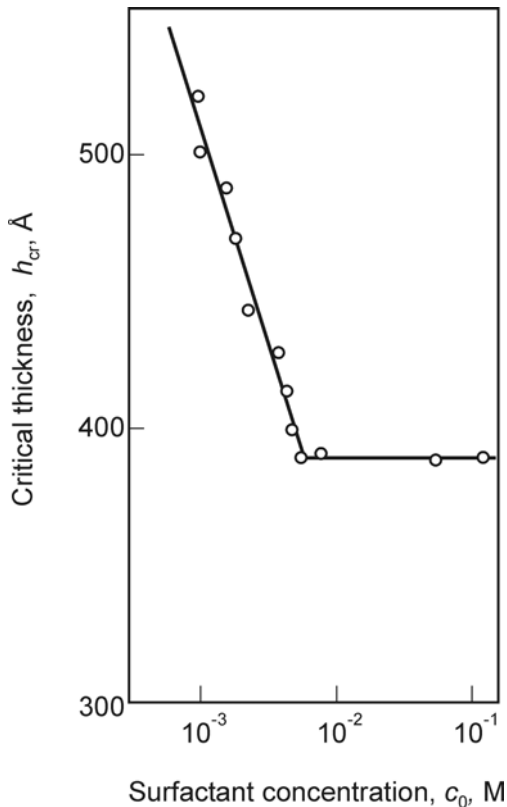
Fig. 43. Experimental dependence of the critical thickness of rupture, h_{cr}, of aniline films on the concentration, c_0, of dodecanol, which plays the role of surfactant [420].

A first attempt to explain the observed decrease of h_{cr} with the increase of c_0 was undertaken by Ivanov and Dimitrov [545], who improved the model from Ref. [492] by accounting for the partial mobility of the film surfaces. Geometrically, the film was modeled as two plane-parallel disks of restricted area, πR^2, in this study. The results show that the latter model does not predict a considerable effect of the surfactant concentration, c_0, in contrast with the experimental observations (Fig. 43). For the time being there is no full solution of this problem. However, there are encouraging evidences that the problem can be solved if the restriction for finite film area is removed and the propagation of the capillary waves into the transition zone between the film and the Plateau border is taken into account. The development in this direction is described below.

Ivanov *et al.* [5,428,547] derived equations approximating the real shape of the surfaces of a draining film (film + Plateau border) formed between two approaching bubbles of radius a

$$h = h_0 + y - h_i \ln\left(1 + \frac{y}{2h_i}\right) - \frac{yh_i}{2h_i + y}, \; V = \frac{Fh_0^3}{2\pi\eta R^4}\left(1 + b_s + \frac{h_s}{h_0}\right) \tag{268}$$

where h_0 is the closest distance between the surfaces of the two bubbles, $V = dh_0/dt$ is the drainage velocity, $y = r^2/a$ is a characteristic radial coordinate, $R = [Fa/(2\pi\sigma)]^{1/2}$ is a characteristic radius of the film formed between the bubbles, and h_i is the inversion thickness, defined by Eq. (246). The analysis of Eq. (268) shows that h has only one extremum (a minimum at $r = 0$) and, in a rather extended region of radius $0 < r < R$ the film profile is almost plane-parallel. If h_f expresses a small perturbation of the film profile, h, the following equation for the fluctuations in the film region can be derived [548] by using the classical linear perturbation analysis:

$$\frac{h_0}{h_f}\frac{\partial h_f}{\partial h_0} = 3 - \frac{2h_s}{h_s + (1 + b_s)h_0} + \frac{h_0 R^2}{12(P_c - \Pi)}\left(\sigma\chi^4 k^4 - 2\Pi'\chi^2 k^2\right) \tag{269}$$

where $\chi \equiv \sqrt{h_0\left[(1 + b_s)h_0 + h_s\right]}$ is a parameter of the radial scaling, $x \equiv \chi r$, used to derive Eq. (269); the profile of the fluctuation is proportional to $J_0(kx)$ where k is the Fourier-Bessel wave number corresponding to the new radial coordinate x. Then one can derive the following expression for calculating the transitional thickness h_t:

$$\frac{3(1 + b_s)h_t + h_s}{(1 + b_s)h_t + h_s} = \frac{h_t R^2}{12\sigma(P_c - \Pi)}\left(\frac{\partial\Pi}{\partial h}\right)^2, \tag{270}$$

see Eq. (247) or the notation. The left-hand side of Eq. (270) varies from 1 for pure (free of surfactant) liquid surfaces ($h_s \to \infty$), up to 3 for tangentially immobile surfaces ($EG \to \infty$, $b_s = h_s = 0$). In the latter case of tangentially immobile surfaces, assuming that only the van der Waals attraction is operative, from Eq. (270) one deduces the following simple expression for h_t:

$$h_t = \left(\frac{aR^2 A_H^2}{288\pi^2\sigma^2} \right)^{1/7} \tag{271}$$

where A_H is the Hamaker constant (see Section VI.1). The values of h_t predicted by Eq. (271) are compared in Fig. 44 with data for the dependence of the critical thickness, h_{cr}, on the film radius R. Curve 1 gives the experimental data for aniline films stabilized by dodecanol [420], Curve 2 presents h_{cr} theoretically calculated from Eq. (267), Curves 3 and 4 present the transitional thickness, h_t, calculated respectively from Eq. (265) and Eq. (271). One sees that the theory from Ref. [492] gives a relatively good agreement with the experimental data for h_{cr}. The transitional thickness, h_t, calculated from Eq. (265) is markedly larger than that calculated from Eq. (271), the latter being close to the critical one. A further development of this theory to explain the dependence of h_{cr} vs c_0 (Fig. 43) is under way.
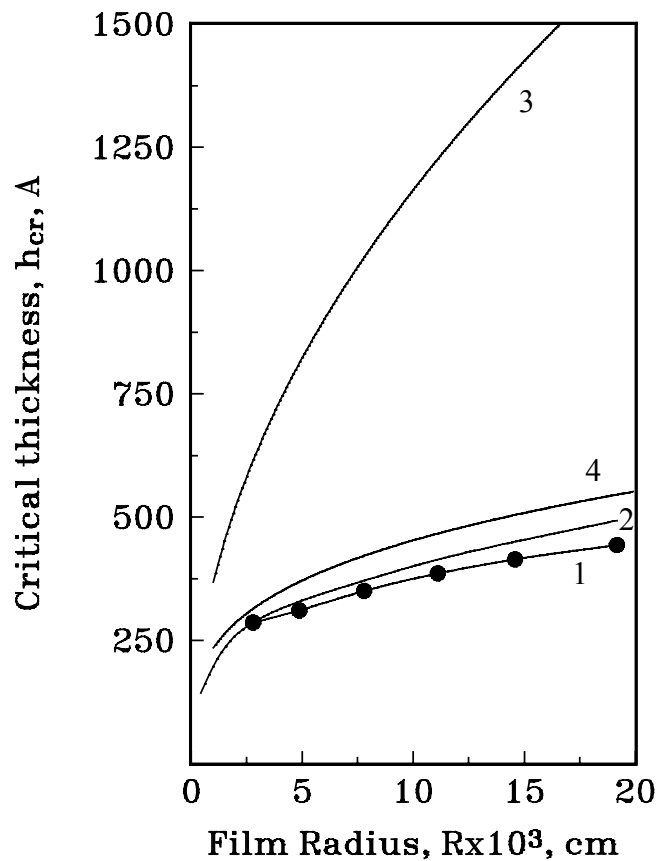
Fig. 44. Dependence of the critical thickness of rupture, h_{cr}, and the transitional thickness, h_t, on the film radius, R. Curve 1 - experimental data for aniline films stabilized by dodecanol [420]; curve 2 - theoretical calculation on the basis of Eq. (267); curves 3 and 4 - the transitional thickness calculated from Eqs. (265) and (271), respectively.

Finally, we consider the effect of interfacial turbulences, which are due to mass transfer across the phase boundaries, on the stability of emulsion films. Experimentally, the diffusion transfer of alcohols, acetic acid and acetone has been studied [549,550]. The observed destabilization of the films can be attributed to the appearance of Marangoni instability [494]. The latter manifests itself through the growth of capillary waves at the interfaces, which eventually can lead to film rupture. Lin and Brenner [521] examined the role of the heat and mass transfer in an attempt to check the hypothesis of Holly [551] that the Marangoni instability can cause the rupture of tear films. Their analysis was extended by Castillo and Velarde [552] who accounted for the tight coupling of the heat and mass transfer and showed that it drastically reduces the threshold for Marangoni convection.

B.2. Stability of thin wetting films

The dispersion relation in the case of wetting film (one of the adjacent phases is solid) can be deduced from Eq. (88), (89) in Ref. [6] in the limit of very large dynamic viscosity of one of the adjacent phases:

$$\tilde{\Omega}^2 = \frac{\sigma k^2 h}{12\eta D}\left[\frac{h^2}{\sigma}\left(\frac{\partial \Pi}{\partial h}\right) - k^2 - \frac{gh^2\Delta\rho}{\sigma}\right]\left(1+\tilde{F}_s\right), \quad \tilde{\Omega} \equiv \left(\frac{\omega h^2}{D}\right)^{1/2} \qquad (272)$$

where $\tilde{\Omega}$ is the dimensionless increment, the fluctuation of the film thickness is

$$h(x,t) \propto \exp\left(\omega t\right)\exp\left(ikx/h\right),$$

k is the dimensionless wave number ($k \ll 1$), and $\Delta\rho$ is the difference between the densities of the lower and upper phases. The surfactant is assumed to be soluble only in the film phase. The dimensionless factor $\tilde{F}_s$, which takes into account the influence of the interfacial viscosity and diffusivity, is defined as follows:

$$\tilde{F}_s \equiv \frac{3h_s}{h_s + 3hk^2\tilde{B}_s}, \quad \tilde{B}_s \equiv \frac{\eta_s D}{h^2 E_G} + \left(\tilde{\Omega}^2 + \frac{h}{h_e}\tilde{\Omega}\tanh\tilde{\Omega} + \frac{D_s k^2}{D}\right)^{-1} \qquad (273)$$

The linear stability analysis of wetting films was first performed for surfactant-free films by Jain and Ruckenstein [553] and this analysis was further extended to surfactant containing films by Edwards et al. [58].

From the dispersion relation (8.14) it follows that the increase of the surface tension,σ, and/or the magnitude of the density difference, $\Delta\rho$, decreases ω (the increment of instability growth) and thus stabilizes the film. The disjoining pressure effect stabilizes the film when $\partial\Pi/\partial h < 0$, but destabilizes the film when $\partial\Pi/\partial h >< 0$.

In general, the presence of surfactant has a stabilizing effect on the wetting films. At a first glance it may seem that the surfactant has destabilizing effect in so far as it decreases the surface tension. However, the main effect of the surfactant on the increment of perturbation growth, ω, comes from the contribution of dynamic factors as E_G and η_s in $\widetilde{F}_s$, see Eqs. (272)-(273). Indeed, F_s changes from 3 (for surfactant free surface) to 0 (for tangentially immobile surface), and the factor $(1 + F_s)$ in Eq. (272) decreases 4 times due to the effect of surfactant.

Gumerman and Homsy [554] have extended this analysis by taking into account the effects of wall and film drainage. Williams and Davis [555] have shown that the nonlinear effects (in the case of a surfactant-free thin liquid films) may have significant effect on the rupture time. The nonlinear stability of evaporating/condensing thin liquid films, free from surfactant, is discussed in Refs. [556-558]. The authors show that the evaporation and the condensation lead to destabilization of the film.

Hatziavramidis [7] investigated the influence of insoluble surfactant on the film stability. He proved that the Marangoni flows driven by gradients of the surface concentration (adsorption) are directed opposite to the thermocapillary flows originating from surface temperature variations. The Marangoni flows are usually predominant; they destabilize condensing films, but stabilize evaporating films. The theory of nonlinear waves on vertical falling films is described in Refs. [559,560] for moderate and high Reynolds numbers.

Another type of interfacial instability are induced by the thermal fluctuations, resulting from temperature inhomogeneity along the interface. When a liquid layer (say a paint film) dries, periodic cellular patterns are often observed; these patterns are known as *Bénard cells*, called after the pioneering experimental studies of Bénard [561]. He has observed that cellular (hexagonal) circulation patterns appear when a liquid film is heated from below. This cellular instability has been first attributed to buoyancy-driven convection until Rayleigh [562] proved that this phenomenon is driven by gradients of the interfacial tension caused by temperature inhomogeneity. Interfacial tension gradients give rise to flows in the interface and the adjacent liquid layer, carrying liquid from the areas of low interfacial tension to those of high tension. Thus, the Bénard convection cells are produced. This coupling of surface concentration and temperature instabilities have been investigated by many authors [131,563-574]. A general conclusion from these works is that the surfactant opposes the surface movement and delays or inhibits the appearance of instability. The theory was experimentally verified by Imaishi *et al.* [575].

The studies of Marangoni-Bénard instabilities have been mostly carried out with *static* films, or with films of initially uniform velocity. The classical works of Benjamin [576] and Yih [577] proved that isothermal flow of a wetting liquid film down a vertical plane is unstable for all finite Reynolds numbers, in the absence of any evaporation and condensation. The surfactant usually has a stabilizing effect on the falling films. Emmert and Pigford [578] found experimentally that the addition of surfactant reduces the rippling in falling liquid films. Whitaker [579] established that the surface elasticity has a primary importance for the stabilizing action. Lin [580] showed that both soluble and insoluble surfactants have a stabilizing effect on falling films, suppressing the natural wave instability.

The surface waves, along with the thermocapillary instability, have been studied with wetting films flowing down an inclined plane, which is subjected to heating [562,581,582]. The authors conclude that three mechanisms may cause the instabilities of the flow. One of them is associated with the shear stress exerted on the film surface from the bulk flow; this stress may bring about instability of the capillary waves. The other two mechanisms are related to the thermocapillary instabilities of *moderate* and of *long* wavelengths. Such an instability can grow in the form of either long transfer waves or short longitudinal rolls, depending on which is the dominant mechanism that triggers the instability.

The desorption of surfactant was found to contribute also to the Marangoni instability. The practical origin of this problem is the process of adsorption refrigeration. Some surfactants, when added in small quantities, increase the capacity of adsorption cooling machines [583]. It is generally believed that the reason for this effect is the Marangoni convection. The enhancing effect of interfacial convection has been experimentally verified with solutions of aqueous lithium bromide adsorbing water vapors [584,585].

IX. SUMMARY

The major property of surfactants is their ability to adsorb at interfaces and thus to decrease the surface excess energy and to modify the interface. Various adsorption and surface tension isotherms are used in the thermodynamic description of this phenomenon, see Section II above.

Many practical processes (foaming, emulsification, dispersing, wetting, washing, solubilization) are influenced by the rate of adsorption from surfactant solutions. This rate depends on whether the adsorption takes place under diffusion, electro-diffusion, barrier or convective control. The presence of surfactant micelles, which serve as carriers and reservoir of surfactant, can strongly accelerate the kinetics of adsorption, see Section III.A-E.

As a rule dynamic processes with fluid interfaces are accompanied by interfacial dilatation, compression and/or two-dimensional flows in the surfactant adsorption monolayer. These processes are affected by the interfacial rheological properties, such as surface (Gibbs) elasticity, dilatational and shear surface viscosity, adsorption relaxation time, see Section III.F. The interfacial rheological properties are especially important for the foaminess of surfactant solutions and the emulsion preparation by homogenization.

The mechanical properties of surfactant adsorption monolayers are characterized not only by the interfacial tension, but also by the interfacial bending moment, which is proportional to the so called spontaneous curvature of the interface. In addition, the variation of the interfacial bending moment with curvature is characterized by the curvature elastic moduli. These interfacial flexural properties are determined mostly by the interactions between the headgroups and tails of the adsorbed surfactant molecules. In their own turn, the interfacial flexural properties influence phenomena and processes such as formation of microemulsions, critical emulsions, holes in foam and emulsion films, fluctuation capillary waves, flocculation in emulsions, etc., see Section IV.

The modification of the fluid interfaces due to surfactant adsorption strongly influences the interactions between fluid particles (droplets, bubbles) in dispersions. Frequently a thin liquid film is formed in the zone of contact of two fluid particles. The contact angle at the periphery of such a film is a measure for the interaction of the two opposite surfactant adsorption monolayers. When the latter adhere to each other, a hysteresis of the contact angle is observed, irrespective of the fact that the fluid interfaces are molecularly smooth. The properties of the thin liquid films are important for the flocculation

in dispersions and the deposition (attachment-detachment) of particles at surfaces, see Section V.

Several types of surface forces determine the interactions across thin liquid films. In addition to the universal van der Waals forces, the adsorbed ionic surfactants enhance the electrostatic (double layer) repulsion. On the other hand, the adsorbed nonionics give rise to a steric repulsion due to the overlap of hydrophilic polymer brushes. The presence of surfactant micelles in the continuous phase gives rise to oscillatory structural forces, which can stabilize or destabilize the liquid films (and dispersions) depending on whether the micelle volume fraction is higher or lower. These and other surface forces, related to the surfactant properties, are considered in Section VI.

The presence of surfactant affects also the hydrodynamic interactions between fluid particles in dispersions. When the surfactant is soluble in the continuous phase, the adsorption monolayers immobilize the drop (bubble) surfaces and decelerate the approach of such two particles. On the contrary, if the surfactant is dissolved in the droplets (in the disperse phase), it efficiently damps the surface tension gradients and accelerates the approach and (eventually) coalescence of the droplets. The processes of surfactant transfer from the continuous toward the disperse phase, or vice versa, also influence the droplet-droplet hydrodynamic interactions, see Section VII.

Another property of surfactants is that they influence the capillary waves. This property is employed by several methods for determining the rheological properties of surfactant adsorption monolayers. Moreover, the breakage of liquid films (and the destruction of foams and emulsions) is often related to the growth of the amplitude of thermally exited capillary waves facilitated by attractive surface forces. The theoretical description of these effects is considered in Section VIII.

We hope that the present review of the thermodynamic, kinetic and mechanical properties of adsorption monolayers and liquid films will be helpful for understanding the role of surfactants in various processes of scientific and practical importance.

REFERENCES

1. E. D. Shchukin, A. V. Pertsov, and E. A. Amelina, <u>Colloid Chemistry</u>, Moscow Univ. Press, Moscow, 1982 [in Russian].

2. B. V. Derjaguin, N. V. Churaev, and V. M. Muller, <u>Surface Forces</u>, Plenum Press: Consultants Bureau, New York, 1987.

3. E. J. W. Verwey, and J. Th. G. Overbeek, <u>The Theory of Stability of Liophobic Colloids</u>, Elsevier, Amsterdam, 1948.

4. J. N. Israelachvili, <u>Intermolecular and Surface Forces</u>, Academic Press, London, 1992.

5. I. B. Ivanov, and D. S. Dimitrov, in: <u>Thin Liquid Films</u> (I. B. Ivanov, ed.), M. Dekker, New York, 1988, p. 379.

6. C. Maldarelli, and R. K. Jain, in: <u>Thin Liquid Films</u> (I. B. Ivanov, ed.), M. Dekker, New York, 1988, p. 497.

7. D. Hatziavramidis, <u>Int. J. Multiphase Flow 18</u>: 517 (1992).

8. J. W. Gibbs, <u>The Scientific Papers of J. W. Gibbs</u>, vol.1, Dover, New York, 1961.

9. S. Ono, and S. Kondo, Molecular theory of surface tension in liquids, in: <u>Handbuch der Physik</u>, vol. 10, Flügge, S., Ed., Springer, Berlin, 1960.

10. A. W. Adamson, <u>Physical Chemistry of Surfaces</u>, Wiley, New York, 1976.

11. I. Langmuir, <u>J. Amer. Chem. Soc. 39</u>: 1883 (1917).

12. T. L. Hill, <u>An Introduction to Statistical Thermodynamics</u>, Addison-Wesley, Reading, MA, 1962.

13. H. Lange, <u>J. Colloid Sci. 20</u>: 50 (1965).

14. P. Joos, and E. Rillaerts, <u>J. Colloid Interface Sci. 79</u>: 96 (1981).

15. R. Miller and K. Lunkenheimer, <u>Colloid Polym. Sci. 261</u>: 585 (1983).

16. R. Miller, and K. Lunkenheimer, <u>Colloid Polym. Sci. 264</u>: 357 (1986).

17. E. H. Lucassen-Reynders, <u>J. Phys. Chem. 70</u>: 1777 (1966).

18. E. H. Lucassen-Reynders, <u>Anionic Surfactants - Physical Chemistry of Surfactant Action</u>, Marcel Dekker, New York, 1981.

19. B. von Szyszkowski, <u>Z. Phys. Chem. 64</u>: 385 (1908).

20. A. Frumkin, <u>Z. Phys. Chem., 116</u> : 466 (1925).

21. R. P. Borwankar, and D. T. Wasan, <u>Chem. Eng. Sci. 43</u>: 1323 (1988).

22. K. Marinova, R. Alargova, N. Denkov, O. Velev, D. Petsev, I. B. Ivanov, and R. P. Borwankar, <u>Langmuir 12</u>: 2045 (1996).

23. T. L. Hill, <u>An Introduction to Statistical Thermodynamics</u>, Addison-Wesley, Reading, MA, 1962.

24. L. D. Landau, and E. M. Lifshitz, <u>Statistical Physics, Part 1.</u> Pergamon Press, Oxford, 1980.

25. J. T. Davies, <u>Proc. Roy. Soc. Ser. A, 208</u>: 224 (1951).

26. S. Hachisu, <u>J. Colloid Interface Sci. 33</u>: 445 (1970).

27. T. D. Gurkov, P. A. Kralchevsky, and K. Nagayama, <u>Colloid Polym. Sci. 274</u>:227 (1996).

28. J. T. Davies, and E. K. Rideal, <u>Interfacial Phenomena.</u> Academic Press, New York, 1963.

29. K. Tajima, M. Muramatsu, and T. Sasaki, <u>Bull. Chem. Soc. Japan 43</u>: 1991 (1970).

30. A. K. Malhotra, and D. T. Wasan, in: <u>Thin Liquid Films</u> (I. B. Ivanov, ed.), M. Dekker, New York, 1988, p. 829.

31. S. S. Dukhin, G. Kretzschmar, and R. Miller, <u>Dynamics of Adsorption at Liquid Interfaces</u>, Elsevier, Amsterdam, 1995.

32. R. Defay, and G. Pétré, Dynamic surface tension, <u>Surface and Colloid Science Vol. 3</u> (E. Matijevic, ed.), Wiley, New York, 1971, p. 27.

33. A. M. Posner, and A. E. Alexander, <u>Trans. Faraday Soc. 45</u>: 651 (1949).

34. K. J. Mysels, <u>Colloids Surf. 43</u>: 241 (1990).

35. P. A. Kralchevsky, Y. S. Radkov, and N. D. Denkov, <u>J. Colloid Interface Sci. 161</u>: 361 (1993).

36. V. B. Fainerman, R. Miller, and P. Joos, <u>Colloid Polym. Sci. 272</u>: 731 (1994).

37. P. Rao, and G. Enhorning, <u>Colloids Surf. B, 4</u>: 159 (1995).

38. V. B. Fainerman, and R. Miller, <u>J. Colloid Interface Sci. 176</u>: 118 (1995).

39. T. S. Horozov, C. D. Dushkin, K. D. Danov, L. N. Arnaudov, O. D. Velev, A. Mehreteab, and G. Broze, <u>Colloids Surf. A, 113</u>: 117 (1996).

40. M. van den Tempel, and E. H. Lucassen-Reynders, <u>Adv. Colloid Interface Sci. 18</u>: 281 (1983).

41. D. Langevin, <u>Colloids Surf. 43</u>: 121 (1990).

42. C. Lemaire, and D. Langevin, <u>Colloids Surf. 65</u>: 101 (1992).

43. D. O. Grigorev, V. V. Krotov, and B. A. Noskov, <u>Colloid J. 56</u>: 562 (1994).

44. R. Miller, and G. Kretzschmar, <u>Adv. Colloid Interface Sci. 37</u>: 97 (1991).

45. C.-H. Chang, and E. I. Franses, <u>J. Colloid Interface Sci. 164</u>: 107 (1994).

46. C.-H. Chang, and E. I. Franses, <u>Chem. Eng. Sci. 49</u>: 313 (1994).

47. K.-D. Wantke, K. Lunkenheimer, and C. Hempt, <u>J. Colloid Interface Sci. 159</u>: 28 (1993).

48. D. O. Johnson, and K. J. Stebe, C.-H. Chang, and E. I. Franses, <u>J. Colloid Interface Sci. 168</u>: 21 (1994).

49. C. Jho, and R. Burke, <u>J. Colloid Interface Sci. 95</u>: 61 (1983).

50. J. van Hunsel, G. Bleys, and P. Joos, <u>J. Colloid Interface Sci. 114</u>: 432 (1986).

51. V. B. Fainerman, and R. Miller, <u>Colloids Surf. A, 97</u>: 255 (1995).

52. J. van Havenbergh, and P. Joos, <u>J. Colloid Interface Sci. 95</u>: 172 (1983).

53. I. Balbaert, G. Bleys, and P. Joos, <u>J. Colloid Interface Sci. 115</u>: 362 (1987).

54. E. I. Franses, O. A. Basaran, and C.-H. Chang, <u>Curr. Opinion Colloid Interface Sci. 1</u>: 296 (1996).

55. R. B. Bird, W. E. Stewart, and E. N. Lightfoot, <u>Transport Phenomena</u>, Wiley, New York, 1960.

56. V. G. Levich, <u>Physicochemical Hydrodynamics</u>, Prentice-Hall, Englewood Cliffs, New Jersey, 1962.

57. J. C. Slattery, <u>Momentum, Energy, and Mass Transfer in Continua</u>, R.E. Krieger Publishing Co.: Huntington, New York, 1978.

58. D. A. Edwards, H. Brenner, and D. T. Wasan, <u>Interfacial Transport Processes and Rheology</u>, Butterworth-Heinemann, Boston, 1991.

59. H. Schlichting, <u>Grenzschicht-Theorie</u>, Verlag G. Braun, Karlsruhe, 1965.

60. V. N. Izmailova, G. P. Yampolskaya, and B. D. Summ, <u>Surface Phenomena in Protein Systems</u>, Himiya, Moscow, 1988 (in Russian).

61. F. van Voorst Vader, Th. F. Erkens, and M. van den Tempel, <u>Trans. Faraday Soc. 60</u>: 1170 (1964).

62. A. F. H. Ward, and L. Tordai, <u>J. Chem. Phys. 14</u>: 453 (1946).

63. R. Miller, and K. Lunkenheimer, <u>Z. Phys. Chem. 259</u>: 863 (1978).

64. R. Miller, <u>Colloid Polym. Sci. 259</u>: 375 (1981).

65. R. P. Borwankar, and D. T. Wasan, <u>Chem. Eng. Sci. 38</u>: 1637 (1983).

66. B. J. McCoy, <u>Colloid Polym. Sci. 261</u>: 535 (1983).

67. M. Ziller, and R. Miller, <u>Colloid Polym. Sci. 264</u>: 611 (1986).

68. R. Miller, and M. Ziller, <u>Colloid Polym. Sci. 266</u>: 532 (1988).

69. K. L. Sutherland, <u>Austr. J. Sci. Res. A5</u>: 683 (1952).

70. M. Abramowitz, and I. A. Stegun, *Handbook of Mathematical Functions,* Dover, New York, 1965.

71. R. Miller, <u>Kolloidn. Zh. 42</u>: 1107 (1980).

72. I. J. Lin, and L. Marszall, <u>Progr. Colloid Polym. Sci. 63</u>: 99 (1978).

73. R. van den Bogaert, and P. Joos, <u>J. Phys. Chem. 83</u>: 2244 (1979).

74. P. Dynarowicz, and W. Jawien, <u>Colloids Surf. A, 70</u>: 171 (1993).

75. R. S. Hansen, <u>J. Chem. Phys. 64</u>: 637 (1960).

76. V. B. Fainerman, A. V. Makievski, and R. Miller, <u>Colloids Surf. A, 87</u>: 61 (1994).

77. E. Rillaerts, and P. Joos, <u>J. Chem. Phys. 96</u>: 3471 (1982).

78. L. K. Filippov, <u>J. Colloid Interface Sci. 164</u>: 471 (1994).

79. X. Y. Hua, and M. J. Rosen, <u>J. Colloid Interface Sci. 124</u>: 652 (1988).

80. X. Y. Hua, and M. J. Rosen, <u>J. Colloid Interface Sci. 141</u>: 180 (1991).

81. M. J. Rosen, Z. H. Zhu, B. Gu, and D. S. Murphy, <u>Langmuir 4</u>: 1273 (1988).

82. P. Joos, J. P. Fang, and G. Serrien, <u>J. Colloid Interface Sci. 151</u>: 144 (1992).

83. T. S. Horozov, K. D. Danov, P. A. Kralchevsky, I. B. Ivanov, and R. P. Borwankar, A local approach in interfacial rheology, <u>Proceedings of the First World Congress on Emulsions, Vol. 2</u>, Paris, 1993, p. 137.

84. T. S. Horozov, P. A. Kralchevsky, K. D. Danov, and I. B. Ivanov, <u>J. Dispersion Sci. Technol.18</u>: 593 (1997).

85. G. K. Batchelor, <u>An Introduction to Fluid Dynamics</u>, University Press, Cambridge, 1970.

86. K. S. G. Doss, <u>Koll. Z. 84</u>: 138 (1938).

87. S. Ross, <u>Am. Chem. Soc. 67</u>: 990 (1945).

88. W. N. Bond, and H. O. Puls, <u>Phil. Mag. 24</u>: 864 (1937).

89. C. M. Blair, <u>J. Chem. Phys. 16</u>: 113 (1948).

90. A. F. H. Ward, <u>Surface Chemistry</u>, London, 1949.

91. R. S. Hansen, and T. Wallace, <u>J. Phys. Chem. 63</u>: 1085 (1959).

92. D. G. Dervichian, <u>Koll. Z. 146</u>: 96 (1956).

93. J. F. Baret, <u>J. Phys. Chem. 72</u>: 2755 (1968).

94. J. F. Baret, <u>J. Chem. Phys. 65</u>: 895 (1968).

95. J. F. Baret, <u>J. Colloid Interface Sci. 30</u>: 1 (1969).

96. R. Miller, and G. Kretzschmar, <u>Colloid Polym. Sci. 258</u>: 85 (1980).

97. C. Tsonopoulos, J. Newman, and J. M. Prausnitz, <u>Chem. Eng. Sci. 26</u>: 817 (1971).

98. A. Yousef, and B. J. McCoy, <u>J. Colloid Interface Sci. 94</u>: 497 (1983).

99. Z. Adamczyk, <u>J. Colloid Interface Sci. 120</u>: 477 (1987).

100. Z. Adamczyk, and J. Petlocki, <u>J. Colloid Interface Sci. 118</u>: 20 (1987).

101. J. Balbaert, and P. Joos, <u>Colloids Surf. 23</u>: 259 (1987).

102. S. S. Dukhin, R. Miller, and G. Kretzschmar, <u>Colloid Polym. Sci. 261</u>: 335 (1983).

103. R. Miller, S. S. Dukhin, and G. Kretzschmar, <u>Colloid Polym. Sci. 263</u>: 420 (1985).

104. R. Miller, S. S. Dukhin, and G. Kretzschmar, <u>Colloid Polym. Sci. 269</u>: 924 (1991).

105. R. Miller, G. Kretzschmar, and S. S. Dukhin, <u>Colloid Polym. Sci. 272</u>: 548 (1994).

106. R. P. Borwankar, and D. T. Wasan, <u>Chem. Eng. Sci. 41</u>: 199 (1986).

107. C. A. McLeod, and C. J. Radke, <u>Langmuir 10</u>: 3555 (1994).

108. P. M. Vlahovska, K. D. Danov, A. Mehreteab, and G. Broze, <u>J. Colloid Interface Sci. 192</u>: 194 (1997).

109. P. M. Vlahovska, K. D. Danov, P. A. Kralchevsky A. Mehreteab, and G. Broze, <u>J. Colloid Interface Sci. </u>: (1998) - submitted.

110. K. W. Wagner, <u>Die Isolierstofe der Elektrotechnik</u>, Springer-Verlag, Berlin, 1924.

111. J. Lucassen, F. Holloway, and J. H. Buckingham, <u>J. Colloid Interface Sci 67</u>: 432 (1978).

112. P. Joos, J. van Hunsel, and G. Bleys, <u>J. Phys. Chem. 90</u>: 3386 (1986).

113. A. Bonfillon, F. Sicoli, and D. Langevin, <u>J. Colloid Interface Sci 168</u>: 497 (1994).

114. E. A. G. Aniansson, and S. N. Wall, <u>J. Phys. Chem. 78</u>: 1024 (1974).

115. E. A. G. Aniansson, and S. N. Wall, <u>J. Phys. Chem. 79</u>: 857 (1975).

116. E. A. G. Aniansson, and S. N. Wall, in: <u>Chemical and Biological Applications of Relaxation Spectrometry</u> (E. Wyn-Jones, ed.), Reidel, Dordrecht, 1975, p. 223.

117. E. A. G. Aniansson, S. N. Wall, M. Almgren, H. Hoffmann, I. Kielmann, W. Ulbricht, R. Zana, J. Lang, and C. Tondre, <u>J. Phys. Chem. 80</u>: 905 (1976).

118. J. Lucassen, <u>J. Chem. Soc., Faraday Trans. I 72</u>: 76 (1976).

119. G. C. Kresheck, E. Hamori, G. Davenport, and H. A. Scheraga, <u>J. Am. Chem. Soc. 88</u>: 264 (1966).

120. N. Muller, <u>J. Phys. Chem. 79</u>: 287 (1975).

121. H. Hoffmann, R. Nagel, G. Platz, and W. Ulbrich, <u>Colloid Polym. Sci. 254</u>: 821 (1976).

122. R. Miller, <u>Colloid Polym. Sci. 259</u>: 1124 (1981).

123. K. D. Danov, P. M. Vlahovska, T. Horozov, C. D. Dushkin, P. A. Kralchevsky, A. Mehreteab, and G. Broze, <u>J. Colloid Interface Sci. 183</u>: 223 (1996).

124. D. H. McQueen, and J. J. Hermans, <u>J. Colloid Interface Sci. 39</u>: 389 (1972).

125. R. H. Weinheimer, D. F. Evans, and E. L. Cussler, <u>J. Colloid Interface Sci. 80</u>: 357 (1981).

126. D. E. Evans, S. Mukherjee, D. J. Mitchell, and B. W. Ninham, <u>J. Colloid Interface Sci. 93</u>: 184 (1983).

127. P. Joos, and L. van Hunsel, <u>Colloids Surf. 33</u>: 99 (1988).

128. V. B. Feinerman, <u>Kolloidn. Zh. 43</u>: 94 (1981).

129. V. B. Feinerman, and Y. M. Rakita, <u>Kolloidn. Zh. 52</u>: 106 (1990).

130. C. D. Dushkin, I. B. Ivanov, and P. A. Kralchevsky, <u>Colloids Surf. 60</u>: 235 (1991).

131. C. D. Dushkin, and I. B. Ivanov, <u>J. Surface Sci. Technol. 6</u>: 269 (1990).

132. C. D. Dushkin, and I. B. Ivanov, <u>Colloids Surf. 60</u>: 213 (1991).

133. B. A. Noskov, <u>Kolloidn Zh. 52</u>: 509 (1990).

134. B. A. Noskov, <u>Kolloidn Zh. 52</u>: 796 (1990).

135. N. Kamenka, B. Lindman, and B. Brun, <u>Colloid Polym. Sci. 252</u>: 144 (1974).

136. C. G. M. Marangoni, <u>Ann. Physik. (Poggendorff) 3</u>: 337 (1871).

137. M. J. Boussinesq, <u>Ann. Chim. Phys. 29</u>: 349 (1913).

138. J. Hunter, <u>Foundation of Colloid Science Vol. I</u>, Clarendon Press, Oxford, 1987.

139. J. Hunter, <u>Foundation of Colloid Science Vol. II</u>, Clarendon Press, Oxford, 1989.

140. L. E. Scriven, <u>Chem. Eng. Sci. 12</u>: 98 (1960).

141. J. C. Slattery, <u>Chem. Eng. Sci. 19</u>: 453 (1964).

142. J. C. Slattery, <u>Interfacial Transport Phenomena</u>, Springer-Verlag, New York, 1990.

143. I. B. Ivanov, and P. A. Kralchevsky, Mechanics and Thermodynamics of Curved Thin Films, in: <u>Thin Liquid Films</u>, I. B. Ivanov, Ed., M. Dekker, New York, 1988, p. 49.

144. C. V. Sterling, L. E. Scriven, <u>AIChE J. 5</u>: 514 (1959).

145. F. G. Goodrich, <u>Proc. Roy. Soc. London A374</u>: 341 (1981).

146. L. D. Landau, and E. M. Lifshitz, <u>Fluid Mechanics</u>, Pergamon Press, Oxford, 1984.

147. A. A. Lebedev, <u>Zhur. Russ. Fiz. Khim. 48</u> (1916).

148. A. Silvey, <u>Phys. Rev. 7</u>: 106 (1916).

149. W. Rybczynski, <u>Bull. Intern. Acad. Sci. (Cracovie) A</u> (1911).

150. J. S. Hadamar, <u>Comp. Rend. Acad. Sci. (Paris) 152</u>: 1735 (1911).

151. W. D. Harkins, R. J. Meyers, <u>Nature 140</u>:465 (1937).

152. D. G. Dervichian, and M. Joly, <u>J. Phys. Radium 10</u>: 375 (1939).

153. J. T. Davies, <u>Proc. 2nd Int. Congr. Surf. Act. 1</u>: 220 (1957).

154. R. J. Mannheimer, and R. S. Schechter, <u>J. Colloid Interface Sci. 32</u>: 195 (1970).

155. A. J. Pintar, A. B. Israel, and D. T. Wasan, <u>J. Colloid Interface Sci. 37</u>: 52 (1971).

156. D. T. Wasan, V. Mohan, Interfacial rheological properties of fluid interfaces containing surfactants, in: <u>Improved Oil Recovery by Surfactant and Polymer Flooding</u> (D. O. Shah, and R. S. Schechter, eds.), Academic Press, New York, 1977, p. 161.

157. F. C. Goodrich, and A. K. Chatterjee, <u>J. Colloid Interface Sci. 34</u>: 36 (1970).

158. P. B. Briley, A. R. Deemer, and J. C. Slattery, <u>J. Colloid Interface Sci. 56</u>: 1 (1976).

159. R. Shail, <u>J. Engng. Math. 12</u>: 59 (1978).

160. S. G. Oh, and J. C. Slattery, <u>J. Colloid Interface Sci. 67</u>: 516 (1978).

161. A. M. Davis, and M. E. O'Neill, <u>Int. J. Multiphase Flow 5</u>: 413 (1979).

162. R. Shail, and D. K. Gooden, <u>Int. J. Multiphase Flow 7</u>: 245 (1981).

163. T. S. Jiang, and J. C. Slattery, <u>J. Colloid Interface Sci. 96</u>: 7 (1983).

164. A. G. Brown, W. C. Thuman, and J. W. McBain, <u>J. Colloid Sci. 8</u>: 491 (1953).

165. N. Lifshutz, M. G. Hedge, and J. C. Slattery, <u>J. Colloid Interface Sci. 37</u>: 73 (1971).

166. F. C. Goodrich, L. H. Allen, <u>J. Colloid Interface Sci. 40</u>: 329 (1972).

167. F. C. Goodrich, L. H. Allen, and A. M. Poskanzer, <u>J. Colloid Interface Sci. 52</u>: 201 (1975).

168. A. M. Poskanzer, and F. C. Goodrich, <u>J. Colloid Interface Sci. 52</u>: 213 (1975).

169. A. M. Poskanzer, and F. C. Goodrich, <u>J. Phys. Chem. 79</u>: 2122 (1975).

170. G. T. Shahin, <u>The Stress Deformation Interfacial Rheometer</u>. Ph.D. Thesis, Department of Chemical Engineering, University of Pennsylvania, State College, Pennsylvania, 1986.

171. J. T. Petkov, N. D. Denkov, K. D. Danov, O. V. Velev, R. Aust, and F. Durst, <u>J. Colloid Interface Sci. 172</u>: 147 (1995).

172. J. T. Petkov, K. D. Danov, N. D. Denkov, R. Aust, and F. Durst, <u>Langmuir 12</u>: 2650 (1996).

173. P. A. Kralchevsky, V. N. Paunov, N. D. Denkov, and K. Nagayama, <u>J. Colloid Interface Sci. 167</u>: 47 (1994).

174. O. D. Velev, N. D. Denkov, V. N. Paunov, P. A. Kralchevsky, and K. Nagayama, <u>J. Colloid Interface Sci. 167</u>: 66 (1994).

175. K. D. Danov, R. Aust, F. Durst, and U. Lange, <u>J. Colloid Interface Sci. 175</u>: 36 (1995).

176. R. L. Bendure, <u>J. Colloid Interface Sci. 35</u>: 238 (1971).

177. K. J. Mysels, <u>Langmuir 2</u>: 428 (1986).

178. R. P. Garrett, and D. R. Ward, <u>J. Colloid Interface Sci. 132</u>: 475 (1988).

179. R. L. Kao, D. A. Edwards, D. T. Wasan, and E. Chen, <u>J. Colloid Interface Sci. 148</u>**:** 247 (1992).

180. R. L. Kao, D. A. Edwards, D. T. Wasan, and E. Chen, <u>J. Colloid Interface Sci. 148</u>**:** 257 (1992).

181. K. D. Watke, R. Miller, K. Lunkenheimer, Theory of diffusion at an oscillatory bubble surface, <u>Abh. Akad. Wiss. DDR, Originalbertr.</u>, Berlin, E. Ger., 1971.

182. K. Malysa, K. Lunkenheimer, R. Miller, and C. Hartenstein, <u>Colloids Surf. 3</u>: 329 (1981).

183. K. Lunkenheimer, C. Hartenstein, R. Miller, and K. D. Watke, <u>Colloids Surf. 8</u>: 271 (1984).

184. J. H. Clint, E. L. Neustadter, and T. J. Jones, <u>Dev. Pet. Sci. 13</u>: 135 (1981).

185. O. Velev, A. Nikolov, N. Denkov, G. Doxastakis, V. Kiosseoglu, and G. Stalidis, <u>Food Hydrocoll. 7</u>: 55 (1993).

186. R. Nagarajan, and D. T. Wasan, <u>J. Colloid Interface Sci. 159</u>: 164 (1993).

187. A. MacLeod, and C. J. Radke, <u>J. Colloid Interface Sci. 160</u>: 43 (1993).

188. D. E. Graham, and M. C. Phillips, <u>J. Colloid Interface Sci. 76</u>: 240 (1980).

189. R. C. Brown, <u>Phys. Soc. Rept. Progress Physics 7</u>: 180 (1940).

190. J. A. Mann, and R. S. Hansen, <u>J. Colloid Sci. 18</u>: 757 (1963).

191. J. Lucassen, and R. S. Hansen, <u>J. Colloid Interface Sci. 22</u>: 32 (1966).

192. J. Lucassen, and M. van den Tempel, <u>J. Colloid Interface Sci. 41</u>: 491 (1972).

193. D. Langevin, <u>J. Colloid Interface Sci. 80</u>: 412 (1981).

194. L Tink, D. T. Wasan, and K. Miyano, <u>J. Colloid Interface Sci. 107</u>: 345 (1985).

195. S. Hard, and Neumann, <u>J. Colloid Interface Sci. 120</u>: 15 (1987).

196. Loglio, E. Rillaerts, and P. Joos, <u>Colloid Polym. Sci. 259</u>: 1221 (1981).

197. P. Somasundaran, M. Danitz, and K. J. Mysels, <u>J. Colloid Interface Sci. 48</u>: 410 (1974).

198. F. Boury, Tz. Ivanova, I. Panaïotov, J. E. Proust, A. Bois, and J. Richou, <u>Langmuir 11</u>: 1636 (1995).

199. F. D. Rumscheid, and S. G. Mason, <u>J. Colloid Interface Sci. 16</u>: 210 (1961).

200. W. J. Phillips, R. W. Graves, and R. W. Flummerfelt, <u>J. Colloid Interface Sci. 76</u>: 350 (1980).

201. J. C. Slattery, J. D. Chen, C. P. Thomas, and P. D. Fleming, <u>J. Colloid Interface Sci. 73</u>: 483 (1980).

202. W. Helfrich, <u>Z. Naturforsch. 28c</u>: 693 (1973).

203. P. M. Naghdi, The Theory of Shells and Plates, in: <u>Handbuch der Physik</u>, S. Flügge, Ed., Vol. VIa/2, Springer, Berlin, 1972, p. 425.

204. Ya. S. Podstrigach, and Yu. Z. Povstenko, <u>Introduction in Mechanics of Surface Phenomena in Deformable Solids</u>, Naukova Dumka, Kiev, 1985 (in Russian).

205. P. A. Kralchevsky, J. C. Eriksson, and S. Ljunggren, <u>Adv. Colloid Interface Sci. 48</u>: 19 (1994).

206. E. A. Evans, and R. Skalak, <u>Mechanics and Thermodynamics of Biomembranes</u>, CRC Press, Boca Raton, Florida, 1979.

207. P. A. Kralchevsky, <u>J. Colloid Interface Sci. 137</u>: 217 (1990).

208. T. D. Gurkov, and P. A. Kralchevsky, <u>Colloids Surf. 47</u>: 45 (1990).

209. F. P. Buff, <u>J. Chem. Phys. 23</u>: 419 (1955).

210. P. A. Kralchevsky, T. D. Gurkov, and I. B. Ivanov, <u>Colloids Surf. 56</u>: 149 (1991).

211. R. C. Tolman, <u>J. Chem. Phys. 17</u>: 333 (1949).

212. P. A. Kralchevsky, and T. D. Gurkov, <u>Colloids Surf. 56</u>: 101 and 119 (1991).

213. P. A. Kralchevsky, T. D. Gurkov, and K. Nagayama, <u>J. Colloid Interface Sci. 180</u>: 619 (1996).

214. J. L. Vivoy, W. M. Gelbart, and A. Ben Shaul, <u>J. Chem. Phys. 87</u>: 4114 (1987).

215. I. Szleifer, D. Kramer, A. Ben Shaul, D. Roux, and W. M. Gelbart, <u>Phys. Rev. Lett.60</u>: 1966 (1988).

216. S. T. Milner, and T. A. Witten, <u>J. Phys. (Paris) 49</u>: 1951 (1988).

217. I. Szleifer, D. Kramer, A. Ben Shaul, W.M. Gelbart, and S. Safran, <u>J. Phys. Chem. 92</u> : 6800 (1990).

218. Z. G. Wang, and S. A. Safran, <u>J. Chem. Phys. 94</u>: 679 (1991).

219. J. Ennis, <u>J. Chem. Phys. 97</u>: 663 (1992).

220. N. Dan, P. Pincus, and S. A. Safran, <u>Langmuir 9</u>: 2768 (1993).

221. P. A. Barneveld, J. M. H. M. Scheutjens, and J. Lyklema, <u>Langmuir 8</u>: 3122 (1993); <u>Langmuir 10</u> : 1084 (1994).

222. J. C. Melrose, <u>Ind. Eng. Chem. 60</u>: 53 (1968).

223. L. Boruvka, and A. W. Neumann, <u>J. Chem. Phys. 66</u>: 5464 (1977).

224. V. S. Markin, M. M. Kozlov, and S. I. Leikin, <u>J. Chem. Soc. Faraday Trans. 2, 84</u>: 1149 (1988).

225. J. C. Eriksson, and S. Ljunggren, <u>J. Colloid Interface Sci. 152</u>: 575 (1992).

226. J. C. Eriksson, S. Ljunggren, and P. A. Kralchevsky, <u>J. Colloid Interface Sci. 161</u>: 133 (1993).

227. H. N. W. Lekkerkerker, <u>Physica A 167</u>: 384 (1990).

228. J. Th. G. Overbeek, Electrochemistry of the Double Layer, in: <u>Colloid Science, Vol. 1</u>, H. R. Kruyt, Ed., Elsevier, Amsterdam, 1953.

229. S. A. Simon, T. J. McIntosh, and A. D. Magid, <u>J. Colloid Interface Sci. 126</u>: 74 (1988).

230. D. N. Petsev, N. D. Denkov, and P. A. Kralchevsky, <u>J. Colloid Interface Sci. 176</u>: 201 (1995).

231. G. J. M. Koper, W. F. C. Sager, J. Smeets, and D. Bedeaux, <u>J. Phys. Chem. 99</u>**:** 13291 (1995).

232. B. P. Binks, <u>Langmuir 9</u>: 25 (1993).

233. P. A. Kralchevsky, V. N. Paunov, N. D. Denkov, and K. Nagayama, <u>J. Chem. Soc. Faraday Trans. 91</u> : 3415 (1995).

234. P. A. Kralchevsky, and I. B. Ivanov,. <u>J. Colloid Interface Sci. 137</u>: 234, (1990).

235. A. I. Rusanov, <u>Phase Equilibria and Surface Phenomena</u>, Khimia, Leningrad, 1967 (in Russian); <u>Phasengleichgewichte und Grenzflächenerscheinungen</u>, Akademie Verlag, Berlin, 1978.

236. B. V. Derjaguin, and M. M. Kussakov, <u>Acta Physicochem. USSR, 10</u>: 153 (1939).

237. D. Exerowa, and A. Scheludko, <u>Bull. Inst. Chim. Phys. Bulg. Acad. Sci. 4</u>: 175 (1964).

238. K. J. Mysels, <u>J. Phys. Chem., 68</u>: 3441 (1964).

239. D. Exerowa, <u>Commun. Dept. Chem. Bulg. Acad. Sci. 11</u>: 739 (1978).

240. P. M. Kruglyakov, Equilibrium properties of free films and stability of foams and emulsions, in: <u>Thin Liquid Films</u>, I.B.Ivanov, Ed., M. Dekker, New York, 1988, p.767.

241. G. A. Martynov, and B. V. Derjaguin, <u>Kolloidn. Zh. 24</u>: 480 (1962).

242. B. V. Toshev, and I. B. Ivanov, <u>Colloid Polym. Sci. 253</u>: 558 (1975).

243. I. B. Ivanov, and B. V. Toshev, <u>Colloid Polym. Sci. 253</u>: 593 (1975).

244. A. Frumkin, <u>Zh. Phys. Khim. USSR, 12</u>: 337 (1938).

245. J. A. de Feijter, Thermodynamics of thin liquid films, in: <u>Thin Liquid Films,</u> I.B.Ivanov, Ed., M. Dekker, New York, 1988, p.1.

246. V. S. Veselovsky, and V. N. Pertzov, <u>Z. Phys. Khim. 8</u>: 245 (1936).

247. B. A. Pethica, <u>Rep. Progr. Appl. Chem. 46</u>: 14 (1961).

248. S. Torza and S. G. Mason, <u>Colloid Polym. Sci. 246</u>: 593 (1971).

249. P. R. Pujado, and L. E. Scriven, <u>J. Colloid Interface Sci. 40</u>: 82 (1975).

250. J. E. Lane, <u>J. Colloid Interface Sci. 52</u>: 155 (1972).

251. I. B. Ivanov, P. A. Kralchevsky, and A. D. Nikolov, <u>J. Colloid Interface Sci. 112</u>: 97 (1986).

252. P. A. Kralchevsky, and I. B. Ivanov, <u>Chem. Phys. Lett., 121</u>**:** 111 (1985); ibid. p. 116 (1985).

253. A. D. Nikolov, P. A. Kralchevsky, I. B. Ivanov, and A. S. Dimitrov, <u>AIChE Symposium Ser. 252, Vol. 82</u>: 82 (1986).

254. V. M. Starov, and N. V. Churaev, <u>Kolloidn. Zh. 42</u>: 703 (1980).

255. N. V. Churaev, V. M. Starov, and B. V. Derjaguin, <u>J. Colloid Interface Sci. 89</u>: 16 (1982).

256. H. M. Princen, The Equilibrium Shape of Interfaces, Drops, and Bubbles, in <u>Surface and Colloid Science, Vol.2</u>, Matijevic, E., Ed., Wiley, New York, 1969, p. 1.

257. J. A. de Feijter, and A. Vrij, <u>J. Electroanal. Chem. 47</u>: 9 (1972).

258. N. D. Denkov, D. N. Petsev, and K. D. Danov, <u>J. Colloid Interface Sci. 176</u>: 189 (1995).

259. A. S. Dimitrov, A. D. Nikolov, P. A. Kralchevsky, and I. B. Ivanov, <u>J. Colloid Interface Sci. 151</u>: 462 (1992).

260. T. D. Gurkov, and P. A. Kralchevsky, <u>J. Dispersion Sci. Technol. 18</u>: 609 (1996).

261. P. Richmond, <u>J. Chem. Soc. Faraday Trans. 2, 70</u>: 1066 (1974).

262. J. A. de Feijter, and A. Vrij, <u>J. Colloid Interface Sci., 70</u>: 456 (1979).

263. R. Kjellander, and S. Marcelja, <u>Chem. Phys. Lett., 112</u>: 49 (1984).

264. L. A. Lobo, A. D. Nikolov, A. S. Dimitrov, P. A. Kralchevsky, and D. T. Wasan, <u>Langmuir, 6</u>: 995 (1990).

265. B. V. Derjaguin, <u>Acta Physicochim. USSR, 12</u>: 181 (1940).

266. H. M. Princen, and S. G. Mason, <u>J. Colloid Sci. 20</u>: 156 (1965).

267. P. A. Kralchevsky, K. D. Danov, and I. B. Ivanov, Thin Liquid Film Physics, in: <u>Foams: Theory, Measurements and Applications</u>, R.K. Prud'homme, Ed.; M. Dekker, New York, 1995, p.1.

268. V. Bergeron, and C. J. Radke, <u>Langmuir 8</u>: 3020 (1992).

269. K. Marinova, private communication.

270. I. B. Ivanov, A. S. Dimitrov, A. D. Nikolov, N. D. Denkov and P. A. Kralchevsky, <u>J. Colloid Interface Sci. 151</u>: 446 (1992).

271. G. A. Martynov, V. M. Starov, and N. V. Churaev, <u>Kolloidn. Zh. 39</u>: 472 (1977).

272. V. M. Starov, <u>Adv. Colloid Interface Sci. 39</u>: 147 (1992).

273. A. Scheludko, and D. Exerowa, <u>Kolloid.-Z. 165</u>: 148 (1959).

274. Z. M. Zorin, and N. V. Churaev, <u>Kolloidn. Zh. 30</u>: 371 (1968).

275. B. V. Derjaguin, I. G. Ershova, and N. V. Churaev, <u>Dokl. AN USSR 182</u>: 368 (1968).

276. B. V. Derjaguin, <u>Kolloid Zeits., 69</u>: 155 (1934).

277. P. Attard, and J. L. Parker, <u>J. Phys. Chem. 96</u>: 5086 (1992).

278. D. Tabor, and R. H. S. Winterton, <u>Nature 219</u>: 1120 (1968).

279. A. Graciaa, G. Morel, P. Saulnier, J. Lachaise, R. S. Schechter, <u>J. Colloid Interface Sci. 172</u>: 131 (1995).

280. A. D. Nikolov, D. T. Wasan, P. A. Kralchevsky, and I. B. Ivanov, "Ordered structures in thinning micellar foam and latex films", in: <u>Ordering and Organisation in Ionic Solutions</u>, N. Ise and I. Sogami, Eds., World Scientific, Singapore, 1988.

281. D. T. Wasan, A. D. Nikolov, P. A. Kralchevsky, and I. B. Ivanov, <u>Colloids Surf. 67</u>: 139 (1992).

282. A. D. Nikolov, P. A. Kralchevsky, I. B. Ivanov, and D. T. Wasan, <u>J. Colloid Interface Sci. 133</u>: 13 (1989).

283. P. Richetti, and P. Kékicheff, <u>Phys. Rev. Lett. 68</u>: 1951, (1992); ibid., p. 1955.

284. W. B. Russel, D. A. Saville, and W. R. Schowalter, <u>Colloidal Dispersions</u>, Cambridge Univ. Press, Cambridge, 1989.

285. W. H. Keesom, <u>Proc. Amst. 15</u>: 850 (1913).

286. P. Debye, <u>Physik, 2</u>: 178 (1920).

287. F. London, <u>Z. Phys., 63</u>: 245 (1930).

288. F. London, <u>Trans. Faraday Soc. 83</u>: 8 (1937).

289. H. C. Hamaker, <u>Physics, 4</u>: 1058 (1937).

290. B. V. Derjaguin, <u>Theory of Stability of Colloids and Thin Liquid Films</u>, Plenum Press: Consultants Bureau, New York, 1989.

291. S. Usui, H. Sasaki, and F. Hasegawa, <u>Colloids Surf. 18</u>: 53 (1986).

292. E. M. Lifshitz, <u>Soviet Phys. JETP (Engl. Transl.) 2</u>: 73 (1956).

293. I. E. Dzyaloshinskii, E. M. Lifshitz, and L. P. Pitaevskii, <u>Adv. Phys. 10</u>: 165 (1961).

294. S. Nir, and C. S. Vassilieff, "Van der Waals interactions in thin films" in: <u>Thin Liquid Films</u>, I. B. Ivanov, Ed., M. Dekker, New York, 1988, p.207.

295. K. D. Danov, D. N. Petsev, N. D. Denkov, and R. Borwankar, <u>J. Chem. Phys. 99</u>: 7179 (1993).

296. H. R. Casimir, and D. Polder, <u>Phys. Rev. 73</u>: 360, 1948.

297. J. Mahanty, and B. W. Ninham, <u>Dispersion Forces</u>, Academic Press, New York, 1976.

298. R. M. Pashley, P. M. McGuiggan, B. W. Ninham, and D. F. Evans, <u>Science 229</u>: 1088 (1985).

299. Y. I. Rabinovich, and B. V. Derjaguin, <u>Colloids Surf. 30</u>: 243 (1988).

300. J. L. Parker, D. L. Cho, and P. M. Claesson, <u>J. Phys. Chem. 93</u>: 6121 (1989).

301. H. K. Christenson, P. M. Claesson, J. Berg and P. C. Herder, <u>J. Phys. Chem. 93</u>: 1472, (1989).

302. H. K. Christenson, J. Fang, B. W. Ninham, and J. L. Parker, <u>J. Phys. Chem. 94</u>: 8004 (1990).

303. J. C. Eriksson, S. Ljunggren, and P. M. Claesson, <u>J. Chem. Soc. Faraday Trans. 2, 85</u>: 163 (1989).

304. H. K. Christenson, J. Fang, and J. N. Israelachvili, <u>Phys. Rev. B, 39</u>: 11750 (1989).

305. V. S. J. Craig, B. W. Ninham, and R. M. Pashley, <u>J. Phys. Chem. 97</u>: 10192 (1993).

306. W. A. Ducker, Z. Xu, and J. N. Israelachvili, <u>Langmuir 10</u>: 3279 (1994).

307. P. H. Elworthy, A. T. Florence, J. A. Rogers, <u>J. Colloid Interface Sci. 35</u>: 23 (1971).

308. D. Exerowa, M. Zacharieva, R. Cohen, and D. Platikanov, <u>Colloid Polym. Sci. 257</u>: 1089 (1979).

309. P. Becher, M. J. Schick, in: <u>Nonionic Surfactants,</u> M. J. Schick Ed., M. Dekker, New York, 1987, p. 435.

310. O. D. Velev, T. D. Gurkov, S. K. Chakarova, B. Dimitrova, I. B. Ivanov, and R. P. Borwankar, <u>Colloids Surf. 83</u>: 43 (1994).

311. I. Langmuir, <u>J. Chem. Phys. 6</u>: 873 (1938).

312. V. M. Muller, <u>Kolloidn. Zh. 38</u>: 704 (1976).

313. B. V. Derjaguin, and L. D. Landau, <u>Acta Physicochim. USSR, 14</u>: 633 (1941).

314. I. F. Efremov, "Periodic Colloidal Structures", in: <u>Colloid and Surface Science,Vol.8</u>, E. Matijevic, Ed., Wiley, New York, 1976, p.85.

315. H. Schultze, <u>J. Prakt. Chem. 25</u>: 431 (1882).

316. W. B. Hardy, <u>Proc. Roy. Soc. (London) 66</u>: 110 (1900).

317. J. N. Israelachvili, and H. Wennerström, <u>J. Phys. Chem. 96</u>: 520 (1992).

318. J. N. Israelachvili, and G. E. Adams, <u>J. Chem. Soc. Faraday Trans. 1, 74</u>: 975 (1978).

319. J. N. Israelachvili, and R. M. Pashley, <u>Nature 300</u>: 341 (1982).

320. R. M. Pashley, <u>J. Colloid Interface Sci. 80</u>: 153 (1981).

321. R. M. Pashley, <u>J. Colloid Interface Sci. 83</u>: 531 (1981).

322. T. W. Healy, A. Homolam, R. O. James, and R. J. Hunter, <u>Faraday Discuss. Chem. Soc. 65</u>: 156 (1978).

323. S. Marçelja, and N. Radiç, <u>Chem. Phys Lett. 42</u>: 129 (1976).

324. B. Jönsson, and H. Wennerström, <u>J. Chem. Soc., Faraday Trans. 2, 79</u>: 19 (1983).

325. S. Leikin, and A. A. Kornyshev, <u>J. Chem. Phys. 92</u>: 6890 1990.

326. D. Henderson, and M. Lozada-Cassou, <u>J. Colloid Interface Sci. 114</u>: 180 (1986); <u>ibid. 162</u>: 508 (1994).

327. S. Basu, and M. M. Sharma, <u>J. Colloid Interface Sci. 165</u>: 355 (1994).

328. V. N. Paunov, R. I. Dimova, P. A. Kralchevsky, G. Broze, and A. Mehreteab, <u>J. Colloid Interface Sci. 182</u>: 239 (1996).

329. J. J. Bikerman, <u>Philos. Mag. 33</u>: 384 (1942).

330. J. S. Rowlinson, "Development of theories of inhomogeneous fluids", in: <u>Fundamentals of Inhomogeneous Fluids</u>: D. Henderson, Ed.., M. Dekker, New York, 1992.

331. P. Claesson, A. M. Carmona-Ribeiro, K. Kurihara, <u>J. Phys. Chem. 93</u>: 917 (1989).

332. R. G. Horn, D. T. Smith, and W. Haller, <u>Chem. Phys. Lett., 162</u>: 404 (1989).

333. P. Debye, and E. Hückel, <u>Z. Phys. 24</u>: 185 (1923).

334. P. Debye, and E. Hückel, <u>Z. Phys. 24</u>: 305 (1923).

335. R. A. Robinson, and R. H. Stokes, <u>Electrolyte Solutions</u>, Butterworths, London, 1959.

336. L. Guldbrand, B. Jönsson, H. Wennerström, and P. Linse, <u>J. Chem. Phys. 80</u>: 2221 (1984).

337. R. Kjellander, and S. Marcelja, <u>J. Phys. Chem., 90</u>: 1230 (1986).

338. P. Attard, D. J. Mitchell, and B. W. Ninham, <u>J. Chem. Phys., 89</u>: 4358 (1988).

339. P. A. Kralchevsky, and V. N. Paunov, <u>Colloids Surf. 64</u>: 245 (1992).

340. V. N. Paunov, and P. A. Kralchevsky, <u>Colloids Surf. 64</u>: 265 (1992).

341. M. J. Grimson, P. Richmond, and C. S. Vassilieff, in: <u>Thin Liquid Films</u>, I. B. Ivanov, Ed., M. Dekker, New York, 1988; p. 298.

342. E. S. Johnnott, <u>Phil. Mag. 70</u>: 1339 (1906).

343. R. E. Perrin, <u>Ann. Phys. 10</u>: 160 (1918).

344. H. G. Bruil, and J. Lyklema, <u>Nature 233</u>: 19 (1971).

345. S. Friberg, St. E. Linden, and H. Saito, <u>Nature 251</u>: 494 (1974).

346. J. W. Keuskamp, and J. Lyklema, <u>ACS Symp. Ser. 8</u>: 191 (1975).

347. P. M. Kruglyakov, <u>Kolloidn. Zh. 36</u>: 160 (1974).

348. P. M. Kruglyakov, and Yu. G. Rovin, <u>Physical Chemistry of Black Hydrocarbon Films</u>, Nauka, Moscow, 1978 [in Russian].

349. E. Manev, S. V. Sazdanova, and D. T. Wasan, <u>J. Dispersion Sci. Technol. 5</u>: 111 (1984).

350. A. D. Nikolov, and D. T. Wasan, <u>J. Colloid Interface Sci. 133</u>: 1 (1989).

351. E. S. Basheva, A. D. Nikolov, P. A. Kralchevsky, I. B. Ivanov, and D. T. Wasan, in: <u>Surfactants in Solution, Vol. 12</u>, K.L.Mittal and D.O. Shah, Eds., Plenum Press, New York, 1991, p.467.

352. A. D. Nikolov, D. T. Wasan, N. D. Denkov, P. A. Kralchevsky, and I. B. Ivanov, <u>Prog. Colloid Polym. Sci. 82</u>: 87 (1990).

353. P. A. Kralchevsky, A. D. Nikolov, D. T. Wasan, and I. B. Ivanov, <u>Langmuir 6</u>: 1180 (1990).

354. K. J. Mysels, <u>J. Phys. Chem. 68</u>: 3441 (1964).

355. N. D. Denkov, and K. Nagayama, <u>Phys. Rev. Lett. 76</u>: 2354(1996).

356. C. D. Dushkin, K. Nagayama, T. Miwa, and P.A. Kralchevsky, <u>Langmuir 9</u>: 3695 (1993).

357. R. G. Horn, and J. N. Israelachvili, <u>Chem. Phys. Lett. 71</u>: 192 (1980).

358. S. Asakura, and F. Oosawa, <u>J. Chem. Phys. 22</u>: 1255 (1954); <u>J. Polym. Sci. 33</u>: 183 (1958).

359. H. de Hek, and A. Vrij, <u>J. Colloid Interface Sci. 84</u>: 409 (1981).

360. I. K. Snook, and W. van Megen, <u>J. Chem. Phys. 72</u>: 2907 (1980).

361. R. Kjellander, and S. Marçelja, <u>Chem. Phys Lett. 120</u>: 393 (1985).

362. P. Tarazona, and L. Vicente, <u>Mol. Phys. 56</u>: 557 (1985).

363. R. Evans, and A. O. Parry, <u>J. Phys. Condens. Matter 2</u>: SA15 (1990).

364. D. Henderson, <u>J. Colloid Interface Sci. 121</u>: 486 (1988).

365. X. L. Chu, A. D. Nikolov, and D. T. Wasan, <u>Langmuir 10</u>: 4403 (1994).

366. X.L. Chu, A. D. Nikolov, and D. T. Wasan, <u>J. Chem. Phys. 103</u>: 6653 (1995).

367. M. L. Pollard, and C. J. Radke, <u>J. Chem. Phys. 101</u>: 6979 (1994).

368. P. A. Kralchevsky, and N. D. Denkov, <u>Chem. Phys. Lett. 240</u>: 385 (1995); <u>Prog. Colloid Polymer Sci. 98</u>: 18 (1995).

369. N. F. Carnahan, and K. E. Starling, <u>J. Chem. Phys. 51</u>: 635 (1969).

370. R. Kjellander, and S. Sarman, <u>Chem. Phys. Lett. 149</u>: 102 (1988).

371. D. T. Mitchell, B. W. Ninham, and B. A. Pailthorpe, <u>J. Chem. Soc. Faraday Trans. II, 74</u>: 1116 (1978).

372. G. Karlström, <u>Chem. Scripta 25</u>: 89 (1985).

373. P. M. Claesson, R. Kjellander, P. Stenius, and H. K. Christenson, <u>J. Chem. Soc. Faraday Trans. I, 82</u>: 2735 (1986).

374. K. G. Marinova, T. D. Gurkov, G. B. Bantchev and P.A. Kralchevsky, "Role of the Oscillatory Structural Forces for the Stability of Emulsions", In: <u>Proceedings of the Second World Congress on Emulsion</u> (Vol.2, Paper 2-3-151), Bordeaux, 1997.

375. C. Bondy, <u>Trans. Faraday Soc. 35</u>: 1093 (1939).

376. P. D. Patel, and W. B. Russel, <u>J. Colloid Interface Sci. 131</u>: 192 (1989).

377. M. P. Aronson, <u>Langmuir 5</u>: 494 (1989).

378. B. van Lent, R. Israels, J. Scheutjens and G. Fleer, <u>J. Colloid Interface Sci. 137</u>: 380 (1990).

379. J. F. Joanny, L. Leibler, and P. G. de Gennes, <u>J. Polym. Sci. 17</u>: 1073 (1979).

380. E. Evans, and D. Needham, <u>Macromolecules 21</u>: 1822 (1988).

381. Th. F. Tadros, , "Steric interactions in thin liquid films", in: <u>Thin Liquid Films,</u> I.B.Ivanov, Ed., M. Dekker, New York, 1988, p.331.

382. S. S. Patel, and M. Tirel, <u>Ann. Rev. Phys. Chem. 40</u>: 597 (1989).

383. H. J. Ploehn , and W. B. Russel, <u>Adv. Chem. Eng., 15</u>: 137 (1990).

384. P. G. de Gennes, <u>Scaling Concepts in Polymer Physics</u>, Cornel Univ. Press, Ithaca, NY, 1979, Chap. III.1.

385. A. K. Dolan, and S. F. Edwards, <u>Proc. Roy. Soc. (London) A337</u>: 509 (1974).

386. A. K. Dolan, and S. F. Edwards, <u>Proc. Roy. Soc. (London) A343</u>: 627 (1975).

387. P. G. de Gennes, <u>C. R.. Acad. Sci. (Paris) 300</u>: 839 (1985).

388. P. G. de Gennes, <u>Adv. Colloid Interface Sci., 27</u>: 189 (1987).

389. S. J. Alexander, <u>Physique 38</u>: 983 (1977).

390. H. J. Taunton, C. Toprakcioglu, L.J. Fetters, and J. Klein, <u>Macromolecules 23</u>: 571 (1990).

391. J. Klein, and P. Luckham, <u>Nature 300</u>, 429 (1982); <u>Macromolecules 17</u>: 1041 (1984).

392. P. F. Luckham, and J. Klein, <u>J. Chem. Soc. Faraday Trans. 86</u>: 1363 (1990).

393. H. Sonntag, B. Ehmka, R. Miller, and L. Knapschinski, <u>Adv. Colloid Interface Sci. 16</u>: 381 (1982).

394. G. A. E. Aniansson, S.N. Wall, M. Almgren, H. Hoffman, I. Kielmann, W. Ulbricht, R. Zana, J. Lang, and C. Tondre, <u>J. Phys. Chem. 80</u>: 905 (1976).

395. G. A. E. Aniansson, <u>J. Phys. Chem. 82</u>: 2805 (1978).

396. W. Helfrich, <u>Z. Naturforsch. 33a</u>: 305 (1978).

397. R. M. Servuss, and W. Helfrich, <u>J. Phys. (France) 50</u>: 809 (1989).

398. L. Fernandez-Puente, I. Bivas, M. D. Mitov, and P. Méléard, <u>Europhys. Lett. 28</u>: 181 (1994).

399. C. R. Safinya, D. Roux, G. S. Smith, S. K. Sinha, P. Dimon, N. A. Clark, and A. M. Bellocq, <u>Phys. Rev. Lett. 57</u>: 2718 (1986).

400. T. J. McIntosh, A. D. Magid, and S. A. Simon, <u>Biochemistry 28</u>: 7904 (1989).

401. O. Abillon, and E. Perez, <u>J. Phys. (France) 51</u>: 2543 (1990).

402. P. Debye, <u>J. Phys. & Colloid Chemistry 51</u>: 18 (1947).

403. M. Kerker, <u>The scattering of light and other electromagnetic radiation</u>, Academic Press, New York, 1969.

404. N.A. Mazer, In <u>Dynamic Light Scattering</u>; Pecora, R., Ed.; Plenum Press: London, 1985; Chapter 8.

405. N. A. Mazer, G. B. Benedek, and M. C. Carey, <u>J. Phys. Chem. 80</u>: 1075 (1976).

406. P. J. Missel, N. A. Mazer, G. B. Benedek, C. Y. Young, and M. C. Carey, <u>J. Phys. Chem. 84</u>: 1044 (1980).

407. S. Hayashi, and S. Ikeda, <u>J. Phys. Chem. 84</u>: 744 (1980).

408. G. Porte, J. Appell, and Y. Poggl, <u>J. Phys. Chem. 84</u>: 3105 (1980).

409. G. Porte, and J. Appell, <u>J. Phys. Chem. 85</u>: 2511 (1981).

410. H. Hoffmann, J. Klaus, H. Thurn, and K. Ibel, <u>Ber. Bunsen-Ges. Phys. Chem. 87</u>: 1120 (1983).

411. J.-M. Chen, T.-M. Su, and C.Y. Mou, <u>J. Phys. Chem. 90</u>: 2418 (1986).

412. P. J. Missel, N. A. Mazer, M. C. Carey, and G. B. Benedek, <u>J. Phys. Chem. 93</u>: 8354 (1989).

413. T.-L. Lin, M.-Y. Tseng, S.-H. Chen, and M. F. Roberts, <u>J. Phys. Chem. 94</u>: 7239 (1990).

414. R. Tausk, and J. Th. G. Overbeek, <u>Colloid Interface Sci. 2</u> [Proc. Int. Conf.]: 379 (1976).

415. D. F. Nicoli, D. R. Dawson, and J. W. Offen, <u>Chem. Phys. Lett. 66</u>: 291 (1979).

416. P. J. Missel, N. A. Mazer, G. B. Benedek, and M. C. Carey, <u>J. Phys. Chem. 87</u>: 1264 (1983).

417. R. Alargova, J. Petkov, D. Petsev, I. B. Ivanov, G. Broze, and A. Mehreteab, <u>Langmuir, 11</u>: 1530 (1995); ibid. <u>13</u>: 5544 (1997).

418. J. N. Israelachvili, D. J. Mitchell, and B. W. Ninham, <u>J. Chem. Soc. Faraday Trans. II, 72</u>: 1525 (1976).

419. P. A. Kralchevsky, K. D. Danov, and N. D. Denkov, Chemical physics of colloid systems and interfaces, in: <u>Handbook of Surface and Colloid Chemistry</u> (K. S. Birdi, ed.), CRC Press, New York, 1997, p. 333.

420. I. B. Ivanov, <u>Pure Appl. Chem. 52</u>: 1241 (1980).

421. L. Lobo, I. B. Ivanov, and D. T. Wasan, <u>AIChE J. 39</u>: 322 (1993).

422. K. D. Danov, I. B. Ivanov, T. D. Gurkov, and R. P. Borwankar, <u>J. Colloid Interface Sci. 167</u>: 8 (1994).

423. K. D. Danov, O. D. Velev, I. B. Ivanov, and R. P. Borwankar, Bancroft rule and hydrodynamic stability of thin films and emulsions, <u>Proceedings of the First World Congress on Emulsion Vol. 2</u>, Paris, 1993, p. 125.

424. O. D. Velev, K. D. Danov, and I. B. Ivanov, Stability of emulsions under static and dynamic conditions, <u>J. Dispersion Sci. Technol. 18</u>: 625 (1997).

425. A. Kabalnov, and H. Wennerström, <u>Langmuir 12</u>: 276 (1996).

426. I. B. Ivanov, B. P. Radoev, T. T. Traykov, D. S. Dimitrov, E. D. Manev, and C. S. Vassilieff, <u>Proceedings of the International Conference on Colloid Surface Science</u> (E. Wolfram, ed.), Akademia Kiado, Budapest, 1975, p. 583.

427. P. Taylor, <u>Proc. Roy. Soc. (London) A108</u>: 11 (1924).

428. I. B. Ivanov, D. S. Dimitrov, P. Somasundaran, and R. K. Jain, <u>Chem. Eng. Sci. 40</u>: 137 (1985).

429. S. D. Stoyanov, K. D. Danov, and I. B. Ivanov - to be published.

430. E. Rushton, and G. A. Davies, <u>Appl. Sci. Res. 28</u>: 37 (1973).

431. S. Haber, G. Hetsroni, and A. Solan, <u>Int. J. Multiphase Flow 1</u>: 57 (1973).

432. L. D. Reed, and F. A. Morrison, <u>Int. J. Multiphase Flow 1</u>: 573 (1974).

433. G. Hetsroni, and S. Haber, <u>Int. J. Multiphase Flow 4</u>: 1 (1978).

434. F. A. Morrison, and L. D. Reed, <u>Int. J. Multiphase Flow 4</u>: 433 (1978).

435. V. N. Beshkov, B. P. Radoev, and I. B. Ivanov, <u>Int. J. Multiphase Flow 4</u>: 563 (1978).

436. Y. O. Fuentes, S. Kim, and D. J. Jeffrey, <u>Phys. Fluids 31</u>: 2445 (1988).

437. Y. O. Fuentes, S. Kim, and D. J. Jeffrey, <u>Phys. Fluids A1</u>: 61 (1989).

438. R. H. Davis, J. A. Schonberg, and J. M. Rallison, <u>Phys. Fluids A1</u>: 77 (1989).

439. X. Zhang, and R. H. Davis, <u>J. Fluid Mech. 230</u>: 479 (1991).

440. S. G. Yiantsios, and R. H. Davis, <u>J. Colloid Interface Sci. 144</u>: 412 (1991).

441. S. G. Yiantsios, and B. G. Higgins, <u>J. Colloid Interface Sci. 147</u>: 341 (1991).

442. J.-L. Joye, G. J. Hirasaki, and C. A. Miller, <u>Langmuir 8</u>: 3085 (1992).

443. J.-L. Joye, G. J. Hirasaki, and C. A. Miller, <u>Langmuir 10</u>: 3174 (1994).

444. J. M. Boulton-Stone, and J. R. Blake, <u>J. Fluid Mech. 254</u>: 437 (1993).

445. S. Frankel, and K. Mysels, <u>J. Phys. Chem. 66</u>: 190 (1962).

446. K. D. Danov, N. D. Denkov, D. N. Petsev, I. B. Ivanov, and R. P. Borwankar, <u>Langmuir 9</u>: 1731 (1993).

447. O. D. Velev, G. N. Constantinides, D. G. Avraam, A. C. Payatakes, and R. P. Borwankar, <u>J. Colloid Interface Sci. 175</u>: 68 (1995).

448. A. Scheludko, <u>Proceedings Koninkl. Ned. Akad. Wet., Amsterdam B65</u>: 76 (1962).

449. B. K. Chi, and L. G. Leal, <u>J. Fluid Mech. 201</u>: 123 (1989).

450. E. P. Ascoli, D. S. Dandy, and L G. Leal, <u>J. Fluid Mech. 213</u>: 287 (1990).

451. S. G. Yiantsios, and R. H. Davis, <u>J. Fluid Mech. 217</u>: 547 (1990).

452. D. Li, <u>J. Colloid Interface Sci. 163</u>: 108 (1994).

453. S. Hartland, Coalescence in dense-packed dispersions, <u>Thin Liquid Films: Fundamentals and Applications</u> (I. B. Ivanov, ed.), M. Dekker, New York, 1988, p. 663.

454. A. Prins, Liquid flow in foams as affected by rheological surface properties: A contribution to a better understanding of the foaming behavior of liquids, <u>Hydrodynamics of Dispersed Media</u> (J. P. Hulin, A. M. Cazabat, E. Guyon, and F. Carmona, eds.), Elsevier Sci. Pub. B.V., North-Holland, 1990, p. 5.

455. R. Pal, <u>Chem. Eng. Comm. 98</u>: 211 (1990).

456. Y. Yuhua, R. Pal, and J. Masliyah, <u>Chem. Eng. Sci. 46</u>: 985 (1991).

457. R. Wessel, and R. C. Ball, <u>Phys. Rev. A46</u>: 3009 (1992).

458. H. Kanai, R. C. Navarrete, C. W. Macosko, and L. E. Scriven, Rheol. Acta 31: 333 (1992).

459. R. Pal, Colloids Surf. A, 71: 173 (1993).

460. V. G. Babak, Colloids Surf. A, 85: 279 (1994).

461. W. R. Schowalter, Ann. Rev. Fluid Mech. 16: 245 (1984).

462. S. Kumar, R. Kumar, and K. S. Gandhi, Chem. Eng. Sci. 46: 2483 (1991).

463. S. Kumar, R. Kumar, and K. S. Gandhi, Chem. Eng. Sci. 47: 971 (1992).

464. M. von Smoluchowski, Phys. Z. 17: 557 (1916).

465. M. von Smoluchowski, Z. Phys. Chem. 92: 129 (1917).

466. O. Reynolds, Phil. Trans. Roy. Soc. (London) A177: 157 (1886).

467. G. E. Charles, and S. G. Mason, J. Colloid Sci. 15: 236 (1960).

468. H. A. Barnes, Rheology of emulsions - a review, Proceedings of the First World Congress on Emulsion Vol. 1, Paris, 1993, p. 267.

469. T. F. Tadros, Fundamental principles of emulsion rheology and their applications, Proceedings of the First World Congress on Emulsion Vol. 1, Paris, 1993, p. 237.

470. B. P. Radoev, D. S. Dimitrov, and I. B. Ivanov, Colloid Polymer. Sci. 252: 50 (1974).

471. I. B. Ivanov, D. S. Dimitrov, and B. P. Radoev, J. Colloid Interface Sci. 63: 166 (1978).

472. E. D. Manev, S. V. Sazdanova, C. S. Vassilieff, and I. B. Ivanov, Ann. Univ. Sofia Fac. Chem. 71(2): 5 (1976/1977).

473. E. D. Manev, Ann. Univ. Sofia Fac. Chem. 70(2): 97 (1975/1976).

474. S. A. K. Jeelany, and S. Hartland, J. Colloid Interface Sci. 164: 296 (1994).

475. J. Teissie, J. F. Toccane, and A. Bandras, Eur. J. Biochem: 77 (1978).

476. D. Vollhardt, Proceeding of the 6th International Conference of Surfactants, Bad Stuer, Akademie Verlag. Berlin, 1985.

477. S.-S. Feng, J. Colloid Interface Sci. 160: 449 (1993).

478. C.-Y. D. Lu, and M. E. Cates, Langmuir 11: 4225 (1995).

479. Z. Zapryanov, A. K. Malhotra, N. Aderangi, and D.T. Wasan, Int. J. Multiphase Flow 9: 105 (1983).

480. A. K. Malhotra, and D. T. Wasan, Chem. Eng. Commun. 55: 95 (1987).

481. D. S. Dimitrov, and I. B. Ivanov, Ann. Univ. Sofia Fac. Chem. 69(1): 83 (1974/1975).

482. D. E. Tambe, and M. M. Sharma, J. Colloid Interface Sci. 147: 137 (1991).

483. P. G. Murdoch, and D. E. Leng, Chem. Eng. Sci. 26: 1881 (1971).

484. X. B. Reed, E. Riolo, and S. Hartland, Int. J. Multiphase Flow 1: 411 (1974).

485. X. B. Reed, E. Riolo, and S. Hartland, Int. J. Multiphase Flow 1: 437 (1974).

486. I. B. Ivanov, and T. T. Traykov, Int. J. Multiphase Flow 2: 397 (1976).

487. T. T. Traykov, and I. B. Ivanov, Int. J. Multiphase Flow 3: 471 (1977).

488. I. B. Ivanov, and P. A. Kralchevsky, Colloids Surf. A, 128: 155 (1997).

489. O. D. Velev, T. D. Gurkov, I. B. Ivanov, and R. P. Borwankar, Phys. Rev. Lett. 75: 264 (1995).

490. O. D. Velev, T. D. Gurkov, and R. P. Borwankar, J. Colloid Interface Sci. 159:497 (1993).

491. K. D. Danov, T. D. Gurkov, T. Dimitrova, I. B. Ivanov, and D. Smith, J. Colloid Interface Sci. 188: 313 (1997).

492. I. B. Ivanov, B. P. Radoev, E. D. Manev, and A. D. Scheludko, <u>Trans. Faraday Soc. 66</u>: 1262 (1970).

493. B. U. Felderhof, <u>J. Chem. Phys. 49</u>: 44 (1968).

494. K. D. Danov, I. B. Ivanov, Z. Zapryanov, E. Nakache, and S. Raharimalala, Marginal stability of emulsion thin film, <u>Proceedings of the Conference of Synergetics, Order and Chaos</u> (M. Velarde, ed.), World Scientific, Singapore, 1988, p. 178.

495. R. S. Hansen, and J. Ahmad, Waves at interfaces, <u>Progress in Surface and Membrane Science vol. 4, 5</u> (J. F. Danielly, M. D. Rosenberg, D. A. Cadenhead, eds.), Academic Press, New York, 1971, p. 1.

496. M. G. Hedge, and J. C. Slattery, <u>J. Colloid Interface Sci. 35</u>: 593 (1971).

497. C. H. Sohl, K. Miyano, and J. B. Ketterson, <u>Rev. Sci. Instrum. 49</u>: 1464 (1978).

498. J Lucassen, <u>Trans. Faraday Soc. 64</u>: 2221 (1968).

499. A. Snik, W. Kouijzer, J. Keltiens, and Z. Houkes, <u>J. Colloid Interface Sci. 93</u>: 301 (1983).

500. J. Lucassen, and R. S. Hansen, <u>J. Colloid Interface Sci. 23</u>: 319 (1967).

501. L Ting, D. T. Wasan, K. Miyano, and S.Q. Xu, <u>J. Colloid Interface Sci. 102</u>: 248 (1984).

502. D. Byrne, J. C. Earnshaw, <u>J. Phys. D12</u>: 1145 (1979).

503. D. Langevin, and C. Griesmar, <u>J. Phys D13</u>: 1189 (1980).

504. S. Hard, and R. D. Neumann, <u>J. Colloid Interface Sci. 83</u>: 315 (1981).

505. S. Chandrasekhar, <u>Hydrodynamic and Hydromagnetic Stability</u>, Clarendon Press, Oxford, 1961.

506. T. K. Scherwood, and J. C. Wie, <u>Ind. Eng. Chem. 49</u>: 1030 (1957).

507. A. Orell, <u>Ph.D. Thesis</u>, University of Illinois, Urbana, 1961.

508. D. Thiessen, <u>Z. Phys. Chem. 232</u>: 27 (1966).

509. M. Hennenberg, T. S. Sorensen, and A. Sanfeld, <u>J. Chem. Soc. Trans. Faraday II 73</u>: 48 (1977).

510. A. Prosperetti, and M. S. Plesset, <u>Phys. Fluids 27(7)</u>: 1590 (1984).

511. R. Aveyard, and B. Vincent, <u>Prog. in Surf. Sci. 8</u>: 59 (1977).

512. P. S. Hahn, T. R. Ramamohan, and J. C. Slattery, <u>AIChE J. 31</u>: 1029 (1985).

513. P. A. Gauglitz, and C. J. Radke, <u>AIChE Symposium Series on Thin Liquid Films 82</u>: 50 (1986).

514. C. S. Dunn, <u>Doctoral Dissertation</u>, SUNY at Buffalo, New York, 1978.

515. L. L. Blyler, and F. Dimarcello, <u>ATT Bell Laboratories Technical Memorandum</u>, JM-850506, 1985.

516. A. D. Ryck, and D. Quéré, <u>C. R. Acad. Sci. Paris 317(2)</u>: 891 (1993).

517. A. D. Ryck, and D. Quéré, <u>C. R. Acad. Sci. Paris 317(2)</u>: 1045 (1993).

518. A. D. Ryck, and D. Quéré, <u>Europhys. Lett. 25(3)</u>: 187 (1994).

519. A. Koulago, V. Shkadov, A. D. Ryck, and D. Quéré, <u>Phys. Fluids 7(6)</u>: 1221 (1995).

520. A. D. Ryck, and D. Quéré, <u>J. Fluid Mech.</u> (1996) - in press.

521. S. D. Lin, and H. Brenner, <u>J. Colloid Interface Sci. 85</u>: 59 (1982).

522. S. D. Lin, and H. Brenner, <u>J. Colloid Interface Sci. 89</u>: 226 (1982).

523. R. K. Jain, C. Maldarelli, and E. Ruckenstein, <u>AIChE Symp. Ser. Biorheology 74</u>: 120 (1978).

524. D. S. Dimitrov, Colloid Polym. Sci. 260: 1137 (1982).

525. A. Steinchen, D. Gallez, and A. Sanfeld, J. Colloid Interface Sci. 85: 5 (1982).

526. D. Galezz, and W. T. Coakley, Prog. Biophys. Molec. Biol. 48: 155 (1986).

527. A. L. Burton, W. L. Anderson, and R. V. Andrews, Blood 32: 819 (1968).

528. F. Brochard, and J. F. Lennon, J. Phys. 36: 1035 (1975).

529. G. L. Nicolson, Int. Rev. Cytol. 39: 89 (1974).

530. G. L. Nicolson, Biochim. Biophys. Acta 457: 57 (1976).

531. K. Porter, D. Prescott, and J. Frye, J. Cell Biology 57: 815 (1973).

532. C. J. Van Oss, Ann. Rev. Microbiol. 32: 19 (1978).

533. M. C. Willingham, and I. Pastan, Proc. Nat. Acad. Sci. USA 72: 1263 (1975).

534. C. Maldarelli, R. K. Jain, I. B. Ivanov, and E. Ruckenstein, J. Colloid Interface Sci. 78: 118 (1980).

535. C. Maldarelli, and R. K. Jain, J. Colloid Interface Sci. 90: 233 (1982).

536. C. Maldarelli, and R. K. Jain, J. Colloid Interface Sci. 90: 263 (1982).

537. D. D. Joseph, Stability of Fluid Motions, vol. I, Springer-Verlag, New York, 1976.

538. P. Drazin, and W. Reid, Hydrodynamic Stability, Cambridge University Press, New York, 1981.

539. I. B. Ivanov, D. Sc. Thesis, University of Sofia, Sofia, 1977.

540. A. J. Vries, Rec. Trav. Chim. Pays-Bas. 77: 44 (1958).

541. A. J. Vries, Third Congress of Detergency Cologne 2: 566 (1960).

542. A. Vrij, Disc. Faraday Soc. 42: 23 (1966).

543. A. Vrij, and J. Overbeek, J. Am. Chem. Soc. 90: 3074 (1968).

544. A. Scheludko, and E. Manev, Trans. Faraday Soc. 64: 1123 (1968).

545. I. B. Ivanov, and D. S. Dimitrov, Colloid Polym. Sci. 252: 983 (1974).

546. I. B. Ivanov, R. K. Jain, P. Somasundaran, and T. T. Traykov, Solution Chemistry of Surfactants vol. 2, (K. L. Mittal, ed.), Plenum, New York, 1979, p. 817.

547. D. S. Dimitrov, and I. B. Ivanov, J. Colloid Interface Sci. 64: 97 (1978).

548. K. D. Danov - to be published.

549. I. B. Ivanov, S. K. Chakarova, and B. I. Dimitrova, Colloids Surf. 22: 311 (1987).

550. B. I. Dimitrova, I. B. Ivanov, and E. Nakache, J. Dispers. Sci. Technol. 9: 321 (1988).

551. F. J. Holly, Wetting, Spreading and Adhesion, (J. F. Padday, ed.), Academic Press, New York, 1978, p. 439.

552. J. L. Castillo, and M. G. Velarde, J. Colloid Interface Sci. 108: 264 (1985).

553. R. K. Jain, and E. Ruckenstein, J. Colloid Interface Sci. 54: 108 (1976).

554. R. J. Gumerman, and G. Homsy, J. Fluid Mech. 68: 191 (1975).

555. M. B. Williams, and S. H. Davis, J. Colloid Interface Sci. 90: 220 (1982).

556. S. H. Davis, Ann. Rev. Fluid Mech. 19: 403 (1987).

557. J. P. Burelbach, S. G. Bankoff, and S. H. Davis, J. Fluid Mech. 195: 463 (1988).

558. S. W. Joo, S. H. Davis, and S. G. Bankoff, J. Fluid Mech. 230: 117 (1991).

559. H.-C. Chang, Chem. Eng. Sci. 42: 515 (1987).

560. J.-J. Lee, and C. C. Mei, J. Fluid Mech. 307: 191 (1996).

561. H. Bénard, <u>Ann. Chim. Phys. 23</u>: 62 (1901).

562. Lord Rayleigh, <u>Phil. Mag. 32</u>: 529 (1916).

563. J. R. A. Pearson, <u>J. Fluid Mech. 4</u>: 489 (1958).

564. L. E. Scriven, C. V. Sterling, <u>J. Fluid Mech. 19</u>: 321 (1964).

565. P. L. T. Brian, <u>AIChE J. 17</u>:765 (1971).

566. P. L. T. Brian, and J. R. Ross, <u>AIChE J. 18</u>:582 (1972).

567. C. L. McTaggart, <u>J. Fluid Mech. 134</u>:301 (1983).

568. K. Ho, and H. Chang, <u>AIChE J. 34</u>:705 (1988).

569. H. A. Dijkstra, <u>Mass Transfer Induced Convection near Gas-Liquid Interface</u>, Ph.D. thesis, Groningen, 1988.

570. H. A. Dijkstra, <u>J. Colloid Interface Sci. 136</u>:151 (1990).

571. D. A. Goussis, and R. E. Kelly, <u>Int. J. Heat Mass Transfer 33</u>:2237 (1990).

572. D. A. Goussis, and R. E. Kelly, <u>J. Fluid Mech. 223</u>:25 (1991).

573. C. Pérez-Garcia, and G. Carniero, <u>Phys. Fluids A 3</u>:292 (1991).

574. W. Ji, H. Bjurström, and F. Setterwall, <u>J. Colloid Interface Sci. 160</u>:127 (1993).

575. N. Imaishi, M. Hozawa, K. Fujinawa, and Y. Suzuki, <u>Int. Chem Engng. 23</u>: 466 (1983).

576. T. B. Benjamin, <u>J. Fluid Mech. 2</u>: 554 (1957).

577. C. S. Yih, <u>Phys. Fluids 6</u>: 321 (1963).

578. R. E. Emmert, and R. L. Pigford, <u>Chem. Engng. Prog. 50</u>: 87 (1954).

579. S. Whitaker, <u>Industr. Eng. Chem. Fundam. Q. 3</u>: 132 (1964).

580. S. P. Lin, <u>AIChE J. 16</u>: 375 (1970).

581. S. P. Lin, <u>Lett. Heat Mass Transfer 2</u>: 361 (1975).

582. R. E. Kelly, S. H. Davies, and D. A. Goussis, On the instability of heated film flow with variable surface tension, <u>Heat Transfer 1986: Proc. 9th Intl. Heat Transfer Conf. vol. 4</u>, San Francisco, 1986, p. 1936.

583. J. R. Bourne, and K. V. Eisberg, Maintaining the effectiveness of an additive in adsorption refrigeration systems, <u>US Patent 3 276 217</u>, 1966.

584. T. Kashiwagi, Y. Kurosaki, and H. Shishido, <u>Nihon Kikai Gakkai Ronbunshu B51</u>: 1002 (1985).

585. T. Kashiwagi, H. Watanabe, K. Omata, and D. H. Lee, Marangoni effect in the process of steam adsorption into the falling film of the aqueous solution of LiBr. <u>KSME-ISME Thermal and Fluid Eng. Conf.</u>, Seoul, Korea, 1988.